MARINE ICOSAHEDRAL MEMBRANE-CONTAINING dsDNA BACTERIOPHAGE PM2: VIRION STRUCTURE AND HOST CELL PENETRATION

HANNA KIVELÄ

Department of Biological and Environmental Sciences

Institute of Biotechnology and

Helsinki Graduate School in Biotechnology and Molecular Biology

University of Helsinki

ACADEMIC DISSERTATION

To be presented with the permission of the Faculty of Biosciences of the University of Helsinki for public criticism in the auditorium 2042 of Biocenter 3, Viikinkaari 1, Helsinki, on June 18th, 2004, at 12 o'clock noon

HELSINKI 2004

Supervisor

Professor Dennis H. Bamford
Institute of Biotechnology and
Faculty of Biosciences
University of Helsinki

Reviewers

Docent Kristiina Mäkinen
Department of Applied Biology
University of Helsinki

Docent Petri Auvinen
Institute of Biotechnology
University of Helsinki

Opponent

Docent Vesa Olkkonen
Department of Molecular Medicine
National Public Health Institute

ISSN 1239-9469
ISBN 952-10-1901-8

Yliopistopaino

Helsinki 2004

Original publications

This thesis is based on the following articles,
which are referred to in the text by their Roman numerals.

I Kivelä, H. M., R. H. Männistö, N. Kalkkinen, and D. H. Bamford. 1999. Purification and protein composition of PM2, the first lipid-containing bacterial virus to be isolated. *Virology* **262,** 364-374.

II Kivelä, H. M., N. Kalkkinen, and D. H. Bamford. 2002. Bacteriophage PM2 has a protein capsid surrounding a spherical proteinaceous lipid core. *J Virol* **76,** 8169-8178.

III Huiskonen, J. T., H. M. Kivelä, D. H. Bamford, and S. J. Butcher. 2004. The PM2 virion has a novel organization with an internal membrane and pentameric receptor binding spikes. *Nat Struct Mol Biol* in press.

IV Kivelä, H. M., R. Daugelavičius, R. H. Hankkio, J. K. H. Bamford, and D. H. Bamford. 2004. Penetration of membrane-containing dsDNA bacteriophage PM2 into *Pseudoalteromonas* hosts. *J Bacteriol* in press.

ABBREVIATIONS

$\Delta\Psi$	membrane voltage
Δp	proton motive force
ΔpH	transmembrane pH difference
σ	standard deviation
Ap	ampicillin
ATP	adenosine triphosphate
BMV	brome mosaic virus
bp	base pair(s)
C-	carboxy-
cfu	colony forming unit(s)
CM	cytoplasmic membrane
Da	Dalton(s), 1 Da= 1.66×10^{-24} g
DNA	deoxyribonucleic acid
ds-	double stranded
EDTA	ethylenediamine-N,N,N'N'-tetraacetic acid
EGTA	ethyleneglycol-bis-N,N'-tetraacetic acid
e	electron
EM	electron microscopy
GlcNAc	N-acetylglucosamine
GD	gramicidin D
gp	gene product
GTP	guanosine triphosphate
HK97	bacteriophage Hong Kong 97
kDa	kilodalton(s)
Km	kanamycin
LC	lipid core(s)
LPS	lipopolysaccharide
MOI	multiplicity of infection
MPa	megapascal
MS	mass spectrometry
MurNAc	N-acetylmuramic acid
N	newton
N-	amino-
nt	nucleotide(s)
OEL	early left operon
OER	early right operon
OL	late operon
OM	outer membrane(s)
ORF	open reading frame(s)
ORI	origin of replication
pac	packaging recognition site
PAGE	polyacrylamide gel electrophoresis
PBCV-1	Paramecium bursaria Chlorella virus 1
PCB^-	phenyldicarbaundeca-borane
PE	phosphatidyletanolamine
PEG	polyethylene glycol
pfu	plaque forming unit(s)
PG	phosphatidylglycerol
p.i.	post infection
pRNA	prohead RNA
RNA	ribonucleic acid
rRNA	ribosomal RNA
S	sedimentation coefficient
SAXS	small angle X-ray scattering
SDS	sodium dodecyl sulfate
ses	SV40 encapsidation signal
SFV	Semliki Forest virus
ss-	single stranded
STMV	satellite tobacco mosaic virus
SV40	Simian virus 40
T	triangulation number
TBSV	tomato bushy stunt virus
TMV	tobacco mosaic virus
TPP^+	tetraphenylphosphonium
Å	ångström, 1 Å=0.1 n

TABLE OF CONTENTS

1 INTRODUCTION

Viruses are obligatory parasites without inherent metabolism. They are dependent on their host's cellular machineries, which they utilise to accomplish their infection-cycle. To ensure efficient reproduction the virus-specific nucleic acid is encapsidated in a protective shell, which functions as a vehicle to encounter a new host. Upon receiving a proper signal following host cell recognition the protective shell has to be disassembled to allow the delivery of the nucleic acid into the host cell to initiate a new reproduction cycle. Thus, the virus structure is a compromise between stability, which drives assembly and packaging of nucleic acid, and metastability, which plays a role in the virus entry.

Viruses are the most abundant forms of life on Earth infecting probably all cellular organisms. It has been estimated that the total number of virus particles is in the order of 10^{31-32}, which exceeds the number of host cells by at least a factor of ten (Bergh *et al*., 1989; Wommack and Colwell, 2000). Viruses having either ribonucleic acid (RNA) or deoxyribonucleic acid (DNA) genomes are known (van Regenmortel *et al*., 2000). Most of the animal virus genomes are RNA molecules, but when viruses infecting bacteria are considered, DNA genomes appear dominant, mostly in the form of double-stranded (ds) DNA. Currently bacteriophages constitute the largest virus group described, including ~5300 examined bacterial viruses organised in 13 virus families (Ackermann, 2003; van Regenmortel *et al*., 2000). The majority of the discovered phages (96%) are polyhedral virions with a tail, while the minority are polyhedral, filamentous, or pleomorphic phages (Fig. 1).

Bacteriophages were discovered independently by two scientists, Twort and d'Herelle, at the beginning of the 20th century. Studies on phages have had a great impact on the development of modern molecular biology and the understanding of the basic mechanisms of life, not the least important being the discovery of DNA carrying the genetic information or mRNA transferring that information further (Fields *et al*., 1996). In general bacteriophages are rather simple organisms and their genomes are often small, but they show remarkable diversity in both structure and function. Viruses can often be obtained rather easily and they usually have regular structures. Thus, they have been utilised widely as model systems. Although viruses have adapted to various cellular environments, several common principles in viral functions have been observed, in many cases elucidating also the cellular life.

1.1 VIRUS STRUCTURE

1.1.1 HELICAL AND ICOSAHEDRAL VIRUS ARCHITECTURES

Viruses have optimised the usage of their limited resources by using certain simple principles to effectively accomplish their infection-cycle. Viruses have solved this minimalism by using symmetry and conformational polymorphism of the subunits in their structure. The viral capsid is often constructed from several copies of one polypeptide building block organised either icosahedrally or helically. The purpose of the capsid is to function as

Morphology	Nucleic acid	Family (-*viridae*)	Example	Members	Characteristics
Tailed	DNA, ds, L	*Myo-*	T4	1243	Tail long, contractile
	ds, L	*Sipho-*	λ	3011	Tail long, noncontractile
	ds, L	*Podo-*	T7	696	Tail short
Polyhedral	DNA, ss, C	*Micro-*	ϕX174	40	
	ds, C, T	*Cortico-*	PM2	1	Complex capsid, lipids
	ds, L	*Tecti-*	PRD1	18	Internal membrane
	RNA, ss, L	*Levi-*	MS2	39	Envelope, lipids
	ds, L, S	*Cysto-*	ϕ6	9	Filaments or rods
Filamentous	DNA, ss, C	*Ino-*	fd	57	Envelope, lipids
	ds, L	*Lipothrix-*	TTV1	6	Resembles TMV
	ds, L	*Rudi-*	SIRV1	2	Envelope, lipids, no capsid
Pleomorphic	DNA, ds, C, T	*Plasma-*	L2	6	Spindle-shaped, no capsid
	ds, C, T	*Fusello-*	SSV1	4	

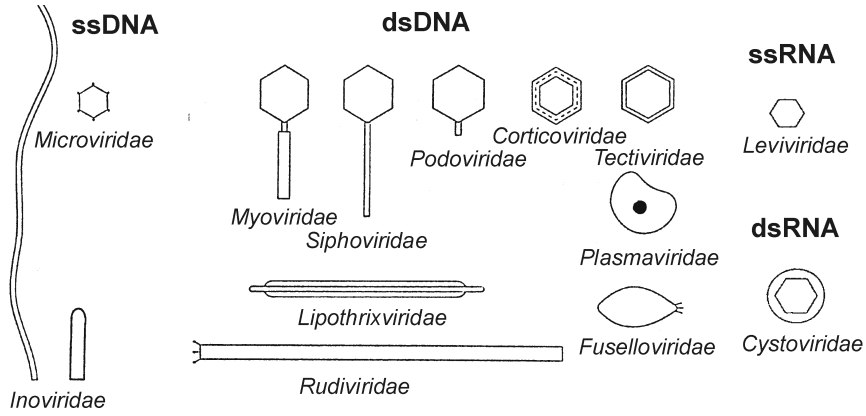

Figure 1. Major bacteriophage groups. Modified from Ackermann (2003). C, circular; L, linear; S, segmented; T, superhelical.

a protective vehicle to deliver the viral genome into the host cell.

The simplest viral structures are helical. They can be rigid rods such as tobacco mosaic virus (TMV; Butler, 1999) or flexible filaments such as bacteriophage fd (Day *et al*., 1988). In TMV a linear ssRNA molecule is inserted between the successive turns of identical proteins in a helical array. In filamentous phages, such as fd, their ssDNA genome is sheathed by capsid subunits and they comprise also specialised minor proteins capping the tips of the filament.

More complexity is found among icosahedral virus structures consisting of several different protein species. The surface architecture of icosahedral viruses can be described following the theory of quasi-equivalence introduced by Caspar and Klug (1962) and presented by its triangulation number (T). The T number describes the number of different environments occupied by one subunit (or the multiples of 60 subunits forming the capsid). The simplest way to build up a capsid is the T=1 architecture, where 60 chemically identical subunits form a continuous protein shell (Baker *et al*., 1999). When more than 60 subunits are assembled into pentamers and hexamers (T>1), the environments of the subunits cannot be equivalent, but ‘quasi-equivalent’. This is achieved when chemically identical

subunits change their bonding. Only certain T numbers (T = 1, 3, 4, 7, 9, 12, 13…) are allowed following the relationship $T=h^2+hk+k^2$, where h and k are integers (Caspar and Klug, 1962). However, there are exceptions such as the T=2 arrangement of fungal virus capsids (Cheng *et al*., 1994) and the inner core of dsRNA viruses (Butcher *et al*., 1997; Grimes *et al*., 1997). The T=2 architecture can be described as a T=1 arrangement of a dimer. In addition, due to the presence of more than one polypeptide building blocks, pseudo-T numbers are used to indicate that the same structural unit does not occupy all of the quasi-equivalent positions. For example, adenoviruses are built up from unique vertex proteins and the major coat proteins are organised in a pseudo T=25 lattice (Burnett, 1985).

Although icosahedral virus structures are mostly regular, a number of structural variations occur; capsids can be elongated or consist of several concentric protein shells. Furthermore, an asymmetric capsid can consist of 11 identical vertices and a unique structure in one vertex. The capsid may include structures projecting out from the capsid such as spikes, fibres, or tails. A lipid envelope surrounding the nucleoprotein core is a frequent feature among animal viruses. A minority of the characterised bacteriophages have envelopes or contain lipids as part of the virion (Fig. 1).

1.1.2 VIRUS ASSEMBLY

Viruses have solved the architectural challenge of assembling a stable structure that can be rapidly disassembled upon infection. There are various mechanisms to achieve accurate assembly, but common for all viruses is that the structural proteins are assembled in an ordered way in various assembly steps to form a virion. The classical example of a complex assembly of a virus is the branched well-described assembly pathway of bacteriophage T4 (Mosig and Eiserling, 1988). Phage tail, head, and tail fibres are built up via separate pathways, and finally combined together to construct an infectious virion.

A nucleation event controls the initiation of assembly. The interactions between the viral components in the nucleation centre induce conformational rearrangements in the building blocks. This creates new surfaces for subsequent interactions and triggers the next step in the assembly pathway (Casjens, 1997). This is the driving-force allowing the assembly to proceed in an ordered manner. Assembly-induced conformational changes are commonly required to accomplish quasi-equivalent interactions in the icosahedral lattice (Dokland, 2000; Tuma *et al*., 2001). There are two fundamentally different mechanisms of conformational switching. Firstly, the conformations observed in the virus capsid can form prior to the assembly of the capsid. This mechanism is employed by bacteriophage Hong Kong 97 (HK97). The coat proteins of HK97 assemble into pentamers and hexamers and their proportions guide the assembly process (Duda *et al*., 1995). Alternatively, the final conformations in the subunits are achieved only during the virus capsid assembly. As an example, bacteriophage PRD1 coat protein folding and multimerisation are assisted by phage and host-encoded proteins. The coat proteins attain their final conformations upon the maturation of an infectious virion (Bamford *et al*., 1995; San Martín *et al*., 2001).

Three types of genome encapsidation mechanisms are known for viruses: i) co-assembly of nucleic acid

and coat proteins, ii) packaging into preformed empty particles, and iii) assembly of a protein shell around precondensed nucleic acid (Casjens, 1997). In all cases the viral nucleic acid is identified and selected for packaging. Viral nucleic acids contain packaging recognition (pac) sites to ensure specific packaging, such as the pac-sites of single-stranded (ss) RNA virus TMV (Turner *et al*., 1988), dsRNA bacteriophage ϕ6 (Pirttimaa and Bamford, 2000), and dsDNA bacteriophage λ (Catalano *et al*., 1995).

1.1.2.1 Co-assembly of viral nucleic acid and coat proteins

In simple viruses such as TMV the assembly of the helical coat occurs simultaneously with the packaging of the ssRNA without any host or virally-encoded accessory factors (Butler, 1999). TMV assembly is initiated by binding of the first coat protein oligomer, a disk, to a specific site in the genome (Turner *et al*., 1988). The subsequent additions of oligomeric protein disks lock the ssRNA genome in a helix structure, which is most likely elongated in two directions, towards the 5' and 3' ends of the RNA genome. Also for satellite tobacco mosaic virus (STMV), a small (T=1) icosahedral virus, it has been proposed that the capsid assembly is mediated by co-condensation of ssRNA with coat protein dimers (Larson and McPherson, 2001). The RNA and coat protein interactions in bacteriophage MS2 also suggest that the capsid formation occurs simultaneously with RNA condensation (Koning *et al*., 2003).

1.1.2.2 Genome packaging into preformed empty particles

The packaging of genomes into preformed empty capsids is best described among the tailed dsDNA bacteriophages. The primary product of the subunit assembly is an empty precursor capsid, called the procapsid. It consists of a coat protein shell, an internal scaffold, and a portal vertex. The portal (or head-tail connector) is a ring of 12 or 13 proteins located at one special vertex used for packaging and delivery of the phage DNA (Bazinet and King, 1985; Valpuesta and Carrascosa, 1994). The portal plays a role in the assembly of the procapsid and provides a docking site for the DNA packaging enzymes, and eventually for the phage tail. In the recently solved crystal structure of the ϕ29 portal protein, the connector appears as a hollow cylinder with a central channel of ~40 Å in diameter, which could easily accommodate dsDNA (Simpson *et al*., 2000). Characteristic to the ϕ29 DNA-packaging device is the presence of a virally-encoded prohead RNA (pRNA) bound to the connector (Guo *et al*., 1987a). Non-structural scaffolding proteins are required for the assembly of the procapsid. For example, the coat proteins of bacteriophage P22, which do not assemble alone, co-polymerise with the scaffolding proteins (Prevelige *et al*., 1988; 1993). Structural analysis of the ϕ29 scaffolding protein before and after the prohead assembly revealed that the scaffold is arranged inside the capsid as a series of concentric shells (Morais *et al*., 2003). It was suggested that DNA binding mediates the structural transition from procapsid to mature ϕ29 virion and release of the scaffold. Prior to the packaging of the DNA the scaffold is removed from the capsid (Dokland, 1999).

Almost all described encapsidation systems using a procapsid state

package a linear molecule. These include ssRNA segments of ϕ6, unit-length DNA genomes with terminal proteins (e.g. PRD1 or ϕ29) or replication generated concatameric DNA molecules (e.g. T7 or P22; King and Chiu, 1997; Mindich, 1999). The concatamers are cleaved into virus genome length molecules by a terminase enzyme residing at the packaging vertex (Catalano, 2000). The packaging is initiated by a specific cutting at the *pac* site. The unidirectional packaging proceeds gradually until the head is full. The cleavage generated by terminase can be either sequence specific (e.g. in λ) or triggered by head-full mechanism (e.g. in P22).

Translocation of the nucleic acid into a precursor capsid is driven by external energy. The most detailed description of a packaging mechanism exists for phage ϕ29. Portal complexes convert the chemical energy from ATP hydrolysis into mechanical pumping of the linear nucleic acid molecule into the procapsid (Guo *et al*., 1987b; Pirttimaa *et al*., 2002). The symmetry mismatch between the packaging machinery and the procapsid is presumably assisting the motion of the packaging device with respect to the capsid upon nucleic acid transport (de Haas *et al*., 1999; Guasch *et al*., 2002; Hendrix, 1978; 1998; Simpson *et al*., 2000). During packaging the procapsid expands and matures to form an infectious virion (Butcher *et al*., 1997; King and Chiu, 1997). For example, the procapsid of HK97 goes through several distinct expansion intermediates (Duda *et al*., 1995). During this dynamic process the major capsid proteins undergo structural transitions, which proceed in a series of stochastically triggered subtransitions (Lata *et al*., 2000).

Osmotic pressure (~1 MPa) has been reported to be required in condensing DNA in solution to a density observed in the phage head (Rau *et al*., 1984). Recent experiments with ϕ29 have estimated the magnitude of the pressure in the packaged phage head to be up to 6 MPa (Smith *et al*., 2001). Within the mature phage, the DNA is tightly packaged to the density of liquid crystal (Cerritelli *et al*., 1997; Lepault *et al*., 1987). In the mature T7 head, modelled by cryo-EM and image analysis, the DNA is organised as a tightly wound coaxial spool, with the DNA coiled around the core in several concentric shells (Cerritelli *et al*., 2003). Thus, the capsid must be stable enough to encounter such a high pressure.

Proteolytic cleavage of structural proteins plays an important role in the assembly of many animal viruses such as herpesviruses (Newcomb *et al*., 2000). In dsDNA bacteriophages this cleavage is associated with DNA packaging, capsid expansion, and scaffold removal (Dokland, 2000). The classic example of proteolysis during virus maturation is the cleavage of T4 coat protein during morphogenesis (Laemmli, 1970). Another example is the HK97 coat protein, which undergoes proteolysis resulting in the removal of its N-terminal domain (Duda *et al*., 1995). In contrast to other tailed dsDNA phages, HK97 does not have a scaffolding protein. Instead, the N-terminal domain of the coat protein might function as a scaffold (Conway *et al*., 1995). Also mechanisms such as cross-linking are used to direct the viral assembly, like in HK97. The coat proteins of HK97 are covalently joined together and form cross-linked hexamers and pentamers (Duda *et al*., 1995). In addition, virally-encoded assembly factors (e.g. proteins P10 and P17 in PRD1; Mindich *et al*., 1982) and cellular chaperonins may guide the folding of coat proteins and thus, prevent premature assembly of the phage particle (e.g. T4, HK97;

Georgopoulos *et al*., 1972; Xie and Hendrix, 1995).

Scaffolding protein-assisted assembly pathways are utilised also by animal herpesviruses (Newcomb *et al*., 2003). Modifications of this theme are also employed by the two icosahedral lipid-containing bacteriophages PRD1 and ϕ6. In PRD1, the internal membrane acts as a scaffold for capsid assembly. The dsDNA genome is packaged through a unique vertex into a precursor capsid containing a lipid membrane (Gowen *et al*., 2003; Mindich *et al*., 1982; Strömsten *et al*., 2003). Unlike packaging ATPases of other phages utilising packaging through a single vertex, the packaging ATPase of PRD1 is a structural protein (Mindich *et al*., 1982; Strömsten N. J. *et al*., unpublished). During packaging, the PRD1 membrane expands analogously to the capsid expansion in the maturation of other dsDNA phages (Butcher *et al*., 1995). ϕ6 packages its segmented ssRNA genome into a preformed nucleocapsid accompanied by expansion of the procapsid (Butcher *et al*., 1997). The dsRNA-containing nucleocapsid is then enveloped (Mindich *et al*., 1976). Also the morphogenesis of small icosahedral bacteriophages of the *Microviridae* family, with circular ssDNA genomes, proceeds via an empty procapsid intermediate. The spikes and coat proteins assemble with the external and internal scaffolding proteins. The resulting open procapsids of ϕX174 (Dokland *et al*., 1999) and α3 (Bernal *et al*., 2003) have prominent pores around three-fold symmetry axes. The openings might be utilised for DNA packaging concomitantly with its synthesis.

1.1.2.3 Assembly of a protein shell around precondensed nucleic acid

The third mechanism to encapsidate the viral genome is the precondensation of nucleic acid. The nucleic acid is first condensed in the presence of specific proteins resulting in a compressed nucleoprotein core, which is covered by a protein capsid. For circular dsDNA of Simian virus 40 (SV40) it has been demonstrated that the genome is complexed with host-encoded histones (Garcea and Liddington, 1997). Cellular transcription factor Sp1 interacts with viral multimeric capsid proteins and recruits them to the packaging signal *ses* of the SV40 genome near the origin of replication (ORI; Gordon-Shaag *et al*., 2002). This functions as a nucleation center for the SV40 capsid assembly. The capsomers are polymerised around the genome and form interactions with adjacent capsomers and the viral genome.

1.1.3 EVOLUTION OF VIRUSES

The rapid sequence divergence in virus genomes makes it difficult to establish relationships between distantly related viruses. RNA virus genomes has been estimated to diverge by a rate of 10^{-2} to 10^{-4} changes per nt per year (Takeda *et al*., 1994; Weaver *et al*., 1997). Sequence data is still valuable in comparisons of closely related species, while the nucleic acid sequences of more distant species have diverged.

1.1.3.1 Viral mosaicism

Comparisons of tailed dsDNA bacteriophage genomes have revealed some of the evolutionary mechanisms detected at the genomic level. Discovery of conserved genomic patterns within specific phage groups has led to proposal that tailed lambdoid phages have a common global gene pool (Hendrix *et al*., 1999). During their propagation phages encounter DNA of bacterial or prophage origin and can recombine to generate new genomic arrangements. Thus, tailed dsDNA phages are considered to be genetic mosaics (Hendrix *et al*., 1999; 2003). The observed mosaicism of lambdoid genomes has evolved by recombination resulting in the addition of genetic modules, morons, described by Juhala *et al*. (2000). Similar evolutionary mosaicisms have been reported for recently described marine cyanophage genomes (Mann, 2003). Although marine cyanophages are quite distinct from the other T4-like phages, their genomes share similarities with that of coliphage T4 (Hambly *et al*., 2001). Most variable areas are found among genes that are thought to facilitate the adaptation to new environments and stresses (Desplats and Krisch, 2003). Very recently it was discovered that recombination between two yersiniaphages, ϕA1122 and ϕYeO3-12, has yielded progeny phages (Garcia *et al*., 2003). It was proposed by the authors that one of these recombinant phages is coliphage T3 described ~50 years ago. Due to recombination, accurate taxonomic or phylogenetic analyses among mosaic viruses may be impossible (Lawrence *et al*., 2002).

Horizontal gene exchange by recombination is rare between phages infecting phylogenetically distant hosts, but coinfection and recombination may occur if their hosts are the same or phylogenetically relatively close (Hendrix *et al*., 1999). It has been observed that in natural aquatic virus communities, genetic similarities exist between phages infecting related hosts (Jiang *et al*., 2003). Furthermore, increasing morphological variance observed among T4-type phages correlates with the increasing phylogenetic distance of their host (Desplats and Krisch, 2003). Exchange between more distant species can be a result of more ancient exchange of the genetic modules or a series of exchanges through intermediate genomes (Hendrix *et al*., 1999). Hambly *et al*. (2001) discovered genetic elements from marine cyanophages similar to terrestrial coliphage T4, which might be a demonstration of an ancient recombination.

While horizontal gene transfer as a viral evolutionary mechanism has been proposed among tailed lambdoid phages, it may not be as universal as concluded. The horizontal genetic exchange in the T7 group of phages has been shown to be limited, as indicated by a strong conservation of essential genes and their organisation

(Chen and Lu, 2002; Hardies *et al*., 2003; Kovalyova and Kropinski, 2003). According to a study of *Lactococcus* prophages, genomic similarity of lysogenic phages is much lower than that of lytic phages (Chopin *et al*., 2001). Thus, virulent phages with a unique replication strategy and rapid and efficient life cycle might evolve by genetic adaptation and accumulation of point mutations rather than recombining and exchanging genetic modules, which is more common for temperate phages (Burch and Chao, 2000; Holder and Bull, 2001).

1.1.3.2 Early viral ancestors

While primary sequences are evolving in response to evolutionary pressure, the variation in two homologous gene sequences might prevent the observation of a shared origin. At the same time, the corresponding three-dimensional structures needed to carry out the fundamental viral functions, may maintain a conserved structure. Structural studies have an increasing importance for analysing phylogeny among distant viruses. Although it is evident that horizontal gene exchange exists, it can be considered that vital conserved key functions and structures comprising a common 'virus-self' diverge slowly and arose a long time ago (Bamford *et al*., 2002).

An illustration of conserved viral structures coupled with vital functions is the jellyroll (β-barrel) topology of capsid proteins. It has been found in an enormously wide range of viruses such as bacterial viruses ϕX174 (McKenna *et al*., 1992) and PRD1 (Benson *et al*., 1999), brome mosaic virus (BMV) infecting plant cells (Lucas *et al*., 2002)**,** and animal viruses SV40 (Liddington *et al*., 1991), adenoviruses (Athappilly *et al*., 1994), and picornaviruses (Hogle *et al*., 1985). A subset of these jellyroll topology proteins is the double-barrel found in PRD1 (Benson *et al*., 1999), Paramecium bursaria Chlorella virus 1 (PBCV-1; Nandhagopal *et al*., 2002), and adenovirus (Athappilly *et al*., 1994) for which the major capsid protein crystal structures are available. These complex dsDNA viruses use this architecture to accomplish large facets. Structural modelling based on sequence information revealed that the fold of the bacillusphage Bam35 coat protein is also a double-β-barrel (Ravantti *et al*., 2003). The strong conservation of the jellyroll fold in coat proteins despite any apparent sequence similarity suggests its utility as a building block throughout evolution. These viruses might share a common ancestor, which arose long time ago (Chelvanayagam *et al*., 1992). Also the glycoprotein structures of alphaviruses and flaviviruses are related with a similar fold (Lescar *et al*., 2001; Pletnev *et al*., 2001). Although there are differences between flavi- and alphaviruses in the capsid architecture and in the genome organisation, it is more likely that the glycoproteins are derived from a common ancestor (Strauss and Strauss, 2001).

Common evolutionary roots have been described for some bacterial and animal viruses. Extensive similarities have been found in bacteriophage PRD1 and adenovirus, strongly suggesting a common evolutionary origin (Benson *et al*., 1999). This descriptive example of conservation between viruses infecting entirely different hosts (bacteria and vertebrates) includes capsid architecture, vertex organisation, and genome replication strategy. Recently two other viruses, chlorella virus PBCV-1 and bacillus phage Bam35, sharing related

structural architectures with PRD1 have been described (Nandhagopal *et al*., 2002; Ravantti *et al*., 2003). This conservation agrees with the current hypothesis by Bamford *et al*. (2002) and proposes that PBCV-1 and Bam35 belong to the virus lineage of PRD1 and adenovirus. Also it has been noticed that animal herpesviruses share structural similarities with tailed dsDNA bacteriophages. The assembly of herpesviruses occurs via procapsid-state with the help of scaffolding proteins similar to complex bacteriophages (King and Chiu, 1997). Discovery of a portal protein in herpesvirus (Newcomb *et al*., 2001), strengthens the idea of a common evolutionary origin among these viruses (Bamford *et al*., 2002; Belnap and Steven, 2000).

High-resolution structural data of several dsRNA viruses revealed that they share structural similarities (Bamford *et al*., 2001). The most striking similarity is the architecture of the inner shell. This unusual "T=2" organisation of the polymerase particle essential for RNA metabolism was described first for bluetongue virus (Grimes *et al*., 1998). The similarities exceed further among the *Reoviridae* family; the folds of the "T=2" shell protein of bluetongue virus (Grimes *et al*., 1998) and reovirus (Reinisch *et al*., 2000) are analogous with no sequence relationship. Bacterial dsRNA virus ϕ6 shares similar organisation and functions with eukaryotic reoviruses (Butcher *et al*., 1997). Thus, it has been suggested that these dsRNA viruses may also belong to the same evolutionary lineage (Bamford *et al*., 2002).

As a conclusion, it seems that viruses constitute a huge, ancient, rapidly evolving population, that was on Earth before the divergence of the three domains of life. The basic structural solutions might have arisen early and have been conserved ever since. Independent evolution of a set of similar structures and functions seems highly improbable. Obviously each virus evolves continuously alongside its host organism to ensure efficient reproduction.

1.2 BACTERIOPHAGE ENTRY

1.2.1 GRAM-NEGATIVE CELL ENVELOPE

The cytoplasm of Gram-negative bacteria is enclosed within two concentric membranes: the outer membrane (OM) and the cytoplasmic membrane (CM). The OM provides a rather passive protective layer for the cell, while most of the metabolic functions are associated with the CM (Kadner, 1996). Additional external layers such as capsules and S-layers can reside outside the OM as an extra protective barrier, which can also contribute to attachment to surfaces (Sleytr and Beveridge, 1999; Whitfield and Roberts, 1999). The periplasm between the two membranes contains a cross-linked peptidoglycan layer and a number of soluble proteins, including nucleases.

Most of the knowledge concerning the organisation of the Gram-negative cell envelope has been obtained from the enteric bacteria *Escherichia coli* and *Salmonella enterica*. The OM of Gram-negative bacteria is highly asymmetric. The inner leaflet consists of phospholipids [70-80% phosphatidyletanolamine (PE), 20-30% of phosphatidylglycerol (PG), and cardiolipin], while lipopolysaccharides (LPS) are found exclusively in the outer leaflet (Nikaido,

1996). The Gram-negative OM functions as a barrier for many external agents. The protecting effect is mainly due to the presence of LPS molecules. The low fluidity of the highly charged LPS molecules decreases the rate of the transmembrane diffusion of lipophilic solutes (Nikaido and Vaara, 1985).

LPS molecules consist of i) a proximal hydrophobic membrane anchor lipid A, ii) a central core oligosaccharide with multiple phosphoryl substituents, and iii) a distal polymer consisting of oligosaccharide repeats, the O-antigen. The structurally diverse O-antigens provide the cell a hydrophilic surface and are the main antigens targeted by host antibody responses. O-antigens also play a role in protection against host defence mechanisms such as phagocytosis (Erridge *et al*., 2002; Nikaido, 1996; Raetz and Whitfied, 2002). The deep rough mutants of *S. enterica* lacking the O-antigen and the distal core region were found to be extremely sensitive to hydrophobic compounds such as dyes, antibiotics, detergents, or mutagens. Thus, the core region is involved in maintaining the barrier properties of the OM (Nikaido, 1996). Negatively charged residues in the proximal core oligosaccharide are particularly important to membrane integrity. The negative charges allow adjacent LPS molecules to be linked by divalent cations (Ca^{2+}, Mg^{2+}) strengthening the OM structurally (Nikaido, 1996). The lethality of the lipid A mutants suggests that the hydrophobic anchor of LPS is essential for the assembly of the OM.

An additional set of proteins contributes in the permeability properties of the OM. Half of the OM mass consists of proteins, that play a role in signal transduction, translocation of solutes, and nutrient uptake. Scarce metal complexes such as iron and vitamins such as vitamin B_{12} are actively taken up by specialised transport complexes operating with the proteins in the CM (Moeck and Coulton, 1998). Porins are one of the most abundant proteins in the OM. They form relatively non-specific pores that allow rapid passage of small hydrophilic molecules across the OM (Nikaido, 1992). A porin consists of three β-barrels forming channels with a ~10 Å width allowing the diffusion of compounds no larger than 600 kDa (Koebnik *et al*., 2000). The OM contains also an abundant lipoprotein. It is covalently bound to the periplasmic peptidoglycan layer contributing to the structural rigidity of the OM by forming a network (Shu *et al*., 2000).

The semipermeability of the CM and the high solute concentration of the cytoplasm contribute to a considerable intracellular turgor pressure. This pressure forces the CM against the stress-bearing bacterial periplasmic cell wall. The cell wall is composed of murein (or peptidoglycan), which surrounds the whole bacterial cell as a single macromolecule (Höltje, 1998). The murein forms a three-dimensional sack maintaining the shape of the cell. Cells have their own enzymes controlling the cleavage of the peptidoglycan needed during the cell division. The peptidoglycan consists of glycan strands and peptide chains covalently joined together forming a meshwork, which restricts the diffusion of large protein complexes (Dijkstra and Keck, 1996). In *E. coli*, particles larger than 50 kDa cannot pass the murein layer (Demchick and Koch, 1996). A neutron small-angle scattering study of *E. coli* sacculus showed that 75-80% of the murein is organised in a single-layer, the remaining being triple-layered with a thickness of 2.5-7.5 nm (Labischinski *et al*., 1991). The glycan strands are polymers of aminosugars, N-acetylglucosamine (GlcNAc) and N-acetyl-

muramic acid (MurNAc), linked together by β-1,4 glycosidic bonds. While variation among the glycans is small, the peptides vary frequently between different bacteria.

1.2.2 DELIVERY OF PHAGE NUCLEIC ACID INTO GRAM-NEGATIVE CELLS

The virion functions as a protective shell for its nucleic acid, which has to enter the cell to reach the site of its replication. In the case of bacteriophages infecting Gram-negative cells the replication of the viral nucleic acid occurs in the cytoplasm. Thus, the rigid three-layered Gram-negative cell envelope forms a barrier to the entering bacteriophage. Depending on the morphology of the virus and the type of the nucleic acid, different strategies for the phage nucleic acid internalisation have evolved (Poranen *et al*., 2002). The nucleic acid transport is essential not only for virus infections, but similar mechanisms are utilised widely also elsewhere. These include the bacterial conjugation, RNA movements across the eukaryotic cell nuclear membrane, and T-DNA transfer from bacteria to plant cells.

The initial step in the phage infection cycle is the recognition of a susceptible host. This is commonly achieved by specific binding of the viral receptor binding protein to a receptor exposed on the bacterial surface. Several OM proteins, LPS, pili, flagella, or capsules act as receptors for bacteriophages (Heller, 1992). The complexities found in the virion structures might be a consequence of the requirement for conformational changes needed for the nucleic acid delivery. Structural rearrangements are trigged when the virus receives a proper signal by host recognition. Upon infection tailed coliphages and bacteriophage PRD1 inject their genome via one vertex, which is structurally metastable. The metastability has commonly been accomplished by symmetry mismatch. Examples of labile structures able to undergo structural rearrangements include the portal proteins with 12 or 13-fold symmetry in tailed bacteriophages at a five-fold symmetry position and the PRD1 spike protein P2 interactions in the vertex complex (Rydman *et al*., 1999; Valpuesta and Carrascosa, 1994).

1.2.2.1 Injection of the genome through the tail

Although the tailed coliphages resemble each other in their gross morphology, they utilise different mechanisms for DNA ejection. Common for the translocation of T4, T5, T7, and λ genomes is that they are injected as linear molecules from the phage heads across the cell membranes via the proteinaceous phage tail. This results in an empty capsid, which remains a hallmark of the DNA injection on the cell surface. In the case of T4 (*Myoviridae*, see Fig. 1), which has a bilayered contractile tail, the initial reversible binding to the receptor triggers conformational changes in the baseplate (Crowther *et al*., 1977). This leads to irreversible binding of T4 to the core region of its LPS by the C-terminal part of the short tail fibres (Riede, 1987; Thomassen *et al*., 2003). This activates a contraction of the external tail sheath resulting in penetration of the OM and peptidoglycan layer by the internal tail tube. The recent structural investigations of T4 proteins in the baseplate complex have given indications that gp5 with lytic activity acts as a membrane-puncturing needle in the tip of the entering tail (Kanamaru *et al*., 2002).

Earlier electron microscopic observations have suggested that infection of phages might take place preferentially at the adhesion sites of the *E. coli* envelope (Bayer, 1968). In these patches the OM and the CM are in close contact. However, it is not clear if these areas are cell-derived, since it has been proposed that the adhesion sites are phage-induced. DNA of tailed phages crosses the bacterial envelope through pores that presumably originate from the phages. Tarahovsky *et al*. (1991) showed that the crossing of the T4 genome induces a fusion between the OM and the CM. A similar fusion event has been proposed to occur during the T5 infection (Letellier *et al*., 2003).

Phage T5 (*Siphoviridae,* see Fig. 1) which has a long, non-contractile tail binds irreversibly by its protein pb5 to the FhuA receptor (Heller, 1984). FhuA is an OM protein of *E. coli* utilised in ferrichrome transport (Boulanger *et al*., 1996). Purified pb5 and FhuA make high-affinity interactions (Plancon *et al*., 2002), and the binding of T5 virions to purified FhuA results in conformational changes in both the phage and the receptor. FhuA is converted into an ion-conductive channel and the phage DNA is ejected (Bonhivers *et al*., 1996; Boulanger *et al*., 1996). T5 DNA transfer occurs in two steps: 8% of the DNA first enters the cytoplasm (Lanni, 1965). The transfer of the remaining DNA is held back until the two virally-encoded proteins A1 and A2 are produced (McCorquodale *et al*., 1977). The interaction between pb5 and FhuA may trigger conformational changes in the straight tail fiber pb2, which is found in the OM and the CM of infected *E. coli* cells (Guihard *et al*., 1992). A cryo-electron tomography study of T5 DNA translocation into FhuA-containing liposomes revealed that pb2 traverses the lipid bilayer (Böhm *et al*., 2001). Thus, it is quite evident that pb2 forms a channel for DNA translocation (Feucht *et al*., 1990). Although T5 binding triggers conformational changes in its receptor and the FhuA channel is wide enough for DNA translocation, the translocation presumably occurs through a channel formed by viral proteins (Letellier *et al*., 2003). Another siphovirus λ requires host-derived mannose transporter proteins in the CM for its DNA entry (Elliott and Arber, 1978; Erni *et al*., 1987). The receptor for λ is the OM channel maltoporin LamB (Randall-Hazelbauer and Schwartz, 1973). λ can deliver its DNA to liposomes carrying LamB. Simultaneously with DNA delivery the liposomes are permeabilised indicating that a transmembrane channel is formed (Roessner and Ihler, 1986). This pore is most probably the channel used by λ DNA to cross the membrane. However, it is not known if LamB functions as a channel or whether viral proteins are involved in the pore formation (Berrier *et al*., 2000).

The non-contractile tail of T7 (*Podoviridae*, see Fig. 1) is too short to span the cell envelope of a Gram-negative cell. The channel for T7 genome injection across the cell envelope is formed by virally-encoded proteins similarly to T5 channel formation. However, the mechanism is totally different. Entry of the T7 genome takes place concomitantly with its transcription (Garcia and Molineux, 1995; Zavriev and Shemyakin, 1982). Following adsorption and conformational changes three internal structural proteins, gp 14, 15, and 16, are ejected from the phage head to the host membrane forming an extension of the short tail. It has been suggested that these proteins together form a channel across the cell envelope (Molineux, 2001).

Almost all studied bacteriophage entry systems involve the penetration of a linear nucleic acid molecule into the cytoplasm. Penetration of a circular DNA molecule into a Gram-negative cell has not been analysed in detail. Examples include the entry of the icosahedral bacteriophage ϕX174 (*Microviridae*, see Fig. 1) with circular ssDNA genome. It adsorbs to the LPS by its spikes gp H and gp G. gp G provides a channel for the DNA translocation from the capsid, while gp H penetrates through the host membrane along with the DNA (Jazwinski *et al*., 1975; McKenna *et al*., 1994). The mechanism of ϕX174 DNA penetration cross the cell envelope is unknown. Once the DNA has reached the cytoplasm, gp H likely directs the binding of the circular ϕX174 ssDNA to a specific site at the membrane, where replication ensues (Hayashi *et al*., 1988).

1.2.2.2 Involvement of phage membranes in entry

Icosahedral bacterial viruses that contain a membrane and no tail belong to three families: the *Tectiviridae*, *Cystoviridae*, and *Corticoviridae* (see Fig. 1). PRD1, ϕ6, and PM2 are the type-organisms of these families, respectively. The structures and the life-cycles of dsDNA phage PRD1 and dsRNA phage ϕ6 are well-characterised, but knowledge of PM2 is still incomplete. The viral membranes are active components during cell entry.

PRD1 adsorption is mediated by the host recognition protein P2 (Grahn *et al*., 1999). P2 is a part of the multiprotein vertex complex. Each of the virion vertices is metastable and capable of releasing the DNA. The removal of the spike complex creates an opening in the binding vertex of the virion (Rydman *et al*., 1999). This activates the transformation of the internal viral membrane to a tubular structure, which protrudes from the vertex (Bamford and Mindich, 1982; Lundström *et al*., 1979). This tubular membrane device, with the help of several viral membrane proteins, is used to deliver the linear genome into the host cell. Fusogenic protein P11 at the viral membrane surface seems to be the first protein needed for a successful DNA delivery, indicating a role in the OM penetration (Bamford and Mindich, 1982; Grahn *et al*., 2002). The genome penetrates the cell envelope via the membrane tail, which most probably interacts with the OM and the CM leaving the empty capsid on the host cell surface.

A totally different strategy is employed by the enveloped dsRNA phage ϕ6. The virion absorbs to the bacterial pilus, which triggers the removal of the spike. Viral transmembrane protein P6 mediates the fusion between the virion envelope and the bacterial OM allowing the nucleocapsid to penetrate into the cytoplasm (Bamford *et al*., 1987). The nucleocapsid penetration across the CM occurs via an endocytic-like pathway, which is mediated by the nucleocapsid shell protein P8 (Poranen *et al*., 1999). This resembles the endocytic entry of animal viruses (Marsh and Helenius, 1989).

1.2.2.3 Cell wall penetration

Once through the OM, the entering phage faces the peptidoglycan layer, which is a barrier to the transport of macromolecules (Dijkstra and Keck, 1996). Numerous hydrolysing enzymes are shown to cleave a range of different bonds in the peptidoglycan polymer (Höltje, 1998). Muramidases degrade the glycan strands and amidases cleave off the peptides from the glycans. Several phages possess genes encoding peptidoglycan hydrolysing enzymes with conserved lytic domains (Koonin and Rudd, 1994; Lehnherr *et al*., 1998). In most cases these enzymes are incorporated into the phage particles, such as T4 protein gp5 and T7 protein gp16, suggesting a role in the cell wall penetration upon entry (Kao and McClain, 1980; Moak and Molineux, 2000; Nakagawa *et al*., 1985). Similarly, particles of the lipid-containing bacteriophages PRD1 and ϕ6 contain lytic activities (Caldentey and Bamford, 1992; Mindich and Lehman, 1979; Rydman and Bamford, 2000). PRD1 protein P7 and ϕ6 protein P5 facilitate the phage nucleic acid transfer across the cell wall during entry.

1.2.2.4 Energy driving phage DNA entry

Transport of phage nucleic acid across the cell envelope is an energy-dependent process. DNA injection through a special vertex is suggested to be driven by the force of the pressurised genome in the virus capsid. In ϕ29, a ~50pN force is built up upon the DNA packaging, thus providing energy for the DNA delivery (Smith *et al*., 2001). Pointing to a similar mechanism, the interactions of phages T5 or λ with their receptors are sufficient to trigger the DNA ejection, which is not dependent on the energetic state of the host CM (Lambert *et al*., 1998; Roessner and Ihler, 1986). The strong stabilisation of receptor binding protein pb5 of T5 upon binding to FhuA suggests that pb5 undergoes structural rearrangements (Plancon *et al*., 2002). Such conformational changes are considered to trigger the DNA release (Heller, 1992). It seems that cellular energy is not required for DNA ejection in these cases, but instead the electrostatic repulsion between the packaged phage DNA phosphates might drive the translocation (Letellier *et al*., 1999). Energy is conserved in the expanded internal membrane during the packaging of the PRD1 genome due to strong electrostatic repulsion between the coat and the membrane. This could be the force driving at least partly the delivery of the PRD1 genome (Grahn *et al*., 2002; San Martín *et al*., 2001). However, in the case of T5, the capsid and the tail can be removed during the DNA translocation leaving the remaining part of the genome freely in the extracellular environment (Letellier *et al*., 1999). The remaining genome is then translocated into the cytoplasm. Thus, relief of the internal pressure in the T5 phage head cannot be the only energy source.

Proton motive force (Δp) consisting of membrane voltage ($\Delta\Psi$) and transmembrane pH gradient (ΔpH) is commonly used in Gram-negative bacteria to drive macromolecular transport across the membranes (Dreiseikelmann, 1994; Grinius, 1980; Palmen *et al*., 1994). T4 and T7 genome delivery is dependent on the energetic state of the host CM. Membrane voltage above 90 mV is required for T4 phage-induced fusion of the OM

and CM at the site of phage adsorption (Kalasauskaite *et al*., 1983; Labedan *et al*., 1980; Tarahovsky *et al*., 1991). Similarly Δp has been shown to be required for successful delivery of phage T7 DNA. The ongoing DNA translocation was arrested by collapsing the membrane potential by a protonophore (Molineux, 2001). Hence, external energy is needed for T7 genome translocation. It has been proposed that the first 850 bp of the entering genome are brought into the cell by a molecular motor formed by viral proteins ejected from the phage head (Molineux, 2001). The remaining genome is internalised by transcription carried out by the cellular RNA polymerase and eventually by the viral enzyme (Moffatt and Studier, 1988; Zavriev and Shemyakin, 1982).

1.3 MARINE BACTERIOPHAGES

Bacteriophages were discovered from oceans ~50 years ago (Spencer, 1955). Currently it is established that viruses in general and bacteriophages in particular are amazingly abundant in marine ecosystems, often with over 10 million virus particles per millilitre of natural sea water (Bergh *et al*., 1989). Since the oceans are the largest biosphere, marine phages are probably the most abundant biological entity on Earth. The exact origin(s), ecological importance, and functions of these bacteriophage particles are unclear at the present. But the abundance of these virus particles suggests that they have a significant ecological impact on the marine environment (Fuhrman, 1999).

The tailed dsDNA bacteriophages being remarkably diverse and the most abundant of all virus types represent also the majority of the marine virus population (Breitbart *et al*., 2002; van Regenmortel *et al*., 2000). This is probably a consequence of the proposed ancient nature of these phages and the virion morphology that can be easily adapted to different conditions (Ackermann, 2003; Tetart *et al*., 2001). Knowledge of viral diversity has been mainly obtained from phages isolated on host bacteria easily grown in laboratory. However, these bacteria represent only a small portion of bacterial diversity (Dojka *et al*., 2000; Hugenholtz *et al*., 1998). Thus, the extent of viral diversity in marine environments is still largely unknown. It has been estimated that less than 0.0002% of the global phage genome population has been sampled (Rohwer, 2003). Since many environmental bacteria and their viruses are difficult to cultivate, culture-independent molecular approaches have been used to investigate the genetic diversity of natural viral communities. A genomic analysis of uncultured marine communities revealed that over 65% of the sequences obtained were previously uncharacterised and the rest of the sequences were mostly virus-derived (Breitbart *et al*., 2002). It has been assumed that bacteriophages in the ocean are genetically more diverse than their bacterial hosts (Jiang *et al*., 2003).

Only a few marine viral genome sequences have been determined (Paul *et al*., 2002). The genome of *Pseudoalteromonads* phage PM2 was the first to be sequenced (see Section 1.4.1; Männistö *et al*., 1999). The study of the genomes of roseophage SIO1, cyanophage P60, and vibriophage VpV262 revealed that genetic elements found in marine phages are similar to well described nonmarine phage genomes (Chen and Lu, 2002; Hardies *et al*., 2003; Rohwer *et al*., 2000). Both SIO1 and P60 belong to the T7-like

podoviruses. Additionally, the marine cyanophage S-PM2 shares conserved genetic elements coding structural components similar to coliphage T4, strongly suggesting that S-PM2 is a marine representative of myoviruses (Hambly *et al*., 2001).

It is obvious that this gigantic population of viruses creates a high selective pressure to cellular organisms. As demonstrated for cyanophages by Waterbury and Valois (1993), marine viruses play an important role in controlling their host population density and influence the genetic diversity of the hosts (Wommack and Colwell, 2000). It has been suggested that marine viruses could mediate horizontal gene transfer through transduction, thus increasing the genetic variability in marine microbial communities (Jiang and Paul, 1998; Paul, 1999). In water samples bacteria harbouring prophages are quite common; 40% of the cultured marine bacteria are lysogens. Lysogeny might have particular importance in the spreading of genes among aquatic bacteria. Interestingly, most toxin and virulence genes as well as antibiotic resistance genes are prophage-derived. An example is the lysogenic filamentous phage CTXϕ of *Vibrio cholerae*, which encodes for chlorella toxin (Waldor and Mekalanos, 1996).

1.4 BACTERIOPHAGE PM2

Viruses have been predominantly classified by the nature of their nucleic acid, particle morphology, and host organism (http://www.ncbi.nlm.nih.gov/ICTV). In the first issue of the International Committee for Taxonomy of Viruses, six bacteriophage genera were presented, including T4, λ, ϕX174, MS2, and fd phage groups and one lonely orphan, newly isolated phage PM2 originating from the coastal seawater of Chile (Espejo and Canelo, 1968a; Wildy, 1971). PM2 was the first phage for which it was demonstrated that lipids could be a structural component of a bacterial virus (Camerini-Otero and Franklin, 1972). Bacteriophage PM2 is an icosahedral particle with an internal lipid bilayer and a highly supercoiled circular dsDNA genome. Due to these unique features it was classified into the *Corticoviridae* family in which it still is the only known isolate (Ackermann, 2000; Bamford and Bamford, 2003; see also Fig. 1).

The host range of PM2 is narrow; it infects *Pseudoalteromonas espejiana* BAL-31 (Gauthier *et al*., 1995). (Formerly the host was named *Pseudomonas* BAL-31 or *Alteromonas espejiana* BAL-31 (Chan *et al*., 1978; Espejo and Canelo, 1968b).) BAL-31 is a gram-negative marine bacterium and the source of the DNA exonuclease *Bal*31. *Pseudoalteromonads* are widespread in marine environments. They are strictly aerobic, polarly flagellated, rod-shaped, heterotrophic *Pseudomonas*–like bacteria originally classified as *Alteromonads* (Baumann *et al*., 1972). Later, the genus *Alteromonas* was divided into *Pseudoalteromonas* and *Alteromonas* (Gauthier *et al*., 1995).

Bacteriophage PM2 has been of interest for two reasons. The virion contains a membrane component, which has made this virus a model system for studies on membrane structure and biosynthesis. In addition, the genome is a small highly supercoiled circular dsDNA molecule ideal for studies on DNA topology. The PM2 genome has been widely used in numerous assays as a substrate.

1.4.1 GENOME

The PM2 genome is a circular 10 097 bp long dsDNA molecule with a 42-43% GC content (Espejo *et al*., 1969; Männistö *et al*., 1999). It contains the highest number of negative supercoils observed in a natural DNA molecule (Gray *et al*., 1971). The number of supercoils in the genome increases when the DNA is packaged into the virion compared to the free intracellular PM2 DNA (Espejo *et al*., 1971a; Ostrander and Gray, 1974). It has been shown that the purified PM2 genome can initiate a productive infection cycle when introduced into spheroplasts by transfection (van der Schans *et al*., 1971).

Determination of the complete nucleotide sequence of the PM2 genome revealed 21 open reading frames (ORF) potentially encoding for protein (Männistö *et al*., 1999). The nomenclature of PM2 proteins and genes/ORF is given by Männistö *et al*. (1999). If an ORF (named with a lowercase letter) has been shown to encode a protein, it is considered to be a gene and designated with Roman numerals. The protein products are named respectively with Arabic numerals with the prefix P. Currently, 13 ORF have been identified to have a function during the PM2 infection-cycle classifying them as genes (Männistö *et al*., 1999; 2003). Genes are clustered in the PM2 genome reflecting their function and organised into three operons; the early left operon (OEL), the early right operon (OER), and the late operon (OL) (Männistö *et al*., 2003). These are controlled by promoters P_{1207}, P_{1193}, and P_{5321}, respectively. Two early promoters P_{1207} and P_{1193} are organised back to back and located in the same region so that their sequences partially overlapp. The OEL operon is transcribed in the opposite direction than the two other operons.

Based on the finding that four virally-encoded transcription factors control the activity of PM2 promoters, a model for PM2 transcriptional regulation was proposed (Männistö *et al*., 2003). The promoters are repressed and activated in a temporal manner. Initially, the early genes of operon OEL (P_{1207}) are most probably transcribed producing gene product (gp) b and transcriptional repressors P15 and P16. P15 represses its own promoter (P_{1207}). Then the genes of operon OER (P_{1193}) for the DNA replication proteins are transcribed. Promoter P_{1193} is repressed by P15 and P16. Finally, the expression of the late operon (OL) is turned on by two transcription factors, P13 and P14. These proteins act concomitantly activating the production of viral structural proteins. Analysis of the P14 amino acid sequence revealed that it has a conserved zinc finger motif similar to the eukaryotic and archaeal transcription factors (Männistö *et al*., 2003; Qian *et al*., 1993; Wang *et al*., 1998). It is noteworthy that P14 is the first transcription factor of bacterial origin with a zinc finger motif similar to archaeal and eukaryotic TFIIS-type transcription factors.

The largest PM2 gene *XII* encoding protein P12 shares significant sequence similarity with the superfamily I group of replication initiation proteins (Männistö *et al*., 1999). This suggests that the PM2 genome is replicated via a rolling circle mechanism. Superfamily I consists of A proteins of bacteriophages such as ϕX174 and P2 and initiation proteins of cyanobacterial and archaeal plasmids (Ilyina and Koonin, 1992). On the basis of conserved ORI sequences among superfamily I replication initiation pro-

teins, the ORI of PM2 genome was mapped inside gene *XII* to nt 2253.

The early operon OEL is homologous to a *Pseudoalteromonas* sp. strain A28 plasmid pAS28 and is thought to be a moron (Kato *et al*., 1998; Männistö *et al*., 2003). The region in the PM2 genome encoding transcriptional repressors P15 and P16, and gp b, is similar to the regulatory region of plasmid pAS28 (Männistö *et al*., 1999; 2003). Moreover, the genes in both of the genomes are organised similarly, they are transcriptionally coupled and in both cases the orientation of the operon is opposite to the other operons in the genomes. The similarity in the DNA and amino acid sequences indicates that *Pseudoalteromonas* phage PM2 might have acquired these genes horizontally from a *Pseudoalteromonas* plasmid or other way around. Although plasmid pAS28 replicates using the rolling circle mechanism similar to PM2, the corresponding ORF in the plasmid does not share any similarity to PM2 gene *XII* encoding the replication initiation protein P12.

1.4.2 VIRION

The PM2 virion is an icosahedral particle containing a protein capsid and an internal lipid bilayer surrounding a dsDNA genome (Camerini-Otero and Franklin, 1972; Espejo and Canelo, 1968c). Based on electron microscopy (EM), small angle X-ray scattering (SAXS), and neutron diffraction studies the diameter of the particle is ~60 nm and the five-fold vertices have clear extensions (Espejo and Canelo, 1968a; Harrison *et al*., 1971; Silbert *et al*., 1969). The estimated mass of the particle (~45 MDa) is distributed among protein (~72%), nucleic acid (~14%), and lipid (~14%) constituents (Camerini-Otero and Franklin, 1975). The viral lipid composition (~64% PG, ~27% PE, ~8% neutral lipids, and small amount of acyl-PG) deviates from that of the host bacterium (Braunstein and Franklin, 1971; Camerini-Otero and Franklin, 1972; Tsukagoshi *et al*., 1976). The sedimentation coefficient and densities of PM2 virion in sucrose and CsCl are $s_{20,w}$=290S, 1.24 g/cm^3 and, 1.29 g/cm^3, respectively (Camerini-Otero and Franklin, 1975). The SAXS based model of the virion proposed three concentric layers in the particle i) an outer protein layer with a thickness of ~60 Å, ii) a lipid bilayer with a thickness of ~40 Å, and iii) a proposed nucleocapsid core with a diameter of 400 Å (Harrison *et al*., 1971). The native virion is stabilised by calcium (Espejo and Canelo, 1968a). Calcium is needed for the assembly of virions and can be replaced with strontium or barium (Snipes *et al*., 1974). It has been proposed that calcium is tightly bound to the coat protein (Schäfer *et al*., 1974). The morphology of PM2 virion resembles the tectiviruses such as PRD1 (Bamford *et al*., 1995; Grahn *et al*., 2003). However, PM2 has been classified to its own family mainly due to the lack of the ability to transform the internal membrane into a tubular structure. Also the host range and the nucleic acid type differ significantly between these two virus families.

Based on SDS-polyacrylamide gel electrophoresis (PAGE) and gel filtration of purified and disrupted PM2 virions, four different structural proteins, P1-P4, were assigned to the particle (Datta *et al*., 1971a). However, it has been presented that a higher number of structural proteins exists in PM2 virion (Brewer and Singer, 1974). Based on dissociation of the virus in the presence of different amounts of

urea the four proteins were assigned to the morphological elements of the virus: the vertex structure, outer protein coat, lipid bilayer, and nucleocapsid (Hinnen *et al*., 1974; Schäfer *et al*., 1974). Based on these assignments a structural model of bacteriophage PM2 was presented (Franklin, 1974; 1977; Franklin *et al*., 1976). This model remained in the literature and is depicted in Figure 2. It is also the only description of the structural organisation of the *Corticoviridae* family (http://www.ncbi.nlm.nih.gov/ICTV).

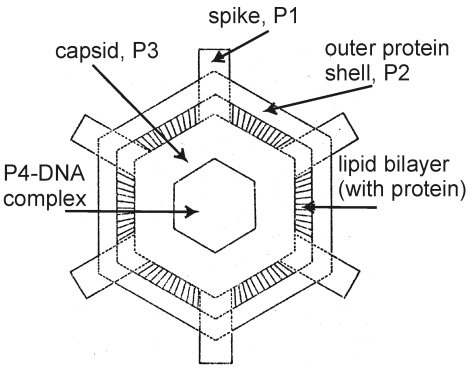

Figure 2. An early structural model of bacteriophage PM2. The names of PM2 structural proteins are according to the nomenclature given by Männistö *et al*. (1999). Modified from Franklin *et al*. (1976).

The structural organisation and locations of the structural proteins were described by Schäfer *et al*. (1974) as follows: "DNA and the nucleoprotein, polypeptide P4, are in the center of the virus. This nucleoprotein complex is enveloped by protein P3, which forms the icosahedral shell of the nucleocapsid core. Protein P1 forms the spikes and protein P2 the outer icosahedral shell of the virus. The phospholipid bilayer is sandwiched between the outer shell and the nucleocapsid core." Further support for the two-shell model was obtained from the "*in vitro*" assembly experiments by reversing the virion degradation steps. It was described that DNA, and purified proteins P3 and P4 were assembled into nucleocapsids similar to the isolated viral nucleocapsids (Schäfer and Franklin, 1975). In addition, infectious virions were reported to be assembled *in vitro* by combining nucleocapsids with phospholipids and proteins P1 and P2 (Schäfer and Franklin, 1975; 1978). Brewer and Singer (1974) did not support the two shell model, and they suggested that two major proteins form the outer layer and other minor proteins are associated with the viral membrane. In fact, it was later reported that the lipid-free nucleocapsids formed by P3, P4, and DNA do not exist, but the viral lipid bilayer is included in these isolated structures (Akutsu *et al*., 1980; Satake *et al*., 1980).

The calculated phospholipid content of PM2 is insufficient to form a complete bilayer (Camerini-Otero and Franklin, 1972). Based on the measured density of the PM2 lipid bilayer (0.30 e/Å^3) the membrane moiety comprises ~2/3 of lipid and the rest is protein constituents (Harrison *et al*., 1971). The phospholipids are distributed asymmetrically between the two leaflets; PG being enriched in the outer leaflet and PE in the inner one (Schäfer *et al*., 1974). The presence of increased amount of PG in the viral membrane compared to that of the host could be due to a higher affinity of viral proteins to negatively charged PG and/or geometric constraints due to the curvature of the membrane in the viral capsid. It has been speculated that neutral PE lipids have hydrophobic interactions with the nucleocapsid and the negatively charged PG make interactions with the positively charged protein P2 (Schäfer *et al*., 1974).

1.4.3 LIFE-CYCLE

The infection cycle of PM2 is relatively poorly known. PM2 is a lytic bacteriophage infecting a marine bacterium *P. espejiana* BAL-31 (Espejo and Canelo, 1968a). The viral DNA is synthesised during the entire infection cycle, whereas the cellular DNA synthesis is inhibited (Franklin *et al*., 1969). The virus replication takes place in association with the CM (Brewer, 1978a). Based on sequence comparisons and the nature of isolated replication intermediates, it is quite evident that the PM2 genome replicates via a rolling circle replication mechanism (Canelo *et al*., 1985; Espejo *et al*., 1971b; Männistö *et al*., 1999). The replication initiation protein is P12, which resembles the A protein of ssDNA bacteriophage ϕX174 (Baas and Jansz, 1988; Männistö *et al*., 1999). Three functional consensus motifs reside in the 30 nt long sequence surrounding the ORI site (van Mansfeld *et al*., 1980). The replication initiation protein functions as an endonuclease. It introduces a nick at the ORI site within its own coding sequence remaining covalently linked to the 5' end. The 3' end is extended by the DNA polymerase. After the DNA polymerase has synthesised one round, the resulting closed ssDNA circle serves as a template for RNA-primed lagging strand synthesis (Kornberg and Baker, 1992).

The viral genes are transcribed by the host RNA polymerase (Zimmer and Millette, 1975a). The DNA-dependent RNA polymerase of BAL-31 is a classic prokaryotic αββσ' holoenzyme (Zimmer and Millette, 1975b). The most efficient transcription is achieved when PM2 DNA is highly supercoiled (Richardson, 1974; Zimmer and Millette, 1975a). Viral mRNA is also synthesised by RNA polymerase of *E. coli* (Richardson, 1975). The formation of a stable complex between the polymerase and DNA is dependent on the number of supercoils in the PM2 DNA.

Early viral functions are under the control of two promoters (Männistö *et al*., 2003). The synthesis of the early proteins starts ~10 minutes p.i. and continues for ~25 minutes (Brewer and Singh, 1982). The late promoter is activated by two virally-encoded transcription factors (Männistö *et al*., 2003). The late proteins appear in the infected cells at ~25 min p.i. (Brewer and Singh, 1982). 21 putative virally-encoded proteins are produced during the infection-cycle (Männistö *et al*., 1999). At least 14 synthesised virus-specific proteins have been observed in the infected cells (Datta *et al*., 1971b). Only one peptide was found soluble in the cytoplasm, while the majority were membrane-associated proteins. Electron microscopic observations of infected cells revealed that the assembly of the virions takes place in association with the CM (Dahlberg and Franklin, 1970). The viral lipids are host-derived (Espejo and Canelo, 1968c). Studies on temperature-sensitive PM2 mutants indicated that empty membrane vesicles are produced in the absence of the coat protein (Brewer, 1976; 1978b). The progeny virions stay associated with the host membranes until ~60 minutes p.i., after which several hundreds particles are released by cell lysis (Cota-Robles *et al*., 1968; Franklin *et al*., 1969).

2 AIMS OF THE PRESENT STUDY

Bacteriophage PM2 is the only representative of the *Corticoviridae* family (http://www.ncbi.nlm.nih.gov/ICTV). At the time when this work was started, the latest studies on PM2 virology were published more than 10 years earlier. During ~16 years, starting from 1968 PM2 was under very intensive investigation. Due to the presence of the membrane in the phage particle, PM2 was used to study lipid biogenesis, protein-lipid interactions, and membrane structure. Unfortunately, the detailed characterisation of PM2 structural features was lacking. The consensus view from the literature was that the PM2 particle consists of four proteins, lipid components, and nucleic acid organised into two concentric protein shells having a lipid bilayer in between and enclosing the genome (Franklin, 1974; 1977; Franklin *et al*., 1976). It was also concluded that two minor proteins and the genome form a lipid-free nucleocapsid. There were reasons to reconsider the structural model of PM2. First, according to Brewer and Singer (1974) the virion contains more structural protein species than had been reported. Second, the arguments presented by Akutsu *et al*. (1980) and Satake *et al*. (1980) against the presence of a lipid-free nucleocapsid. Also Harrison *et al*. (1971) had concluded that the lipid bilayer contains protein species. Recently, the complete nucleotide sequence of the PM2 genome and its organisation suggested that the amount of PM2 structural protein species had been underestimated (Männistö *et al*., 1999).

The first aim of this study was to establish methods for production of highly infectious virus particles and identify the structural proteins forming the infectious virion. The second aim was to describe the structural organisation of PM2 using biochemistry and cryo-electron microscopy combined with image analysis. The PM2 infection-cycle is poorly understood. Specifically the initial stages of the virus infection have not been described. In addition there are no examples of penetration of a circular, highly supercoiled dsDNA residing inside lipid bilayer into a Gram-negative cell. Our attempt was to study the entry of PM2 into marine Gram-negative *Pseudoalteromonads*. These results together could refine the structure and functions of PM2 and establish the knowledge on the *Corticoviridae* family on a reliable basis.

The specific aims of the present study were

- To set up methods for virus propagation and particle purification to obtain highly infectious material
- To identify the viral structural proteins
- To describe the particle architecture
- To study PM2 entry

3 MATERIALS AND METHODS

Bacteriophage PM2 used in this study was obtained from the American Type Culture Collection (ATCC 27025-B1; Espejo and Canelo, 1968a). Bacterial strains and plasmids are listed in Tables 1 and 2, respectively. Experimental procedures are summarised in Table 3 and described in the original publications. The references for the published methods can be found in the articles.

Table 1. Bacterial strains used in this study

Bacteria	Relevant property or usage	Reference
Pseudoalteromonas		
espejiana BAL-31	PM2 host	(Espejo and Canelo, 1968b; Gauthier *et al*., 1995)
sp. ER72M2	PM2 host	I
sp. strain A28	Tested for virus sensitivity; Adsorption assay	(Kato *et al*., 1998)
nigrifaciens	16S rRNA comparison; Tested for virus sensitivity	(Gauthier *et al*., 1995; White, 1940)
atlantica	16S rRNA comparison; Tested for virus sensitivity	(Akagawa-Matsushita *et al*., 1992; Gauthier *et al*., 1995)
carrageenovora	16S rRNA comparison; Tested for virus sensitivity	(Akagawa-Matsushita *et al*., 1992; Gauthier *et al*., 1995)
undina	16S rRNA comparison; Tested for virus sensitivity	(Chan *et al*., 1978; Gauthier *et al*., 1995)
haloplanktis subsp. *haloplanktis*	16S rRNA comparison; Tested for virus sensitivity	(Gauthier *et al*., 1995; ZoBell and Upham, 1944)
haloplanktis subsp. *tetraodonis*	16S rRNA comparison; Tested for virus sensitivity	(Gauthier *et al*., 1995; Simidu *et al*., 1990)
luteoviolacea	16S rRNA comparison; Tested for virus sensitivity	(Gauthier, 1976; Gauthier *et al*., 1995)
Alteromonas macleodie	16S rRNA comparison; Tested for virus sensitivity	(Baumann *et al*., 1972; Gauthier *et al*., 1995)
PM2 resistant ER72M2 mutants	Adsorption assay	IV
Escherichia coli		
K12	16S rRNA comparison; Tested for virus sensitivity	(Carbon *et al*., 1979)
HB101	Adsorption assay	(Boyer and Roulland-Dussoix, 1969)
DH5α	Molecular cloning, protein expression, and source of peptidoglycan	(Sambrook and Russell, 2001)
HMS174(DE3)	Protein expression	(Studier and Moffatt, 1986)
Salmonella enterica LT2	16S rRNA comparison; Tested for virus sensitivity	(Chang *et al*., 1997)
Pseudomonas syringae pv. Phaseolicola	16S rRNA comparison; Tested for virus sensitivity	(Moore *et al*., 1996)

Table 2. Plasmids used in this study

Plasmid	Relevant property	Reference
pDS12	Expression vector, colE1 replicon, Ap^r	(Bujard *et al.*, 1987)
pJJ2	Expression vector, colE1 replicon, Ap^r	(Ojala *et al.*, 1993)
pET24	Expression vector, pMB1 replicon, Km^r	Novagen
pDMI	Contains the gene for *lac* repressor, p15A replicon, Km^r	(Certa *et al.*, 1986)
pRM203	pDS12 + PM2 gene *III*	IV
pRM206	pDS12 + PM2 gene *I*	IV
pRM301	pJJ2 + PM2 gene *VI*	IV
pRM315	pJJ2 + PM2 gene *IV*	IV
pRM318	pJJ2 + PM2 gene *VII*	IV
pRM319	pJJ2 + PM2 gene *V*	IV
pRM325	pJJ2 + PM2 gene *VIII*	IV
pRM607	pET24 + PM2 gene *II*	IV

Table 3. Methods used in this study

Method	Described and used in			
Amino terminal amino acid sequencing	I	II		IV
ATP measurements				IV
Computational analysis of DNA or protein sequences	I		III	IV
Cryo electron microscopy and image analysis			III	
Determination of 16S rRNA sequence	I			
Dissociation of phage particles		II	III	
Immunoprecipitation of phage particles	I	II		
Ion flux measurements and $\Delta\Psi$ determination				IV
Isolation of phage resistant ER72M2 cell lines				IV
Labeling of phage particles				IV
LC isolation		II		
LPS isolation				IV
Mass spectrometry			III	
Molecular cloning techniques				IV
Phage adsorption assay				IV
Phage lipid isolation and analysis		II		
PM2 growth and purification	I	II	III	IV
Polyclonal antiserum production	I	II		
Protease treatment of phage particles		II	III	
Protein concentration measurement	I	II	III	IV
Protein overexpression				IV
Protein purification		II		IV
Reconstitution of phage particles		II		
SDS polyacrylamide gel electrophoresis	I	II	III	IV
Transmission electron microscopy	I	II		IV
Western blotting	I	II		
Zymogram analysis and isolation of peptidoglycan				IV

4 RESULTS AND DISCUSSION

4.1 HOST BACTERIA - TWO MARINE GRAM-NEGATIVE *PSEUDOALTEROMONADS*

In addition to the original PM2 host *Pseudoalteromonas espejiana* BAL-31, another host bacterium, ER72M2, was isolated from East River, New York City, by Dr. Leonard Mindich. In order to identify ER72M2 we determined its 16S rRNA gene sequence (I; GenBank accession number AF155038). When it was compared with sequences in GenBank, the closest sequence similarities were with *Pseudoalteromonad* strains. The closest matches were to *Pseudoalteromonas nigrifaciens* (99.8%), *Pseudoalteromonas atlantica* (99.7%), *Pseudoalteromonas carrageenovora* (99.5%), and *Pseudoalteromonas espejiana* BAL-31 (99.5%; I, Table 1). Morphology and colour of ER72M2 colonies and the growth requirements distinctly differed from the other *Pseudoalteromonad* strains indicating that ER72M2 was a new *Pseudoalteromonas* isolate.

The sensitivity of various *Pseudoalteromonads* to PM2 was tested using a plaque-assay, but only ER72M2 and BAL-31 supported the growth of the virus indicating that the host-range of PM2 is narrow (I; IV). Since PM2 did not infect the other tested strains, the ability of the cells to support the virus reproduction was tested further by transfecting the cells with purified PM2 genome. It has been demonstrated that transfected PM2 genome can initiate the virus production in BAL-31 cells (van der Schans *et al*., 1971) and also in ER72M2 (IV). Interestingly, *Pseudoalteromonas* strain sp. A28 produced plaques after the transfected A28 cells were plated on a lawn of PM2 sensitive cells (IV). Other tested cells failed to support formation of plaques in this assay. Furthermore, we also showed that the binding of PM2 to A28 cell surface is prevented and that the PM2 entry-derived ion effluxes across the A28 cell envelope were not detectable, demonstrating that PM2 virion cannot penetrate the envelope of A28 (IV). Although A28 does not have the cell surface receptor for PM2, when introduced into A28 cell, the PM2 genome can initiate a productive infection cycle. This is in concordance with the observation that the maintenance region of the plasmid pAS28 originating from the A28 strain shares significant sequence similarity with the replication and regulatory region of PM2 genome (Kato *et al*., 1998; Männistö *et al*., 1999). So far there is no evidence of the presence of indigenous plasmids in PM2 host cells or a prophage state of PM2.

4.2 PRODUCTION OF VIRUS PARTICLES

4.2.1 VIRUS PROPAGATION AND INFECTION CYCLE

PM2 was propagated either on BAL-31 or ER72M2 cells in rich SB-media resembling seawater (I). Both hosts are thermosensitive, the optimal growth temperature (25-28°C) reported for BAL-31 (Espejo and Canelo, 1968a) was also the optimal for ER72M2. At 37°C growth of the cells is inhibited, but even at 4°C cells are slowly dividing (data not shown).

Although hosts grow well at temperatures under 20°C, the growth of the virus slows down at these temperatures. PM2 grows at temperatures between 22-30°C and 28°C is routinely used. Both host cells require sodium and magnesium for growth, but ER72M2 grows also in a medium containing less salt (I; Chan *et al*., 1978). However, the lower NaCl concentration in the growth medium affected negatively the quality of the purified virus particles. When PM2 was plated with the host cells using SB-soft agar, equivalent amounts of plaques were observed with both cells lines. The plaque count was independent of the host used to grow the virus. The size of the plaques is homogeneous on ER72M2, but varies on BAL-31.

To obtain a high number of phage particles, the growth of the virus was optimised in liquid SB-medium. The best results were obtained when logarithmically growing BAL-31 or ER72M2 cells (~6-7$\times10^8$ cfu/ml) were infected using a freshly made virus agar-stock (~1$\times10^{12}$ pfu/ml) with a multiplicity of infection (MOI) of 10, which yielded over 10^{11} pfu/ml of the lysate. The lysate titers were the same regardless of the host used for the propagation and comparable with previously reported BAL-31 lysates (Espejo and Canelo, 1968a; Franklin *et al*., 1969).

Under optimal conditions in SB media the lysis starts at ~60 min p.i. and is complete in ~80 min with both host cells. Thin-section electron microscopy of infected BAL-31 and ER72M2 cells revealed only few particles associated with the cell surfaces at 10 min p.i. (I; IV; see Section 4.7.1). The earliest detectable intracellular virus assemblies (at 50 min p.i.) were associating with the host CM, but no mature particles were observed in the cell interior (I). An infected ER72M2 cell released ~300 progeny virions. These results agree with the previous ones obtained with infected BAL-31 cells (Cota-Robles *et al*., 1968; Dahlberg and Franklin, 1970).

4.2.2 OPTIMISING THE PURIFICATION OF VIRUS PARTICLES

Sodium and calcium ions are needed for PM2 virion viability (I; Espejo and Canelo, 1968a; Snipes *et al*., 1974). In order to determine the optimal condition for virus storage as well as for particle purification, effects of different sodium and calcium ion concentrations on phage viability were tested. It appeared that the most critical ion for PM2 infectivity was calcium (I, Fig. 2). The virus preserved its infectivity in much lower salt concentration than earlier has been utilised (I; Hinnen *et al*., 1974). Thus, high ionic strength is not needed for the virion stability. The virus was stable even in 10 mM NaCl and 2.5 mM $CaCl_2$ (I). Also Snipes *et al*. (1974) reported that 1.5 mM Ca^{2+} ion concentration is needed to preserve virus infectivity. (The mechanism of inactivation in low ion conditions is described in Section 4.4.) Although high salt concentration (2.5 M) did not affect the phage viability, the combination of sucrose (~16%, w/v) and salt (>0.5 M) caused a loss of infectivity (I, Fig. 3). Moreover sucrose alone (concentration >20%, w/v) significantly inactivated PM2 (I, Fig. 4). Thus, higher than 20% concentration of sucrose during PM2 particle purification could not be used. Reason for the sensitivity of the virion to sucrose remained obscure.

We defined buffer conditions for PM2 purification and storage (I; 20 mM Tris, pH 7.2, 100 mM NaCl, 5 mM $CaCl_2$). Although viruses were stored in optimised buffer conditions or in SB-medium at +4°C, a significant decay of

the infectivity was observed. After one week of storage the titer was reduced to ~50%. PM2 stored at –20°C or –80°C is non-infectious regardless of cryo-protectants used. However, virus preparations supplemented with glycerol and stored in liquid nitrogen were reasonable stable (I).

Several purification methods have been described for PM2 (Hinnen *et al*., 1974; Salditt *et al*., 1972; Silbert *et al*., 1969). In our hands the recovery of infectious particles purified by these methods was low; the specific infectivity being $<1\times10^{11}$ pfu/mg of protein. The development of an optimal virus purification procedure was initiated based on the method by Hinnen *et al*. (1974). The new ER72M2 was chosen as host, since it had several advantages over BAL-31. During purification the yield and the quality of the virus specimen originating from ER72M2 were superior to those obtained with BAL-31 (I). The quality of the virus preparation was followed during the purification process by determining the specific infectivity and analysing the protein components in tricine-SDS-PAGE (I, Table 2 and Fig. 5a). The tricine-gel protocol (Schägger and von Jagow, 1987) was slightly modified to enable easier separation of small PM2 proteins (<10 kDa; I).

The recovery of infectious virus particles was improved when the following steps were optimised (I; II). i) The ER72M2 lysate was treated with DNase to decrease the viscosity due to the host chromosomal DNA. ii) The most critical step in the PM2 purification was the polyethylene glycol (PEG) precipitation (Yamamoto *et al*., 1970) of the particles from the lysate. Increasing the PEG concentration to 10% (w/v) and prolonging the centrifugation time during virus collection improved the yield from ~5% to ~40%. iii) Purification by rate-zonal centrifugation in a linear sucrose gradient (5-20%, w/v) in 20 mM Tris, pH 7.2, 1 M NaCl, and 10 mM $CaCl_2$ according to Hinnen *et al*. (1974) produced only a low amount of infectious virions. However, lowering the NaCl concentration to 100 mM increased the recovery of infectious particles by a factor of ten (I, Fig. 3). Infectious virions sedimented in one light scattering zone. Empty DNA-less particles have not been observed during purifications. Other light scattering zones observed in the gradient were host-derived. iv) PM2 virions equilibrated in sucrose (1.26 g/cm^3) were non-infectious regardless of the salts used, but other tested density gradient media, CsCl or iodixanol, did not inactivate the virus (I, Fig. 4). The optimised PM2 purification procedure included PEG precipitation, rate-zonal centrifugation in sucrose, and equilibrium centrifugation in CsCl or iodixanol (I; II).

This purification protocol for PM2 yields highly infectious, pure, and homogenous virus material with a specific infectivity of up to $\sim1\times10^{13}$ pfu/mg of protein (I, Table 2; II), which is approximately hundred fold higher than obtained with previously described methods. Similar high specific infectivities have been reported for ultra pure preparations of phage PRD1 (Walin *et al*., 1994) and ϕ6 (Olkkonen and Bamford, 1989). Analysis of the protein composition of the highly purified virus preparation by tricine-SDS-PAGE revealed in addition to the virally-encoded proteins (see Section 4.3.2) a protein band with the N-terminal amino acid sequence ISVNTXVTI. This sequence was not virus-derived and comparison to the databank did not reveal the origin of the protein. Based on the examination of the negatively stained virus preparation and the observation that the protein sedimented slightly differently than the virus particles, we concluded that the protein was host-derived flagellin. Isopycnic CsCl

density gradient centrifugation separates virus particles from the contaminating flagella.

4.3 PM2 VIRION

4.3.1 AN ICOSAHEDRAL VIRION WITH AN INTERNAL MEMBRANE BILAYER

In this study, the three-dimensional structure of PM2 at 12 Å resolution was solved using cryo-EM and image processing techniques (III; Baker *et al*., 1999). The material for cryo-EM was produced using the optimised purification method described above (I; II). Virions were vitrified immediately after purification to avoid dissociation. The PM2 virion appeared as an icosahedron with slightly convex facets. There were clear extensions (~7 nm) projecting out from the virion vertices (III, Fig. 2b-d), which agree with the previous observations (Harrison *et al*., 1971). The distance between the opposite facets was ~56.5 nm. Edge-to-edge and vertex-to-vertex dimensions were 59 nm and 63.5 nm, respectively. Negative-stain and thin-section EM of the virions revealed icosahedral particles with an average diameter of ~60 nm, consistent with cryo-EM data (II, Fig. 1a,b; III, Fig. 2). Densities of the virion in sucrose and in CsCl were determined to be 1.26 g/cm^3 and 1.28 g/cm^3, respectively (I). These densities and diameters of the virion are in agreement with the previously reported measurements (Camerini-Otero and Franklin, 1975; Espejo and Canelo, 1968c).

The central section through the PM2 density map showed clearly that the outer capsid, giving the strongest density, surrounds concentric layers with weaker densities (III, Fig. 2b). These different layers of the virion were also apparent in the calculated radial density profile (III, Fig. 3b). The outermost layer (between radii ~32-39 nm) was the spike consisting of protein P1 (see Section 4.4.1). The layer with the strongest density (between radii ~24-32 nm) was interpreted as the protein capsid formed of protein P2 (see Section 4.4.2). The lipid bilayer (between radii ~19-24 nm) was assigned to the two density peaks under the capsid. Three concentric layers (between radii ~12-19 nm) were assigned to DNA. At lower radii the layers were less defined due to the reduced icosahedral order. The data correspond well to the previously presented SAXS-model of the PM2 particle (Harrison *et al*., 1971). The positions of the capsid and the membrane were equivalent.

The different parts of the PM2 structure are not equally defined: the highest resolution (8.4 Å) was assigned to the capsid region, and the resolution of the internal portion of the particle as well as the spike was higher than 12 Å (III, Fig. 3). We interpret this variation to represent different degrees of order in the structure. The membrane region consists of a lipid bilayer and membrane proteins (see Section 4.5.1). Thus, it would be expected to contain less ordered components than the capsid region.

4.3.2 STRUCTURAL PROTEINS

The conclusion from the previous PM2 literature was that four structural protein species build up the PM2 virion (Datta *et al*., 1971a). For the analysis of the PM2 structural proteins, proteins in purified virus preparations with high specific infectivity (~1×10^{13} pfu/mg of protein) were separated in tricine-SDS-PAGE gels (I, Fig. 5a). All detected protein bands were subjected to N-terminal amino acid sequencing and mass spectrometric (MS) analyses. The obtained N-terminal peptides were compared to the translated PM2 genomic sequence (I, Fig. 5b; Männistö *et al*., 1999) and to the protein database. We observed that nine determined N-terminal sequences matched the putative protein products of PM2 ORF and were identified as proteins P1-P9 (I; II). MS analysis of the tryptic peptides obtained from the position of the major capsid protein in the SDS-PAGE gel revealed three specific peptides, which matched ORF j. This newly found protein product was named P10 (III). The only detected nonviral protein in the virus preparation was host-derived flagellin. The molecular masses of proteins P1-P10 range from 37.5 to 3.7 kDa and the corresponding genes are *I-X*.

Previously described four structural proteins I-IV (Datta *et al*., 1971a; Hinnen *et al*., 1974; 1976) or alternatively sp43, sp27, sp13, sp6.6 (Brewer, 1976) were identified. These were renamed P1–P4 to maintain the previous numbering (Datta *et al*., 1971a). Brewer and Singer (1974) described two additional PM2 structural proteins, which could not be assigned to proteins defined by us. Proteins P5 - P8 were named according to their mobility in tricine-SDS-PAGE, protein P5 having the highest molecular mass (I, Fig. 5a). Eventually the most recently identified proteins were designated as P9 and P10 (II; III). The determined N-terminal amino acid sequences were equivalent to the protein sequences deduced from the PM2 genome except for the N-terminal amino acids of proteins P6 and P9 (I; II). The first methionine of protein P6 is removed after translation and gene *IX* starts with TTG initiation codon, which encodes leusine. This amino acid has been replaced with methionine residue in P9.

Currently 15 PM2 genes (*I-X*, *XII-XVI*) have been characterised encoding protein (I; II; III; Männistö *et al*., 1999; 2003). PM2 genes *I-X* coding for structural proteins comprise ~50% of the coding capacity of the genome (Fig. 3). Genes *I-VIII* and *X* belong to the late operon, OL (Männistö *et al*., 1999; 2003). This operon also includes small ORF k and l, which have not been so far shown to encode structural proteins. Gene *IX* belongs to the early right operon (OER) being presumably produced before the other structural proteins. Transcription of genes *I-VIII* and *X* in the OL operon is activated by two viral transcription factors, P13 and P14 (Männistö *et al*., 2003).

Protein P9 contains an ATP/GTP-binding consensus site (II; Männistö *et al*., 1999). Other PM2 structural proteins do not have sequence similarity to any proteins in the protein databank. Based on computer analysis of the amino acid sequences of the PM2 structural proteins (using TMPRED, TMHMM, and DAS), P3–P8 and P10 contain putative hydrophobic helices (I; III; Cserzo *et al*., 1994; Hofmann and Stoffel, 1993; Krogh *et al*., 2001; Männistö *et al*., 1999; Rost *et al*., 1996; von Heijne, 1992). Proteins P6, P10 and the gp h contain putative Ca^{2+}-binding sites (Männistö *et al*., 1999).

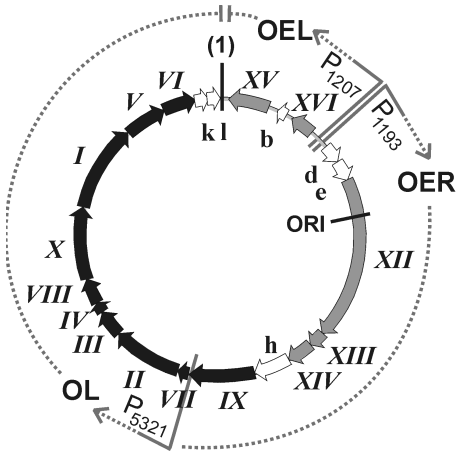

Figure 3. PM2 genome. The nucleotides of the circular genome are numbered starting from the unique *Eco*RII restriction site proceeding in the direction in which most of the ORFs are transcribed as described by Männistö *et al*. (1999). The genes marked by Roman numerals and the ORF by lowercase letters are visualised as arrows indicating the direction of transcription. Genes encoding structural, non-structural proteins, and ORF are coloured black, grey, and white, respectively. The genome is organised in three operons: the early left, the early right, and the late operon named OEL, OER, and OL, respectively. The arrows with dashed lines show the mRNA start sites for the three promoters (P). The origin of replication (ORI) is indicated.

4.4 CAPSID

Calcium ions are a requisite for the PM2 virion (Espejo and Canelo, 1968a; Snipes *et al*., 1974). In this study it was shown that Ca^{2+} ions control capsid stability and uncoating of the virion. It was found that below 2.5 mM $CaCl_2$, infectivity of the virions was significantly reduced (I). Further analyses revealed that Ca^{2+} depletion triggered the dissociation of the outer capsid (II, Fig. 2b). Analysis of the virion dissociation products allowed us to identify the capsid components: the spike protein P1 (37.5 kDa) and the major coat protein P2 (30.2 kDa; II). It has been estimated that P2 and P1 together account for ~40% of the protein mass in the PM2 virion. The analysis was consistent with the previous description of the capsid (Brewer and Singer, 1974; Hinnen *et al*., 1974; Schäfer *et al*., 1974). The removal of soluble proteins P1 and P2 from the virion resulted in aggregation of the rest of the viral material. Also freezing and thawing completely removes the protein shell (II, Fig. 2b; Brewer and Singer, 1974). Moreover, even during storage under optimised conditions, similar dissociation was observed over time indicating the metastable nature of the PM2 particle. In conditions where Ca^{2+} were present but NaCl was omitted the virus titer was reduced due to partial removal of the vertices (II, Fig. 2b).

Proteins P1 and P2 can be purified from virions in a soluble form. The purified proteins P1 and P2 were used to raise polyclonal antisera (II). The obtained antibodies were used in virus aggregation and neutralisation assays. Viruses treated with antiserum against P2 aggregated and made virus-multimers confirming the surface location of P2 (II, Fig. 3). However, antiserum against protein P1 did not neutralise viruses.

4.4.1 PROTEIN P1 FORMS RIGID PENTAMERIC SPIKES

There are obvious brush-like protrusions at the five-fold vertices of the PM2 virion (Harrison *et al*., 1971). Three-dimensional image reconstruction of the PM2 virion revealed that the vertices are occupied by prominent pentameric protein complexes (III, Fig. 2b-d). The vertex structure is shaped like a hand with well-defined five fingers forming a distal domain, which is attached to a central domain. The base of the vertex structure, a proximal domain, is embedded in the capsid (see below).

Protease treatments were used to probe the accessibility of the proteins on the virion surface. It was possible to produce particles with different protein compositions using proteinase K or bromelain treatment (II, Fig. 2). After protease treatment the particles had negligible infectivity and they sedimented faster than the virions. SDS-PAGE analysis of purified particles revealed that only protein P1 was susceptible to proteolysis resulting in particles with truncated peptides. The cleaved peptides were identified to originate from the N-termini of P1 molecules (II). Three-dimensional difference imaging between the PM2 virion density map and that of either bromelain or proteinase K - treated particles revealed the domains of the P1 protein. Mass spectrometric analyses were use to determine the bromelain and proteinase K cleavage sites on P1 defining the boundaries between the domains (III). It appeared that the cleavages occurred between the predicted secondary structure elements. After bromelain treatment a ~6.4 kDa N-terminal fragment of P1 remained with the virus defining the wrist domain interacting with the P2 capsid. For proteinase K digested particles, a ~17.4 kDa N-terminal P1 fragment was identified. This fragment includes the proximal and central domains devoid of the distal domain. These masses correspond well to the mass estimates from the SDS-PAGE analysis (II). Thus, the distal 20.1 kDa C-terminal domain of P1 (Val159-Thr335) is exposed to the medium and is essential for infectivity.

A major portion of the spike protrudes from the capsid (III, Fig. 2d). There are 60 copies of P1 monomers (37.5 kDa) per virion and the mass of the pentameric P1 is 187.5 kDa. This mass accounts for the density observed at virion vertices in the three-dimensional virion density map. Segmentation of the P2 trimers from the PM2-native reconstruction defined the boundary of the pentameric spike base (III, Fig. 2c, 5a–c). Moreover, the bases of the spike can readily fit in the five-fold holes in the P2-shell. Thus, the vertices are occupied by pentameric spikes formed entirely of P1. Based on sequence analyses the PM2 spike protein P1 belongs to the class of α/β-proteins with no similarity to known proteins in Protein Databank (III; Rost and Sander, 1993).

Gel filtration, sedimentation, and cross-linking experiments showed that P1 is a monomer in solution (II, Fig. 4). Behaviour in the sedimentation assay and size-exclusion chromatography strongly suggests an elongated shape for isolated P1. However, in the virion, radially orientated P1 monomers form pentameric complexes with interactions occurring along the length of the proximal and central domains. The interactions between P1 monomers seem to be weak and other factors are needed for pentamerisation. Assembly of the spike proteins into the P2-shell may lead to the multimerisation.

4.4.2 PM2 CAPSOMERS ARE ORGANISED ON A NOVEL PSEUDO T=21 LATTICE

The major components of the PM2 capsid are the P2 trimers (II, Fig. 4). Based on sequence analysis, P2 belongs to the class of α/β-proteins (III; Rost and Sander, 1993). According to the size exclusion chromatography and sedimentation analysis the P2 trimer is a compact complex. Surface presentation of the PM2 virion three-dimensional reconstruction at 8.4 Å resolution (for the capsid) revealed protrusions clustering into three-fold and local six-fold coordinated positions (III). The protrusions were assigned to P2 trimers resolving the organisation of the PM2 capsomers. Three P2 monomers pack closely together forming a trimer (3×30.2 kDa) with a pseudo-hexagonal shape (III, Fig 4a). The mean height and width of a trimer are ~50 Å and ~90 Å, respectively (III, Fig. 4f). The hexagonal shape of the trimer agrees well with negatively stained images of isolated viral donut-shaped P2 trimers having a diameter of ~7 nm (II). The capsomers are organised in a pseudo T=21 icosahedral lattice skewed to the right (*dextro*; III, Fig. 4b). Each of the 60 asymmetric units is composed of ten P2 monomers and one monomer of P1 occupying the vertex. Thus, the copy-number of P2 is 600, which agrees well with the previous estimate (Harrison *et al*., 1971). When rendered at 4σ above the mean density, the boundaries between the P2 monomers could be defined (not shown). A P2 monomer consists of two distinct domains (P and Q) giving the trimer its pseudo-hexagonal shape (III, Fig 4d). The P domain is slightly higher than the Q domain, otherwise they appear to be similar, although any duplication can not be found in the P2 amino acid sequence. The pseudo T=21 capsid lattice arrangement is unique and has not described previously for other viruses. The PM2 capsid architecture some what resembles the pseudo T=25 capsid organisation of PRD1 (Butcher *et al*., 1995). The pseudo T=25 capsid lattice is constructed of 240 copies of the major coat protein trimers with pseudo-hexagonal shape forming the facets and 12 copies of protein complexes residing at the vertices. A notable difference is that the homopentameric vertex structure of PM2 deviates from the vertices of PRD1, which are composed of several different protein species (II; III; Rydman *et al*., 1999; Xu *et al*., 2003).

Icosahedral viruses (T>1) have developed various strategies to employ identical polypeptides to occupy different environments, while forming a continuous protein shell. In PM2 P2 trimers 1-4 occupy four positions with chemically different environments (III, Fig. 4b,c). Type 1 trimers circle the five-fold vertices and type 3 trimers reside at the three-fold axes of symmetries. Type 2 and 4 trimers are situated on both sides of the two-fold axes. The resolution obtained (8.4 Å) allowed putative α-helices to be seen on the membrane side of the P2 trimers (III, Fig. 4e,f). The different composition and orientation of the α-helices in P2 trimers occupying different positions reflect conformational switching. Similarly, the X-ray structure of SV40 revealed that capsid protein pentamers have either two or three α-helices depending on the location of the pentamer on the capsid surface lattice (Liddington *et al*., 1991). The most significant difference between the PM2 trimers is seen at the bottom of the adjacent trimers 2 and 4. These trimers are connected to the underlying

membrane through strong densities (anchors), which are described in section 4.5.2 (III, Fig. 2b and 4e,g).

In addition to the anchors, other capsid stabilising features like calcium binding sites, α-helices, or accessory glue proteins might function to hold this pseudo T=21 capsid together. Although the capsid protein P2 and the spike protein P1 do not contain apparent calcium binding sites, the uncoating of the virion is regulated by Ca^{2+} proposing the presence of Ca^{2+} binding sites in the PM2 capsid (II). Tenfold molar excess of EGTA to remove calcium ions reduced the phage titer only by ~50%, but the corresponding amount of EDTA did not have any effect on virion stability (I). Thus, calcium ions seem to be tightly bound. The best candidates for binding calcium are membrane proteins P6 and P10 and the protein product of ORF h with predicted putative calcium-binding motifs (Männistö *et al*., 1999). It has been proposed that P2 binds calcium (Schäfer *et al*., 1974), and it is also noteworthy that P2 solubility is increased by calcium ion chelation (J.T. Huiskonen and S.J. Butcher, unpublished). Thus, Ca^{2+} ions might be located at the P2 trimer interfaces favouring the assembly state. It has been shown for several viruses that calcium ions play a role in the capsid assembly and stability. These examples include the outer capsid proteins (VP4 and VP7) of rotavirus, (Ruiz *et al*., 1996), the intermediate shell of bacteriophage ϕ6 protein P8 (Olkkonen *et al*., 1991), and SV40 capsid (Brady *et al*., 1977; Stehle *et al*., 1996).

Flexible portions of major capsid proteins like in tomato bushy stunt virus (TBSV; Olson *et al*., 1983) and polyoma virus (Stehle *et al*., 1996), ordered regions of nucleic acid like in Flock House virus (Fisher and Johnson, 1993) or glue proteins/minor capsid proteins like in adenovirus (Stewart *et al*., 1991) and PRD1 (Rydman *et al*., 2001; San Martín *et al*., 2002) are used to stabilise the lattices. The membrane facing surface of the PM2 major capsid protein trimers have conformational variation as seen in different compositions and positions of the α-helices (III, Fig. 4e,f). In many viruses alternative conformations of the N- and/or C-termini of major capsid proteins stabilise the protein shells, like in SV40 and HK97 (Liddington *et al*., 1991; Wikoff *et al*., 2000). This might also be the case in PM2 trimer stabilisation. In addition to the putative N-/C-terminal P2 contacts the N-terminal wrist domains of the spike protein P1 embedded to the P2 shell may function as glue. It is not excluded that PM2 capsid contains small additional proteins.

4.5 LIPID CORE – A DNA-FILLED PROTEINACEOUS MEMBRANE VESICLE

Two different models have been presented for the organisation of the internal part of PM2 virion. The previous PM2 model is based on studies by Franklin and his collaborators (Franklin, 1974; 1977; Franklin *et al*., 1976). This model suggested that the lipid bilayer is located between two protein shells: the outer shell formed of protein P2 and the inner shell formed of protein P3 (Fig. 3; Schäfer *et al*., 1974). Predominantly based on particle dissociation studies with urea, the previously identified proteins P1-P4 were localised to the virion and it was proposed that a distinct nucleocapsid (composed of proteins P3, P4, and the genome) resides under the membrane (Hinnen *et al*., 1974; Schäfer *et al*., 1978). The current model based on the results of this study is described below (I; II; III).

4.5.1 DEFINING THE LIPID CORE COMPONENTS AND THEIR ORGANISATION

A central section of the PM2 cryo-EM based density map visualised an apparent 4 nm thick internal lipid bilayer (III, Fig. 2b). In cryo-EM micrographs smaller, round dissociation products with a diameter of ~48 nm were detected in addition to virions (III, Fig. 2a). These internal membrane vesicles were isolated from PM2 virions by removing the protein capsid with 2 - 4.5 M urea as previously described (II; Hinnen *et al*., 1974; Schäfer *et al*., 1978). The diameter of isolated vesicles agrees with the position of the bilayer in the virion density map (II). These membrane vesicles were soluble only in the presence of urea. The products of virions dissociated with urea were separated in sucrose gradients containing urea. The protein, lipid, and DNA contents of the dissociation products were analysed by SDS-PAGE and thin layer chromatography (II, Fig. 5b). Phospholipids PG and PE forming the majority of the PM2 lipid bilayer, the viral genome, and structural proteins P3-P9 (and most probably P10) were detected in the isolated subviral particles. Proteins associated with the lipid bilayer were also analysed from viral membranes obtained by freeze-thawing or calcium depletion experiments: proteins P3-P10 were localised in the membrane fraction (II, Fig. 2b; III, 1b). The subviral particles lacking P1 and P2 were designated lipid cores (LC). Urea-isolated LC with two different buoyant densities were detected (1.15 and 1.19 g/cm^3); the lighter contained smaller amount of protein P5, but otherwise their protein composition was similar. Different phospholipid contents of the LC might also explain the density difference.

By subtracting the P2 shell density, from the PM2 virion density the surface of the LC can be visualised (III, Fig. 2d). The PM2 membrane is asymmetric; the inner membrane leaflet is denser than the outer leaflet (III, Fig. 2b, 4g). The circular dsDNA genome resides next to the inner membrane leaflet. The increased order of the inner leaflet might be a consequence of the close association with the genome. PM2 phospholipids are distributed asymmetrically between the two leaflets; PG being enriched in the outer membrane leaflet (Schäfer *et al*., 1974). This could be explained by the specific interactions between PG mole-

cules and the membrane proteins, similarly as observed in bacteriophage PR4 (Davis and Cronan, 1985). However, the enrichment of PG in the PR4 membrane does not seem to be a prerequisite for the assembly of infectious particles (Vanden Boom and Cronan, 1988). The asymmetric distribution of phospholipids may also be a consequence of geometrical constrains (de Kruijff, 1987; 1997).

Only the outermost concentric DNA layers can be seen in the icosahedrally-averaged PM2 density map. The average distance between the phospholipid head groups and the inner leaflet to the DNA phosphates is ~17 Å. Concentric rings of DNA have been observed also in capsids of other dsDNA bacteriophages and herpesviruses (Booy *et al*., 1991; Cerritelli *et al*., 1997; Olson *et al*., 2001; San Martín *et al*., 2001). The spacing between the outermost adjacent DNA layers in PM2 is unequal, which is also seen in bacteriophage PRD1 (San Martín *et al*., 2001). Calculations based on the genome size and the LC interior volume indicate that the PM2 genome is less densely packaged (0.35 bp/nm^3) than that of tailed bacteriophages or herpesviruses, but similar to the PRD1 genome (III; Casjens, 1997).

According to the previous structural model of PM2, the first layer of density below the membrane (radius of 18.5 nm) was suggested to be the inner protein shell formed of P3 (see III, Fig. 3b; Harrison *et al*., 1971; Hinnen *et al*., 1974; Schäfer *et al*., 1974). This model also proposed that the lipid bilayer could be stripped off, leaving an intact lipid-free nucleocapsid (Hinnen *et al*., 1974; Schäfer *et al*., 1978). In this study we present a different interpretation for this layer. No evidence for distinct lipid-free nucleocapsid was observed (II; III). Our data agree well with the results of Satake *et al*. (1980) who showed that 95% of the viral phospholipids are associated with isolated LC. According to Akutsu *et al*. (1980) and Satake *et al*. (1980) a lipid-free nucleocapsid does not exist, but the lipids are found in the form of a bilayer both in the virion and the LC. Furthermore, SAXS analysis of the PM2 membrane demonstrated that proteins occupy ~1/3 of the membrane volume (Harrison *et al*., 1971). This is consistent with our analysis, since secondary structure predictions identified a putative transmembrane helix in proteins P3-P8 and P10, which associate with the isolated LC (II; III; Männistö *et al*., 1999). Thus, these proteins are likely to be partially embedded in the viral membrane. In the case of protein P9 no transmembrane regions were detected and its incorporation to the LC is most probably mediated by protein-protein interactions. Although protein P3 is the major LC-protein, it is more likely to be embedded into the lipid bilayer, rather than forming a continuous shell. The observation that the recombinant protein P3 expressed in *E. coli* is insoluble and found in the membrane fraction of the cells also supports a membrane location for P3 (IV). A putative candidate for a protein constituent residing in the interior of the virion is the small protein P4, which supposedly binds DNA (Marcoli *et al*., 1979; Satake *et al*., 1981). Proteolytic treatment of isolated LC produced pleomorfic membranes containing only P4 (II). Thus, P4 might be located completely inside the LC as previously has been proposed (Armour and Brewer, 1990; Hinnen *et al*., 1976). Although the other LC-associated proteins were cleaved with trypsin in isolated LC (II), small domains of these proteins could possibly reside inside the LC. As a conclusion, the density underneath the membrane could consist of both protein and DNA closely juxtaposed to the membrane (III).

4.5.2 ANCHORS LINK THE MEMBRANE TO THE CAPSID

Although the isolated LC seem to be spherical, the membrane in the virion follows the curvature of the icosahedral capsid (II; III). Underneath the five-fold vertices the membrane is more rounded than the interior of the protein capsid (III). Therefore, the icosahedral shape of the membrane vesicle is imposed by its interactions with the P2 capsid. A similar phenomenon is seen also in PRD1, where the internal membrane also follows the shape of the icosahedral capsid (Butcher *et al*., 1995).

In all of the membrane-containing virus structures examined so far, there appear to be connections between each of the major capsid protein molecules and the membrane. Examples include the P3 α-helical contacts in PRD1 (San Martín *et al*., 2002), the E2 transmembrane helices in Semliki Forrest virus (SFV; Mancini *et al*., 2000) and the M and E α-helices in dengue virus (Kuhn *et al*., 2002; Zhang *et al*., 2003). In this respect, the connection between the PM2 membrane and the capsid is different. The three-dimensional reconstruction of the PM2 virion revealed that near the two-fold axis of symmetry the membrane is brought together with the capsid by 60 anchors (III, Fig. 2b and 4g). Each anchor is most likely formed by a bundle of α-helices, which extend from the capsid to the membrane under the type 2 and 4 trimers of the adjacent facets. Thus, only a subset of 120 P2 polypeptides is linked to the membrane. P2 is most likely not connected to the membrane, since the protein capsid can be removed from the virion exposing the intact membrane surface (II). Moreover, the P2 amino acid sequence does not contain any predicted transmembrane helices. Furthermore, the density forming the anchors is not part of the averaged P2 trimer (III, Fig 4f). The most probable candidates for anchor proteins are the LC-associated proteins such as protein P10 (29 kDa), which could readily account for the anchor density.

4.5.3 IS THE LIPID CORE AN ASSEMBLY INTERMEDIATE?

Does the disassembly product, the LC, have a real biological function? Previous analyses of temperature-sensitive PM2 mutants identified an assembly intermediate apparently similar to the LC (Brewer, 1978b; 1979). These mutants had defective capsid formation and the DNA packaging was blocked producing only virus-sized empty membrane vesicles. This indicates that PM2 membrane vesicle formation is not dependent on the presence of the major capsid proteins. Thin section EM of PM2 infected cells showed viral assembly intermediates smaller than progeny virions lining with the CM (Cota-Robles *et al*., 1968; Dahlberg and Franklin, 1970). This is consistent with the idea that LC is an assembly intermediate. The majority of the proteins synthesised during PM2 infection are membrane-bound (Brewer and Singh, 1982; Datta *et al*., 1971b). Thus, the CM containing the viral proteins could acts as an assembly site for the LC.

There are no examples of how a circular supercoiled dsDNA molecule could be encapsidated inside the viral lipid bilayer. All described encapsidation systems of dsDNA bacteriophages proceed via a procapsid state including also the membrane-containing bacteriophage PRD1 (Bamford *et al*., 1995; King and Chiu, 1997). There is no evidence so far for an empty PM2 pro-

capsid. It is intriguing how PM2 has solved the packaging puzzle. The intracellular, newly replicated PM2 genome is supercoiled as the packaged DNA in the virion (Ostrander and Gray, 1974). The only encapsidation system for highly supercoiled circular dsDNA is that described for papovavirus SV40. The SV40 genome is first precondenced and then surrounded by the major capsid proteins (Gordon-Shaag *et al*., 2002). The presence of the putative packaging ATPase P9 in the PM2 LC suggests that energy is required for packaging (II). Is the LC assembled around a condenced genome like in SV40 or is the circular dsDNA packaged into a preformed empty LC? Brewer (1976) favoured the latter option based on the finding that virus-sized membrane vesicles are formed without DNA or scaffolding protein. Thus, the membrane vesicle containing integral membrane proteins could wrap around the circular supercoiled genome at the host CM. Assuming that the LC is an assembly intermediate, P1 and P2 are subsequently co-assembled on the LC surface. The most potential candidates for the shell nucleation are the anchor pairs at the two-fold axis of symmetry.

The packaged nucleic acid in the bacteriophage head is highly pressurised (Casjens, 1997; Smith *et al*., 2001). Thus, the capsid must resist an extensive force derived from the packaged DNA. PM2 DNA-filled LC can be isolated suggesting that they can withstand any forces that may have arisen during DNA encapsidation. The supercoiling of the DNA might decrease the pressure against the LC wall.

4.6 'RECONSTITUTION' OF THE PM2 VIRION

An *in vitro* reconstitution of the PM2 virion using purified viral components have been described by Schäfer and Franklin (1975; 1978). The assembly experiments were carried out by combining separated viral structural proteins, nucleic acid, and phospholipids obtained from urea-dissociated virions. It was reported that PM2 nucleocapsids were assembled from denatured proteins P3 and P4, and from the viral genome (Schäfer and Franklin, 1975). Subsequently, combining P1, P2, PE, and PG with reconstituted or isolated nucleocapsids was reported to produce infectious virions (Schäfer and Franklin, 1975; 1978). Criticisms against these experiments have been presented. According to Satake *et al*. (1980) isolated nucleocapsid contained 95% of the viral phospholipids and the viral lipids could not be removed from the nucleocapsids. Knowing that the PM2 particle consists at least of ten different structural protein species (I; II; III), it is puzzling to imagine how the infectious virion could be assembled from the described pure components. Therefore, we repeated the reconstitution experiments using these newly defined viral components and tried to assemble a protein shell around the LC.

As mentioned above, treatment of PM2 virions with 4.5 M urea results in the removal of proteins P1 and P2 from the particle thus exposing the LC (II, Fig. 5). For reconstitution the dissociation was carried out in the presence of 20 mM 2-mercaptoethanol as described by Schäfer and Franklin (1975; 1978). In 4.5 M urea P1, P2, and LC are soluble. To repeat the experiments described earlier we lowered the urea concentration gradually by dialysis. The dialysed material was analysed by rate zonal centrifugation revealing that the depletion of urea from the reconstitution mixture resulted in aggregation of the viral material.

However, when 0.5 M urea was left in the reconstitution mixture some P1 and P2 were assembled on the LC producing soluble non-infectious particles (II, Fig. 6). The amount of assembled P1 and P2 on the LC was significantly lower than in the virions.

Also the ability of P1 and P2 obtained from freeze-thawed virions to assemble on urea-isolated LC was tested. P1 and P2 obtained by freeze-thawing precipitated when the urea concentration exceeded 1 M and we were restricted to use <1 M urea concentrations in these reconstitution experiments. Combining P1 and P2 with isolated LC resulted in non-infectious aggregates of viral components. Addition of either bovine serum albumin as proposed by Schäfer and Franklin (1975) or PEG did not result in any specific assembly products. In conclusion, the repeated reconstitution experiments were not successful and did not produce infectious virions in contradiction to previously published results.

4.7 BACTERIOPHAGE PM2 ENTRY

4.7.1 PHAGE ADSORPTION TRIGGERS DISSOCIATION OF THE VIRION EXPOSING A FUSION-ACTIVE LIPID CORE

Bacteriophage PM2 has to deliver its genome into the host cell cytoplasm to initiate the infection-cycle. There is no description of the events during the penetration of phage PM2 into its host cells. It is known that purified PM2 DNA can initiate an infection cycle when introduced into BAL-31 cells by transfection (van der Schans *et al*., 1971). Also ER72M2 and A28 spheroplasts can be infected with purified PM2 DNA (IV). Thus, only the PM2 genome has to enter the cell, no parental protein or lipid components are needed to carry out the reproduction cycle.

On the basis of binding assays, hundreds of PM2 particles were bound to the cell surface of the two marine Gram-negative *Pseudoalteromonads* demonstrating a high abundance of PM2 receptor molecules on the sensitive cells (IV, Fig. 1b). This correlates well with the high rate of the phage binding to the cells (IV, Fig. 1a). As mentioned above (Section 4.1) other tested *Pseudoalteromonads* do not support PM2 growth, although they are closely related to the hosts (I). This indicates that the receptor molecule/complex is not a common surface structure of *Pseudoalteromonads*. In order to identify the PM2 receptor, virus binding inhibition in the presence of LPS and the soluble and insoluble fractions of sensitive cell were analysed (IV). No inhibition of virus binding was observed. The reason for this may be that disruption of the cell envelope inactivates the receptor, which might be functional only when organised properly on the cell surface. This is the case in the PRD1 non-extractable receptor-complex (Daugelavičius *et al*., 1997b). Moreover, an extensive protease treatment of the sensitive cells did not affect the virus binding (IV).

Proteins P1 and P2 on the surface of the PM2 virion encounter the receptor on the host cell. In the present study we purified recombinant proteins P1 and P2 as well as the corresponding proteins obtained from disrupted PM2 particles (II; IV). The proteins were added into phage adsorption assay to test their capability to interfere with the phage binding to the sensitive cells. It was shown that the P1 monomers (recombinant and virus-derived) prevented phage adsorption, while P2

trimers had a negligible effect. Thus, the specific binding to the cellular receptor is mediated by protein P1 (IV).

The lability of the interactions in the PM2 capsid might assist in initiating DNA delivery upon receptor recognition. Association experiments of the ^{35}S-methionine- and the ^{33}P-labeled PM2 virions to host cells revealed that receptor binding is followed by release of virion components (IV, Fig 2). The major coat protein P2 was found to be soluble after the phage adsorption. In addition to this, a fraction of the viral DNA was released. We propose that binding of PM2 to the cellular receptor leads to the uncoating of the virion. Several observations support this hypothesis. Calcium depletion or freeze-thawing of the virions trigger dramatic rearrangements in the outer capsid. The spikes and the capsomers are simultaneously released and the fusogenic LC is exposed (II; III). Analogous uncoating triggered by calcium depletion has been described for the P8 layer of bacteriophage ϕ6 and VP7 of rotavirus forming the T=13 middle shell lattice (Olkkonen *et al*., 1991; Ruiz *et al*., 1996). This uncoating event is essential for infection. On the other hand, obviously the interactions between the PM2 spike and the cellular receptor activates the next step in the infection leading to the transfer of the viral DNA into the host cell. After genome injection of various dsDNA bacteriophages including internal membrane-containing tectiviruses PRD1 and Bam35, the empty protein capsid stays bound to the cell surface (Lundström *et al*., 1979; Ravantti *et al*., 2003). In contrast no empty viral capsids were seen on the host cell surface after all the PM2 entry-derived changes on the cell envelope were completed (IV, Fig. 1c-e). In fact, the observed cell-associated particles had a diameter of ~40 nm, which corresponds to the diameter of the LC. Thus, the exposed LC is an entry-intermediate, which faces the cell surface and is needed for the penetration of the highly supercoiled circular dsDNA through the cell envelope.

4.7.2 PENETRATION OF PM2 INDUCES CHANGES IN HOST CELL ENVELOPE PERMEABILITY

The electrochemical characteristics of the cell envelope of marine Gram-negative *Pseudoalteromonads* have not been described. It is known that the phospholipid composition and ratio of BAL-31 membranes are similar to that of Enterobacteria such as *E. coli* (Espejo and Canelo, 1968b). The OM of Gram-negative bacteria are permeable to small hydrophilic compounds and inorganic ions, which freely diffuse though porins. However, the outer leaflet of the OM forms a permeability barrier to lipophilic compounds such as tetraphenylphosphonium (TPP^+), phenyldicarbaundecaborane (PCB^-), and ionophoric antibiotics like gramicidin D (GD) (Daugelavičius *et al*., 1997a; Nikaido, 1996). The bacterial CM is permeable to lipophilic ions and GD, but inorganic ions like K^+ can not penetrate the membrane. The penetration of the viral nucleic acid across a Gram-negative cell envelope induces changes in the OM and the CM (Letellier *et al*., 1999). Thus, the ion fluxes across the cell envelope are indicators of the energetic state of the CM and the permeability of the OM. The ion flows can be measured using selective electrodes. They monitor the concentrations of the used indicator ions in the media surrounding the cells. In this study three indicator ions were used: TPP^+, PCB^-, and K^+. If phage infection increases OM permeability, it

should be observed as an increased uptake of lipophilic ions. Furthermore the ionophoric antibiotic GD can then reach the CM thus inducing depolarisation, which results in exit of intracellular K^+.

Analyses of the electrochemical characteristics of the cell envelopes of *Pseudoalteromonads* revealed that their OM are highly permeable to the lipophilic compound TPP^+ (IV). In this respect their OM are different from the well-characterised Gram-negative cell envelopes of *E. coli* or *S. enterica* (Nikaido, 1996). Chelating agents such as EDTA destabilise the OM of Gram-negative bacteria by removing the stabilising divalent cations (Vaara, 1992). This results in a partial release of LPS molecules. The permeability observed in the OM of the *Pseudoalteromonad* resembles that of enteric bacteria when their OM have been permeabilised by Tris-EDTA treatment (Daugelavičius *et al*., 1997a). Interestingly, the EDTA treatment did not increase the OM permeability of *Pseudoalteromonads*. *Pseudoalteromonads* are grown in a medium resembling seawater. High salt in the growth medium results in an increased concentration of cellular solutes (Ingraham and Marr, 1996). Thus, the high intracellular K^+ concentration of *Pseudoalteromonads* (IV) and the high permeability of the OM might be an adaptation to their natural marine environment.

Ion fluxes across the cell envelope were measured during PM2 entry into *Pseudoalteromonds*, BAL-31 and ER72M2 (IV). Although the OM of *Pseudoalteromonads* were permeable to lipophilic TPP^+, it formed a permeability barrier for lipophilic but rather large GD molecules. However, the phage addition allowed GD to penetrate the OM and cause depolarisation in the CM. (IV, Fig. 6). This virus-induced transient permeabilisation of the OM can be interpreted as a fusion between the viral membrane and the OM. This results in a virus-derived membrane patch in the outer leafter of the OM. Less than two minutes after virus addition the OM was recovered possibly due to the diffusion of the lipids and movements of the LPS molecules. Also the uncoating of the virions upon the penetration of the viral DNA across the cell envelope supports the proposal of a fusion between the LC and the host OM.

Penetration of the membrane by the PM2 nucleic acid induced a release of accumulated TPP^+ from the cells and a leakage of intracellular K^+, as well as PCB^- binding to the cellular membranes (IV, Fig. 3, 4). These phage-induced effects on the CM started ~15 s after the addition of the virions into the cell suspension and were over in approximately two minutes showing that the initial stages of PM2 infection are fast. The transfer of the PM2 DNA across the CM only slightly destabilised the membrane. The CM was partially depolarised, but the intracellular ATP concentration did not decrease during the infection. The strong uptake of PBC^- by the cellular membranes upon phage infection correlates with the pore formation in the bacterial envelope during T4 and λ infections (Boulanger and Letellier, 1988; Daugelavičius *et al*., 2001; Grinius and Daugelavičius, 1988). Also it has been shown that there is an efflux of K^+ simultaneously with T4, T5, and T7 DNA injection (Letellier *et al*., 1999). Similarly strong binding of PBC^- and release of K^+ are triggered by PM2 infection (IV, Fig. 4b,c). Presumably the CM is transiently reorganised allowing K^+ to leak out through a pore. This putative pore is impermeable to ATP and sealed after the DNA passage minimising the harmful effects for the cell energy balance.

Calcium has a role in controlling the stability of the PM2 virion (II). According to the electrochemical measurements the stage when PM2 penetrates the CM is also controlled by calcium. The cells were incubated without calcium and highly infectious virus particles were added. (Amount of calcium coming from the virus preparation into the adsorption mixture was small, <0.01 mM $CaCl_2$). In the absence of calcium the phage-induced effect on the OM permeability is seen, but the CM is not depolarised indicating that the infection process is blocked (IV, Fig. 7). Different interpretations of the role of the calcium ions during PM2 infection have been presented (Snipes *et al*., 1974). According to these experiments PM2 binding to the cell does not require calcium ions, but calcium is needed only for the particle assembly.

4.7.3 LIPID CORE-ASSOCIATED PROTEIN P7 HAS LYTIC ACTIVITY

The PM2 virion contains a particle-associated lytic activity previously assigned to protein P3 (Tsukagoshi *et al*., 1977). We analysed the virion associated lytic activities by zymogram analysis (Bernadsky *et al*., 1994). In this assay proteins are first separated by SDS-PAGE in a gel that contains peptidoglycan isolated from Gram-negative bacteria. The electrophoresis is followed by renaturation of the separated proteins into their proper conformation. The lytic enzymes that have regained their active conformation digest the peptidoglycan in the gel, which results in visible zones in the stained gels.

Zymogram analyses of purified PM2 virions and isolated LC particles derived from freeze-thawed particles produced one clear zone (IV, Fig. 8). Thereby the PM2 lytic enzyme was localised to the LC. The molecular mass of the protein responsible for the digestion as determined by SDS-PAGE was small (below 17 kDa) assigning one of the putative membrane proteins, P3-P8, as the lytic enzyme. Proteins P3-P8 were expressed separately in *E. coli* and the cell extracts were screened by the zymogram assay. The expression of two small proteins P4 and P8 could not be detected by Coomassie blue staining. Cell extracts containing PM2 recombinant proteins P3, P5, P6, or P7 were compared to the negative control (bacteria with the cloning vector). This revealed that the cell extract containing recombinant protein P7 had a similar peptidoglycan hydrolysing activity than that observed with purified PM2 virion and isolated LC (IV, Fig. 8).

Since the PM2 lytic enzyme P7 is a component of the virus particle, it is more likely that it facilitates DNA delivery rather than being involved in the liberation of progeny virions by host cell lysis. Bacteriophages T7, T4, ϕ29, and ϕ6 contain a particle-associated peptidoglycan-hydrolysing enzyme, which aids the penetration of the viral nucleic acid into the cytoplasm (Caldentey and Bamford, 1992; Kao and McClain, 1980; Moak and Molineux, 2000; 2004; Nakagawa *et al*., 1985). For T4 and T7 it is known that host cell lysis is induced by non-structural viral proteins. In contrast, the PRD1 virion contains two different types of lytic enzymes associated with the internal viral membrane. P15 causes host cell lysis, while P7 acts during phage DNA entry (Caldentey *et al*., 1994; Rydman and Bamford, 2000; 2002).

The lytic enzymes are harmful for the cell if not controlled properly. During PM2 assembly P7 is incorporated into the membrane, in a similar manner to PRD1 P7 (Rydman and Bamford, 2000). The embedding of P7

into the membrane might limit its enzymatic activity until it is needed. PRD1 membrane-connected lytic enzymes reach the peptidoglycan layer when the viral membrane is transformed into a tubular tail-like structure, which penetrates the OM (Grahn *et al*., 2002). Conceivably PM2 P7 is connected to the inner surface of the viral bilayer by its putative transmembrane helix. The small size of the protein (3.7 kDa) makes it more likely that it can not reach the outer surface of the viral bilayer. Thus, it is presumably activated by the viral membrane fusion.

4.7.4 A MODEL FOR PM2 ENTRY

Combining all the observations presented here, a model for PM2 entry process can be proposed as follows (Fig. 4); i) receptor recognition, ii) OM penetration, iii) peptidoglycan digestion, and iv) CM penetration. The outermost capsid of PM2 functions in viral attachment to the cell surface, while the innermost LC is needed for penetration of the cell envelope.

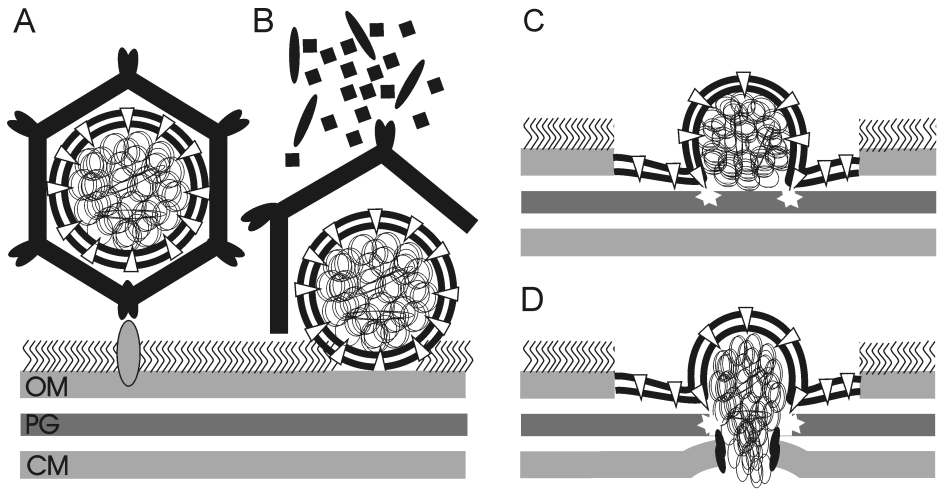

Figure 4. A model for PM2 entry into the Gram-negative *Pseudoalteromonads* (for details see the text). A) Receptor binding B) Uncoating of the virus C) LC fuses with the OM and the membrane-bound viral lytic enzymes locally digests the peptidoglycan layer. D) The CM is transiently opened for the DNA translocation and is sealed ~2 min after infection.

PM2 recognises a cellular receptor on the surface of two *Pseudoalteromonads* (IV). It is likely that each of the pentameric P1 spikes at the vertices can bind to the receptor. The distal C-terminal domains of P1 contain the host recognition site (III). The receptor binding is a signal, which is transmitted to the P2 protein capsid through the N-terminal wrist domain of P1, which is directly in contact with the capsid (III). This leads to release of the protein shell exposing the LC to the cell surface (IV).

Fusion between viral and host membranes is a common event during

enveloped animal virus entry. Among bacteriophages, membrane-containing ϕ6 fuses with the bacterial OM allowing the internalisation of the nucleocapsid (Bamford *et al*., 1987). An indication of a fusion event during PM2 DNA entry was obtained by electrochemical measurements (IV). It can be postulated that the protein-rich LC fuses with the host OM resulting in transient permeability to lipophilic ions. Some protein components in the LC, which are exposed after the uncoating might mediate fusion with the host membrane. Following fusion, the LC interior faces the peptidoglycan layer, which may be locally opened by the membrane-bound lytic enzyme P7.

To cross the bacterial CM, the circular supercoiled dsDNA of PM2 supposedly needs a pore to bypass the barrier. Tailed bacteriophages T5, T7, and λ have accomplished this task by forming a pore built up from virally- or host-encoded proteins for linear DNA translocation (Feucht *et al*., 1990; Molineux, 2001; Roessner and Ihler, 1986). Concomitant efflux of K^+ with the virus entry indicates that the CM is permeabilised due to the phage DNA translocation through a channel (Letellier *et al*., 1999). Analogously a transient efflux of K^+ from the cytoplasm was measured during PM2 entry (IV). However, the slight decrease in the membrane voltage as well as the steady cellular ATP level observed during PM2 DNA passage indicate that there is a well-controlled pore in the CM formed of host or virus proteins or both. At this stage the proteins present in the LC might act and induce the formation of a channel for the PM2 genome.

Bacteriophages typically use a single vertex for the delivery of their dsDNA. Here we propose a novel mechanism for the entry of PM2 genome. It deviates considerably from previously described phage DNA delivery mechanisms. Bacteriophage PRD1 possesses a similar general architecture as PM2. The proteinaceous internal membranes of PRD1 and PM2 play important roles in the phage DNA translocation. However, the mechanisms deviate considerably. The injection of the PRD1 genome occurs through a tail-tube formed of the membrane (Bamford and Mindich, 1982; Grahn *et al*., 2002). There is no evidence of tube formation in PM2, but the PM2 membrane most probably fuses with the bacterial OM. The difference observed in the electrochemical measurements during PRD1 and PM2 entry also indicate, that the entry pathways are different (IV; Daugelavičius *et al*., 1997a). The role of the PM2 membrane in DNA injection resembles more that of the membrane of the enveloped animal viruses. An example of this mechanism can be also found in another bacterial virus, dsRNA phage ϕ6 (Bamford *et al*., 1987).

5 CONCLUSIONS

As a result of the present study, understanding of the marine dsDNA membrane-containing bacteriophage PM2 representing the *Corticoviridae* family has considerably advanced. The microbiological, biochemical, and electrochemical techniques combined with the cryo-EM and image analysis methods provided a vast amount of information on the virion structure and led to insights into the life-cycle of PM2. Today, 15 genes out of 21 putative ORF have been assigned to function during the PM2 infection-cycle (I; II; III; Männistö *et al*., 1999; 2003). Previously published purification methods were optimised to considerably increase the recovery of infectious virus particles (I). Currently virions can be purified to high homogeneity with a reasonable yield (~2.5 mg of pure virus/ litre of lysate). This allowed detailed structural studies of the PM2 virion.

A new host for PM2, *Pseudoalteromonas* sp. ER72M2 was introduced (I). Among several *Pseudoalteromonads* only two strains were shown to be sensitive to PM2. In addition we showed that PM2 can replicate in resistant *Pseudoalteromonas* sp. strain A28 cells (IV). PM2 and plasmid pAS28 originating from strain A28 have homologous genome regions transcribed autonomously (Männistö *et al*., 2003). In lambdoid phages such regions acquired by horizontal gene exchange are called morons (Hendrix *et al*., 1999; Juhala *et al*., 2000). The concomitant replication of PM2 with plasmid pAS28 in A28 cells has most probably enabled the recombination between the genomes.

This study provides the first three-dimensional description of the PM2 virion, which determines the structural organisation of virions in the *Corticoviridae* family. A schemantic model of the PM2 virion is shown in Figure 5.

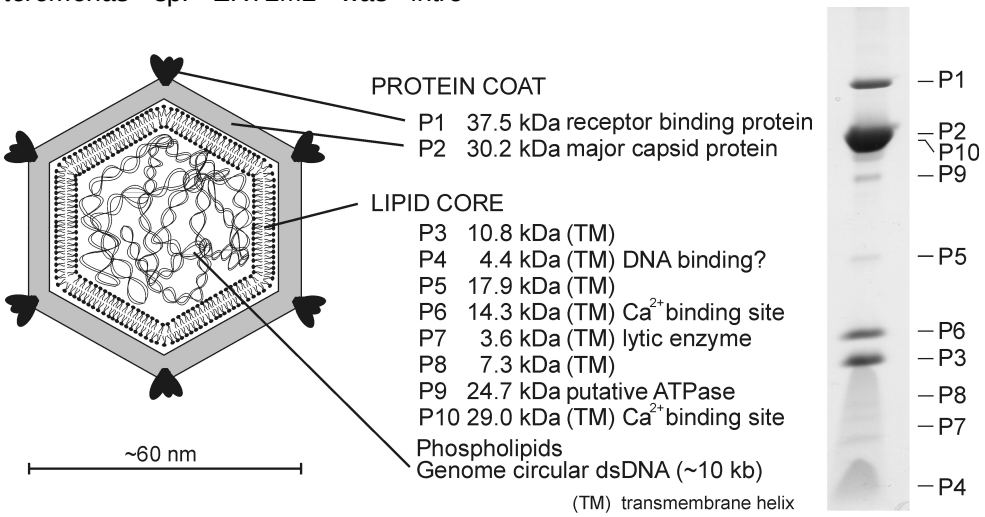

Figure 5. The current model of bacteriophage PM2 virion. Schematic presentation of PM2 is modified from II. Structural proteins of PM2 separated in tricine-SDS-PAGE (Coomassie blue stained) are shown on the right.

The virion architecture is unique, not described for other viruses. The capsid has a pseudo T=21 *dextro* organisation (III). The membrane bilayer closely follows the internal surface of the icosahedral capsid with 60 evident protein anchors, which link a subset of the capsomers to the underlying membrane near the two-fold axes of symmetry. This is a novel arrangement of interactions between a viral lipid bilayer and capsomers. The proteinaceous membrane bilayer encloses the circular supercoiled dsDNA genome designated as the LC particle (II). Inside the LC the genome closely interacts with the inner leaflet of the viral membrane. The capsid is a metastable structure able to undergo rapid structural rearragements leading to a total dissociation of the protein shell. Calcium ions located most probably at the capsomer interfaces stabilise the lattice (II).

It was demonstrated that the protein composition of highly infectious PM2 virions is more complex than previously described (I; Datta *et al*., 1971a). Having also the PM2 genome sequence available, ten structural proteins, P1-P10, were identified (I; II; III; Männistö *et al*., 1999). The proteins were biochemically localised either to the capsid (P1 and P2) or to the LC associated with the membrane (P3-P10) (II; III). The pseudo T=21 capsid architecture is built from 200 pseudohexagonal trimers of the major capsid protein P2 (III). Depending on the location of four different quasi-equivalent P2 trimers, the base of the capsomer has from one to three α-helices parallel to the membrane. The large pentameric spikes formed by the receptor-binding protein P1 fill the vertices (II; III). These rigid, three-domain structures are radially oriented and multimerised upon particle assembly. The distal C-terminus of P1 protrudes from the vertices and the proximal N-terminus interacts with the P2 capsomers (II; III). The virion structure presented in this study agrees well with the SAXS based model of PM2 particles (Harrison *et al*., 1971), but partially disagrees with the model dominating the previous PM2 literature (Fig. 2 and 5). The previous model proposed that the PM2 virion has two concentric icosahedral protein shells, similar to the structure of SFV (Franklin *et al*., 1976; Mancini *et al*., 2000). We found no evidence for two protein shells.

This work together with earlier observations yielded also insights into the PM2 infection-cycle, which is summarised in Figure 6. The viral membrane plays a role both in entry and assembly. A model for the PM2 entry pathway is proposed here (Fig. 4). It provides the first model of how a circular supercoiled dsDNA viral genome is introduced into a Gram-negative cell. Binding of the receptor by the distal C-terminus of spike P1 triggers a cascade of events leading to dissociation of the viral capsid and fusion of LC with the host OM (IV). A lytic enzyme associated with the PM2 virion was assigned to the membrane protein P7 (IV). We propose that P7 assists the phage DNA delivery. The novel entry pathway of PM2 deviates significantly from other described phage DNA delivery mechanisms.

The virion structure suggested a probable mechanism for the particle assembly. The LC might be an assembly intermediate, which packages DNA and acts as a scaffold for co-assembly of the capsomers and the spikes on the LC surface. Two pieces of evidence have been presented supporting that the assembly proceeds via a preformed viral membrane vesicle. Transmission EM of PM2 infected cells has revealed the maturation of virus-sized empty vesicles into virions

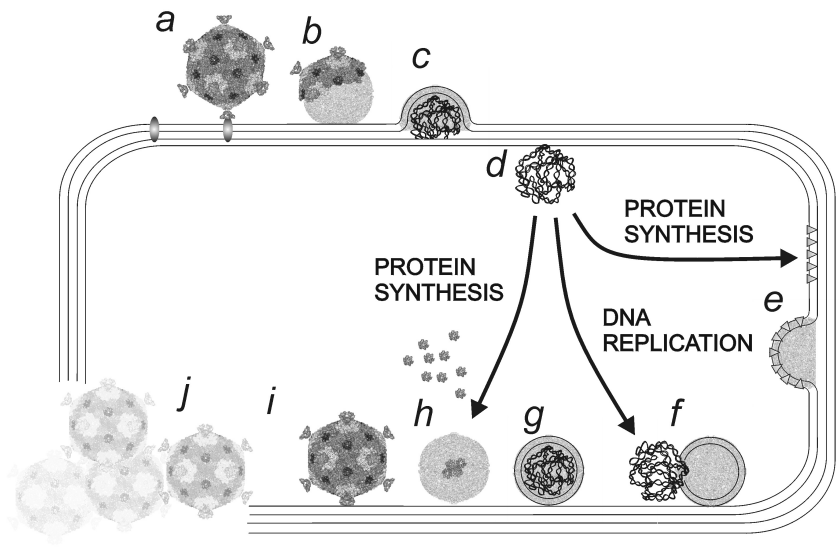

Figure 6. Life cycle of PM2. ***a***, The PM2 virion binds to the host cell receptor with the spike protein distal domain. ***b***, Receptor binding triggers uncoating of the virion. ***c***, Lipid core fuses with the host outer membrane leading to genome delivery. ***d***, DNA replication and protein synthesis is associated with the host cytoplasmic membrane. ***e***, A lipid vesicle buds internally with the help of viral membrane proteins. ***f***, The empty vesicle associates with the circular, supercoiled genome. ***g***, The vesicle wraps around the genome. ***h***, Assembly of the capsid nucleates from the P2 trimers interacting with the lipid core anchor proteins. ***i***, Lateral interactions between P2 trimers mediate the assembly of the rest of the capsid. Monomeric P1 proteins associate into pentameric spikes. ***j***, Host cell lysis.

(Dahlberg and Franklin, 1970). Additionally, shifting to a permissive temperature induced the maturation of the temperature-sensitive PM2 mutant membrane vesicles into infectious virions (Brewer, 1976; 1980). The anchors on the LC surface might act as a nucleation center for capsid assembly.

Characteristics of PM2 are unusual for a bacteriophage. It does not have a tail and it has an internal membrane bilayer (Fig. 1). It resembles the tectiviruses (Bamford *et al*., 1995; Grahn *et al*., 2003). Even though PRD1 and PM2 have common features, they have significant differences such as the detailed capsid architecture, genome organisation, and replication mechanism. Also the assembly processes and infection mechanisms seem to be different. PM2 does not have structural similarity to any other membrane-containing viruses. PM2 is also very distinct from phage ϕX174 that has a similar DNA replication mechanism (Männistö *et al*., 1999). Obviously, unique mechanisms for delivery and packaging of circular highly supercoiled dsDNA molecule have evolved. However, only a minor fraction of available phages have been sampled (Rohwer, 2003). Thus, it is quite apparent that similarities to PM2 may emerge when new membrane-containing viruses are discovered. The results presented in this thesis support the placement of PM2 into its own family, the *Corticoviridae*.

6 ACKNOWLEDGEMENTS

This study was carried out at the Department of Biological and Environmental Sciences, Faculty of Biosciences (formerly the Department of Biosciences, the Faculty of Science) and at the Institute of Biotechnology, University of Helsinki under the supervision of Professor Dennis Bamford. Professor Hannu Saarilahti, the head of the Division of Genetics, is acknowledged for his flexible attitude towards my studies. Helsinki Graduate School in Biotechnology and Molecular Biology and Academy of Finland are acknowledged for the financial support.

I am grateful to my excellent supervisor Dennis, whose inspiring scientific attitude and optimism, together with the excellent working facilities in the Bamford's lab, has had the greatest impact to my work. I wish to thank Dennis for all that he has contributed to my education as a scientist; especially for the freedom he has allowed me to develop my own ideas.

Docents Kristiina Mäkinen and Petri Auvinen are warmly acknowledged for their expert review of this manuscript.

I express my deepest gratitude to my excellent co-authors, Dr Riina Hankkio, MSc Juha Huiskonen, Dr Sarah Butcher, Dr Rimantas Daugelavičius, Dr Nisse Kalkkinen, and Dr Jaana Bamford for their contributions in the papers.

Docents Petri Auvinen and Jaana Bamford, the follow-up members of my thesis work, are thanked for their supportive attitude towards this study. Jaana is warmly thanked for her ideas and contributions to my projects during these years, although most of our collaboration is not included in this thesis.

I gratefully acknowledge all the former and present members of the Bamford's lab for help, advice, and the warm and joyful atmosphere in the lab. Warm thanks are especially due to Riina Hankkio, Minna Poranen, Marika Grahn, Pia Rydman, Janne Ravantti, Markus Pirttimaa, and Anja Paatero for all the (scientific) discussions, enjoyable moments, and especially the fun in and out of the lab. Thanks for all the old good times! I am grateful to Riina for our fruitful collaborations. It was a great pleasure to work with you. I really miss the time of our shared projects (the time when the dead cats were thrown around) with all the discussions about the challenging nature of PM2.

Special thanks are reserved for our accurate and skilled previous and present technical personnel of the lab for their valuable technical assistance. I especially thank Marja-Leena Perälä, Sari Korhonen, Riitta Tarkiainen, Anna Rantala, and Sara Ollila.

I express my gratitude to Nelli Strömsten for her rapid review of English of this manuscript.

All work is made easier with family. I am deeply grateful to my parents Timo and Maarit Kivelä together with my sister and brother for their loving support. I indebted to them together with my parents-in-law Rauno and Ritva Oksanen for their invaluable help e.g. in babysitting. My sincerest appreciation goes to my husband Juha Oksanen and to our son Atte for their love and care. Without you none of this would be possible. I want to thank Juha also for his expert and patient technical support with the computers. The sunshine of my life, Atte has not only taught me what time-management is really all about, but also shown me a new perspective of life with his 3-year enthusiasm.

Helsinki, May 2004

Hanna

7 REFERENCES

Ackermann, H. W. (2000). Family Corticoviridae. *In* "Virus Taxonomy. Classification and Nomenclature of Viruses." (M. H. V. van Regenmortel, C. M. Fauquet, D. H. L. Bishop, E. B. Carstens, M. K. Estes, S. M. Lemon, J. Maniloff, M. A. Mayo, D. J. McGeoch, C. R. Pringle, and R. B. Wickner, Eds.), pp. 117-120. Academic Press, San Diego, California.

Ackermann, H. W. (2003). Bacteriophage observations and evolution. *Res Microbiol* **154,** 245-251.

Akagawa-Matsushita, M., Matsuo, M., Koga, Y., and Yamasato, K. (1992). *Alteromonas atlantica* sp. nov. and *Alteromonas carrageenovora* sp. nov. bacteria that decompose algal polysaccharides. *Int J Syst Bacteriol* **42,** 621-627.

Akutsu, H., Satake, H., and Franklin, R. M. (1980). Phosphorus nuclear magnetic resonance studies on the lipid-containing bacteriophage PM2. *Biochemistry* **19,** 5264-5270.

Armour, G. A., and Brewer, G. J. (1990). Membrane morphogenesis from cloned fragments of bacteriophage PM2 DNA that contain the sp6.6 gene. *FASEB J* **4,** 1488-1493.

Athappilly, F. K., Murali, R., Rux, J. J., Cai, Z., and Burnett, R. M. (1994). The refined crystal structure of hexon, the major coat protein of adenovirus type 2, at 2.9 Å resolution. *J Mol Biol* **242,** 430-455.

Baas, P. D., and Jansz, H. S. (1988). Single-stranded DNA phage origins. *Curr Top Microbiol Immunol* **136,** 31-70.

Baker, T. S., Olson, N. H., and Fuller, S. D. (1999). Adding the third dimension to virus life cycles: three-dimensional reconstruction of icosahedral viruses from cryo-electron micrographs. *Microbiol Mol Biol Rev* **63,** 862-922.

Bamford, D. H., and Bamford, J. K. H. (2003). Lipid-containing bacteriophage PM2, the type-organism of *Corticoviridae*. *In* "The Bacteriophages" (R. Calendar, Ed.). Oxford University Press. In press.

Bamford, D., and Mindich, L. (1982). Structure of the lipid-containing bacteriophage PRD1: disruption of wild-type and nonsense mutant phage particles with guanidine hydrochloride. *J Virol* **44,** 1031-1038.

Bamford, D. H., Romantschuk, M., and Somerharju, P. J. (1987). Membrane fusion in prokaryotes: bacteriophage ϕ6 membrane fuses with the *Pseudomonas syringae* outer membrane. *EMBO J* **6,** 1467-1473.

Bamford, D. H., Caldentey, J., and Bamford, J. K. H. (1995). Bacteriophage PRD1: a broad host range dsDNA tectivirus with an internal membrane. *Adv Virus Res* **45,** 281-319.

Bamford, D. H., Gilbert, R. J., Grimes, J. M., and Stuart, D. I. (2001). Macromolecular assemblies: greater than their parts. *Curr Opin Struct Biol* **11,** 107-113.

Bamford, D. H., Burnett, R. M., and Stuart, D. I. (2002). Evolution of viral structure. *Theor Popul Biol* **61,** 461-470.

Baumann, L., Baumann, P., Mandel, M., and Allen, R. D. (1972). Taxonomy of aerobic marine eubacteria. *J Bacteriol* **110,** 402-429.

Bayer, M. E. (1968). Areas of adhesion between wall and membrane of *Escherichia coli*. *J Gen Microbiol* **53,** 395-404.

Bazinet, C., and King, J. (1985). The DNA translocation vertex of dsDNA bacteriophages. *Annu Rev Microbiol* **39,** 109-129.

Belnap, D. M., and Steven, A. C. (2000). 'Deja vu all over again': the similar structures of bacteriophage PRD1 and adenovirus. *Trends Microbiol* **8,** 91-93.

Benson, S. D., Bamford, J. K. H., Bamford, D. H., and Burnett, R. M. (1999). Viral evolution revealed by bacteriophage PRD1 and human adenovirus coat protein structures. *Cell* **98,** 825-833.

Bergh, O., Borsheim, K. K., Bratbak, G., and Heldal, M. (1989). High abundance of viruses found in aquatic environments. *Nature* **340,** 467-468.

Bernadsky, G., Beveridge, T. J., and Clarke, A. J. (1994). Analysis of the sodium dodecyl sulphate-stable peptidoglycan autolysins of select gram-negative pathogens by using renaturing polyacrylamide gel electrophoresis. *J Bacteriol* **176,** 5225-5232.

Bernal, R. A., Hafenstein, S., Olson, N. H., Bowman, V. D., Chipman, P. R., Baker, T. S., Fane, B. A., and Rossmann, M. G. (2003). Structural studies of bacteriophage α3 assembly. *J Mol Biol* **325,** 11-24.

Berrier, C., Bonhivers, M., Letellier, L., and Ghazi, A. (2000). High-conductance channel induced by the interaction of phage lambda with its receptor maltoporin. *FEBS Lett* **476,** 129-133.

Böhm, J., Lambert, O., Frangakis, A. S., Letellier, L., Baumeister, W., and Rigaud, J. L. (2001). FhuA-mediated phage genome transfer into liposomes: a cryo-electron tomography study. *Curr Biol* **11,** 1168-1175.

Bonhivers, M., Ghazi, A., Boulanger, P., and Letellier, L. (1996). FhuA, a transporter of the *Escherichia coli* outer membrane, is converted into a channel upon binding of bacteriophage T5. *EMBO J* **15,** 1850-1856.

Booy, F. P., Newcomb, W. W., Trus, B. L., Brown, J. C., Baker, T. S., and Steven, A. C. (1991). Liquid-crystalline, phage-like packing of encapsidated DNA in herpes simplex virus. *Cell* **64,** 1007-1015.

Boulanger, P., and Letellier, L. (1988). Characterization of ion channels involved in the penetration of phage T4 DNA into *Escherichia coli* cells. *J Biol Chem* **263,** 9767-9775.

Boulanger, P., le Maire, M., Bonhivers, M., Dubois, S., Desmadril, M., and Letellier, L. (1996). Purification and structural and functional characterization of FhuA, a transporter of the *Escherichia coli* outer membrane. *Biochemistry* **35,** 14216-14224.

Boyer, H. W., and Roulland-Dussoix, D. (1969). A complementation analysis of the restriction and modification system of DNA in *Escherichia coli*. *J Mol Biol* **41,** 459-472.

Brady, J. B., Winston, V. D., and Consigli, R. A. (1977). Dissociation of polyoma virus by the chelation of calcium ions found associated with purified virions. *J Virol* **23,** 717-724.

Braunstein, S. N., and Franklin, R. M. (1971). Structure and synthesis of a lipid-containing bacteriophage. V. Phospholipids of the host BAL-31 and of the bacteriophage PM2. *Virology* **43,** 685-95.

Breitbart, M., Salamon, P., Andresen, B., Mahaffy, J. M., Segall, A. M., Mead, D., Azam, F., and Rohwer, F. (2002). Genomic analysis of uncultured marine viral communities. *Proc Natl Acad Sci U S A* **99,** 14250-14255.

Brewer, G. J. (1976). Control of membrane morphogenesis in bacteriophage PM2. *J Supramol Struct* **5,** 73-79.

Brewer, G. J. (1978a). Membrane-localized replication of bacteriophage PM2. *Virology* **84,** 242-245.

Brewer, G. J. (1978b). Characterization of temperature-sensitive mutants of bacteriophage PM2: membrane mutants. *Mol Gen Genet* **167,** 65-74.

Brewer, G. J. (1979). *In vivo* assembly of a biological membrane of defined size, shape, and lipid composition. *J Virol* **30,** 875-882.

Brewer, G. J. (1980). Control of membrane morphogenesis in bacteriophage. *Int Rev Cytol* **68,** 53-96.

Brewer, G. J., and Singer, S. J. (1974). On the disposition of the proteins of the membrane-containing bacteriophage PM2. *Biochemistry* **13,** 3580-3588.

Brewer, G. J., and Singh, M. (1982). Kinetics and characterization of the proteins synthesized during infection by bacteriophage PM2. *J Gen Virol* **60,** 135-146.

Bujard, H., Gentz, R., Lanzer, M., Stueber, D., Mueller, M., Ibrahimi, I., Haeuptle, M. T., and Dobberstein, B. (1987). A T5 promoter-based transcription-translation system for the analysis of proteins *in vitro* and *in vivo*. *Meth Enzymol* **155,** 416-433.

Burch, C. L., and Chao, L. (2000). Evolvability of an RNA virus is determined by its mutational neighbourhood. *Nature* **406,** 625-628.

Burnett, R. M. (1985). The structure of the adenovirus capsid. II. The packing symmetry of hexon and its implications for viral architecture. *J Mol Biol* **185,** 125-143.

Butcher, S. J., Bamford, D. H., and Fuller, S. D. (1995). DNA packaging orders the membrane of bacteriophage PRD1. *EMBO J* **14,** 6078-6086.

Butcher, S. J., Dokland, T., Ojala, P. M., Bamford, D. H., and Fuller, S. D. (1997). Intermediates in the assembly pathway of the double-stranded RNA virus ϕ6. *EMBO J* **16,** 4477-4487.

Butler, P. J. (1999). Self-assembly of tobacco mosaic virus: the role of an intermediate aggregate in generating both specificity and speed. *Philos Trans R Soc Lond B Biol Sci* **354,** 537-550.

Caldentey, J., and Bamford, D. H. (1992). The lytic enzyme of the *Pseudomonas* phage ϕ6. Purification and biochemical characterization. *Biochim Biophys Acta* **1159,** 44-50.

Caldentey, J., Hänninen, A. L., and Bamford, D. H. (1994). Gene XV of bacteriophage PRD1 encodes a lytic enzyme with muramidase activity. *Eur J Biochem* **225,** 341-346.

Camerini-Otero, R. D., and Franklin, R. M. (1972). Structure and synthesis of a lipid-containing bacteriophage. XII. The fatty acids and lipid content of bacteriophage PM2. *Virology* **49,** 385-393.

Camerini-Otero, R. D., and Franklin, R. M. (1975). Structure and synthesis of a lipid-containing bacteriophage. The molecular weight and other physical properties of bacteriophage PM2. *Eur J Biochem* **53,** 343-348.

Canelo, E., Phillips, O. M., and del Roure, R. N. (1985). Relating cistrons and functions in bacteriophage PM2. *Virology* **140,** 364-367.

Carbon, P., Ehresmann, C., Ehresmann, B., and Ebel, J. P. (1979). The complete nucleotide sequence of the ribosomal 16-S RNA from *Escherichia coli*. Experimental details and cistron heterogeneities. *Eur J Biochem* **100,** 399-410.

Casjens, S. (1997). Principles of virion structure, function, and assembly. *In* "Structural biology of viruses" (W. Chiu, R. M. Burnett, and R. Garcea, Eds.), pp. 3-37. Oxford University Press, Inc., New York, Oxford.

Caspar, D. L. D., and Klug, A. (1962). Physical principles in the construction of regular viruses. *Cold Spring Harb Symp Quant Biol* **27,** 1-24.

Catalano, C. E. (2000). The terminase enzyme from bacteriophage lambda: a DNA-packaging machine. *Cell Mol Life Sci* **57,** 128-148.

Catalano, C. E., Cue, D., and Feiss, M. (1995). Virus DNA packaging: the strategy used by phage lambda. *Mol Microbiol* **16,** 1075-1086.

Cerritelli, M. E., Cheng, N., Rosenberg, A. H., McPherson, C. E., Booy, F. P., and Steven, A. C. (1997). Encapsidated conformation of bacteriophage T7 DNA. *Cell* **91,** 271-280.

Cerritelli, M. E., Conway, J. F., Cheng, N., Trus, B. L., and Steven, A. C. (2003). Molecular mechanisms in bacteriophage T7 procapsid assembly, maturation, and DNA containment. *Adv Protein Chem* **64,** 301-323.

Certa, U., Bannwarth, W., Stüber, D., Gentz, R., Lanzer, M., le Grice, S., Guillot, F., Wendler, I., Hunsmann, G., Bujard, H., and Mous, J. (1986). Subregions of a conserved part of the HIV gp41 transmembrane protein are differentially recognized by antibodies of infected individuals. *EMBO J* **5,** 3051-3056.

Chan, K. Y., Baumann, L., Garza, M. M., and Baumann, P. (1978). Two new species of *Alteromonas*: *Alteromonas espeijiana* and *Alteromonas undida*. *Int J Syst Bacteriol* **28,** 217-222.

Chang, H. R., Loo, L. H., Jeyaseelan, K., Earnest, L., and Stackebrandt, E. (1997). Phylogenetic relationships of *Salmonella typhi* and *Salmonella typhimurium* based on 16S rRNA sequence analysis. *Int J Syst Bacteriol* **47,** 1253-1254.

Chelvanayagam, G., Heringa, J., and Argos, P. (1992). Anatomy and evolution of proteins displaying the viral capsid jellyroll topology. *J Mol Biol* **228,** 220-242.

Chen, F., and Lu, J. (2002). Genomic sequence and evolution of marine cyanophage P60: a new insight on lytic and lysogenic phages. *Appl Environ Microbiol* **68,** 2589-2594.

Cheng, R. H., Caston, J. R., Wang, G. J., Gu, F., Smith, T. J., Baker, T. S., Bozarth, R. F., Trus, B. L., Cheng, N., Wickner, R. B., and Steven, A. C. (1994). Fungal virus capsids, cytoplasmic compartments for the replication of double-stranded RNA, formed as icosahedral shells of asymmetric Gag dimers. *J Mol Biol* **244,** 255-258.

Chopin, A., Bolotin, A., Sorokin, A., Ehrlich, S. D., and Chopin, M. (2001). Analysis of six prophages in *Lactococcus lactis* IL1403: different genetic structure of temperate and virulent phage populations. *Nucleic Acids Res* **29,** 644-651.

Conway, J. F., Duda, R. L., Cheng, N., Hendrix, R. W., and Steven, A. C. (1995). Proteolytic and conformational control of virus capsid maturation: the bacteriophage HK97 system. *J Mol Biol* **253,** 86-99.

Cota-Robles, E., Espejo, R. T., and Haywood, P. W. (1968). Ultrastructure of bacterial cells infected with bacteriophage PM2, a lipid-containing bacterial virus. *J Virol* **2,** 56-68.

Crowther, R. A., Lenk, E. V., Kikuchi, Y., and King, J. (1977). Molecular reorganization in the hexagon to star transition of the baseplate of bacteriophage T4. *J Mol Biol* **116,** 489-523.

Cserzo, M., Bernassau, J. M., Simon, I., and Maigret, B. (1994). New alignment strategy for transmembrane proteins. *J Mol Biol* **243,** 388-396.

Dahlberg, J. E., and Franklin, R. M. (1970). Structure and synthesis of a lipid-containing bacteriophage. IV. Electron microscopic studies of PM2-infected *Pseudomonas* BAL-31. *Virology* **42,** 1073-1086.

Datta, A., Camerini-Otero, R. D., Braunstein, S. N., and Franklin, R. M. (1971a). Structure and synthesis of a lipid-containing bacteriophage. VII. Structural proteins of bacteriophage PM2. *Virology* **45,** 232-239.

Datta, A., Braunstein, S., and Franklin, R. M. (1971b). Structure and synthesis of a lipid-containing bacteriophage. VI. The spectrum of cytoplasmic and membrane-associated proteins in *Pseudomonas* BAL 31 during replication of bacteriophage PM2. *Virology* **43,** 696-707.

Daugelavičius, R., Bamford, J. K. H., and Bamford, D. H. (1997a). Changes in host cell energetics in response to bacteriophage PRD1 DNA entry. *J Bacteriol* **179,** 5203-5210.

Daugelavičius, R., Bamford, J. K. H., Grahn, A. M., Lanka, E., and Bamford, D. H. (1997b). The IncP plasmid-encoded cell envelope-associated DNA transfer complex increases cell permeability. *J Bacteriol* **179,** 5195-5202.

Daugelavičius, R., Bakiene, E., Berzinskiene, J., and Bamford, D. H. (2001). Use of lipophilic anions for estimation of biomass and cell viability. *Biotechnol Bioeng* **71,** 208-216.

Davis, T. N., and Cronan, J. E., Jr. (1985). An alkyl imidate labeling study of the organization of phospholipids and proteins in the lipid-containing bacteriophage PR4. *J Biol Chem* **260,** 663-671.

Day, L. A., Marzec, C. J., Reisberg, S. A., and Casadevall, A. (1988). DNA packing in filamentous bacteriophages. *Annu Rev Biophys Biophys Chem* **17,** 509-539.

de Haas, F., Paatero, A. O., Mindich, L., Bamford, D. H., and Fuller, S. D. (1999). A symmetry mismatch at the site of RNA packaging in the polymerase complex of dsRNA bacteriophage ϕ6. *J Mol Biol* **294,** 357-372.

de Kruijff, B. (1987). Polymorphic regulation of membrane lipid composition. *Nature* **329,** 587-588.

de Kruijff, B. (1997). Lipid polymorphism and biomembrane function. *Curr Opin Chem Biol* **1,** 564-569.

Demchick, P., and Koch, A. L. (1996). The permeability of the wall fabric of *Escherichia coli* and *Bacillus subtilis*. *J Bacteriol* **178,** 768-773.

Desplats, C., and Krisch, H. M. (2003). The diversity and evolution of the T4-type bacteriophages. *Res Microbiol* **154,** 259-267.

Dijkstra, A. J., and Keck, W. (1996). Peptidoglycan as a barrier to transenvelope transport. *J Bacteriol* **178,** 5555-5562.

Dojka, M. A., Harris, J. K., and Pace, N. R. (2000). Expanding the known diversity and environmental distribution of an uncultured phylogenetic division of bacteria. *Appl Environ Microbiol* **66,** 1617-1621.

Dokland, T. (1999). Scaffolding proteins and their role in viral assembly. *Cell Mol Life Sci* **56,** 580-603.

Dokland, T. (2000). Freedom and restraint: themes in virus capsid assembly. *Structure Fold Des* **8,** R157-162.

Dokland, T., Bernal, R. A., Burch, A., Pletnev, S., Fane, B. A., and Rossmann, M. G. (1999). The role of scaffolding proteins in the assembly of the small, single-stranded DNA virus ϕX174. *J Mol Biol* **288,** 595-608.

Dreiseikelmann, B. (1994). Translocation of DNA across bacterial membranes. *Microbiol Rev* **58,** 293-316.

Duda, R. L., Hempel, J., Michel, H., Shabanowitz, J., Hunt, D., and Hendrix, R. W. (1995). Structural transitions during bacteriophage HK97 head assembly. *J Mol Biol* **247,** 618-635.

Elliott, J., and Arber, W. (1978). *E. coli* K-12 pel mutants, which block phage lambda DNA injection, coincide with ptsM, which determines a component of a sugar transport system. *Mol Gen Genet* **161,** 1-8.

Erni, B., Zanolari, B., and Kocher, H. P. (1987). The mannose permease of *Escherichia coli* consists of three different proteins. Amino acid sequence and function in sugar transport, sugar phosphorylation, and penetration of phage lambda DNA. *J Biol Chem* **262,** 5238-5247.

Erridge, C., Bennett-Guerrero, E., and Poxton, I. R. (2002). Structure and function of lipopolysaccharides. *Microbes Infect* **4,** 837-851.

Espejo, R. T., and Canelo, E. S. (1968a). Properties of bacteriophage PM2: a lipid-containing bacterial virus. *Virology* **34,** 738-747.

Espejo, R. T., and Canelo, E. S. (1968b). Properties and characterization of the host bacterium of bacteriophage PM2. *J Bacteriol* **95,** 1887-1891.

Espejo, R. T., and Canelo, E. S. (1968c). Origin of phospholipid in bacteriophage PM2. *J Virol* **2,** 1235-1240.

Espejo, R. T., Canelo, E. S., and Sinsheimer, R. L. (1969). DNA of bacteriophage PM2: a closed circular double-stranded molecule. *Proc Natl Acad Sci U S A* **63,** 1164-1168.

Espejo, R., Espejo-Canelo, E., and Sinsheimer, R. L. (1971a). A difference between intracellular and viral supercoiled PM2 DNA. *J Mol Biol* **56,** 623-626.

Espejo, R. T., Canelo, E. S., and Sinsheimer, R. L. (1971b). Replication of bacteriophage PM2 deoxyribonucleic acid: a closed circular double-stranded molecule. *J Mol Biol* **56,** 597-621.

Feucht, A., Schmid, A., Benz, R., Schwarz, H., and Heller, K. J. (1990). Pore formation associated with the tail-tip protein pb2 of bacteriophage T5. *J Biol Chem* **265,** 18561-18567.

Fields, B. N., Knipe, D. M., Howley, P. M., Chanock, R. M., Melnick, J. L., Monath, T. P., and Roizman, B. (1996). "Fields Virology, 3rd ed." Lippincott-Raven press, Philadelpia, New York.

Fisher, A. J., and Johnson, J. E. (1993). Ordered duplex RNA controls capsid architecture in an icosahedral animal virus. *Nature* **361,** 176-179.

Franklin, R. M. (1974). Structure and synthesis of bacteriophage PM2, with particular emphasis on the viral lipid bilayer. *Curr Top Microbiol Immunol* **68,** 107-159.

Franklin, R. M. (1977). *In vitro* and *in vivo* assembly of bacteriophage PM2: a model for protein-lipid interactions. *In* "Cell Surface Reviews Vol 4, The synthesis, assembly and turnover of cell surface components" (G. Poste, and G. L. Nicolson, Eds.), Vol. 4, pp. 803-827. North-Holland Publishing Company, Amsterdam, New York, Oxford.

Franklin, R. M., Salditt, M., and Silbert, J. A. (1969). Structure and synthesis of a lipid-containing bacteriophage. I. Growth of bacteriophage PM2 and alterations in nucleic acid metabolism in the infected cell. *Virology* **38,** 627-640.

Franklin, R. M., Hinnen, R., Schäfer, R., and Tsukagoshi, N. (1976). Structure and assembly of lipid-containing viruses, with special reference to bacteriophage PM2 as one type of model system. *Philos Trans R Soc Lond B Biol Sci* **276,** 63-80.

Fuhrman, J. A. (1999). Marine viruses and their biogeochemical and ecological effects. *Nature* **399,** 541-548.

Garcea, R. L., and Liddington, R. C. (1997). Structural biology of polyomaviruses. *In* "Structural biology of viruses" (W. Chiu, R. M. Burnett, and R. Carcea, Eds.), pp. 187-208. Oxford University Press, Inc., New York, Oxford.

Garcia, L. R., and Molineux, I. J. (1995). Rate of translocation of bacteriophage T7 DNA across the membranes of *Escherichia coli*. *J Bacteriol* **177,** 4066-4076.

Garcia, E., Elliott, J. M., Ramanculov, E., Chain, P. S., Chu, M. C., and Molineux, I. J. (2003). The genome sequence of *Yersinia pestis* bacteriophage ϕA1122 reveals an intimate history with the coliphage T3 and T7 genomes. *J Bacteriol* **185,** 5248-5262.

Gauthier, M. J. (1976). Morphological, physiological, and biochemical characteristics of some violet-pigmented bacteria isolated from seawater. *Can J Microbiol* **22,** 138-149.

Gauthier, G., Gauthier, M., and Christen, R. (1995). Phylogenetic analysis of the genera *Alteromonas*, *Shewanella* and *Moritella* using genes coding for small-subunit rRNA sequences and division of the genus *Alteromonas* into two genera, *Alteromonas* (emended) and *Pseudoalteromonas* gen. nov., and proposal of twelve new species combinations. *Int J Syst Bacteriol* **45,** 755-761.

Georgopoulos, C. P., Hendrix, R. W., Kaiser, A. D., and Wood, W. B. (1972). Role of the host cell in bacteriophage morphogenesis: effects of a bacterial mutation on T4 head assembly. *Nat New Biol* **239,** 38-41.

Gordon-Shaag, A., Ben-Nun-Shaul, O., Roitman, V., Yosef, Y., and Oppenheim, A. (2002). Cellular transcription factor Sp1 recruits Simian virus 40 capsid proteins to the viral packaging signal, *ses*. *J Virol* **76,** 5915-5924.

Gowen, B., Bamford, J. K. H., Bamford, D. H., and Fuller, S. D. (2003). The tailless icosahedral membrane virus PRD1 localizes the proteins involved in genome packaging and injection at a unique vertex. *J Virol* **77,** 7863-7871.

Grahn, A. M., Caldentey, J., Bamford, J. K. H., and Bamford, D. H. (1999). Stable packaging of phage PRD1 DNA requires adsorption protein P2, which binds to the IncP plasmid-encoded conjugative transfer complex. *J Bacteriol* **181,** 6689-6696.

Grahn, A. M., Daugelavičius, R., and Bamford, D. H. (2002). Sequential model of phage PRD1 DNA delivery: active involvement of the viral membrane. *Mol Microbiol* **46,** 1199-1209.

Grahn, A. M., Butcher, S. J., Bamford, J. K. H., and Bamford, D. H. (2003). PRD1-Dissecting the genome, structure and entry. *In* "The Bacteriophages" (R. Calendar, Ed.). Oxford University Press. In press.

Gray, H. B. J., Upholt, W. B., and Vinograd, J. (1971). A buoyant method for the determination of superhelix density of closed circular DNA. *J Mol Biol* **62,** 1-19.

Grimes, J. M., Jakana, J., Ghosh, M., Basak, A. K., Roy, P., Chiu, W., Stuart, D. I., and Prasad, B. V. (1997). An atomic model of the outer layer of the bluetongue virus core derived from X-ray crystallography and electron cryomicroscopy. *Structure* **5,** 885-893.

Grimes, J. M., Burroughs, J. N., Gouet, P., Diprose, J. M., Malby, R., Zientara, S., Mertens, P. P., and Stuart, D. I. (1998). The atomic structure of the bluetongue virus core. *Nature* **395,** 470-478.

Grinius, L. (1980). Nucleic acid transport driven by ion gradient across cell membrane. *FEBS lett* **113,** 1-10.

Grinius, L., and Daugelavičius, D. (1988). Depolarization of *Escherichia coli* cytoplasmic membrane by bacteriophage T4 and lambda: evidence for induction of ion-permeable channels. *Bioelectrochem Bioenerg* **19,** 235-245.

Guasch, A., Pous, J., Ibarra, B., Gomis-Ruth, F. X., Valpuesta, J. M., Sousa, N., Carrascosa, J. L., and Coll, M. (2002). Detailed architecture of a DNA translocating machine: the high-resolution structure of the bacteriophage ϕ29 connector particle. *J Mol Biol* **315,** 663-676.

Guihard, G., Boulanger, P., and Letellier, L. (1992). Involvement of phage T5 tail proteins and contact sites between the outer and inner membrane of *Escherichia coli* in phage T5 DNA injection. *J Biol Chem* **267,** 3173-3178.

Guo, P. X., Erickson, S., and Anderson, D. (1987a). A small viral RNA is required for *in vitro* packaging of bacteriophage ϕ29 DNA. *Science* **236,** 690-694.

Guo, P., Peterson, C., and Anderson, D. (1987b). Prohead and DNA-gp3-dependent ATPase activity of the DNA packaging protein gp16 of bacteriophage ϕ29. *J Mol Biol* **197,** 229-236.

Hambly, E., Tetart, F., Desplats, C., Wilson, W. H., Krisch, H. M., and Mann, N. H. (2001). A conserved genetic module that encodes the major virion components in both the coliphage T4 and the marine cyanophage S-PM2. *Proc Natl Acad Sci U S A* **98,** 11411-11416.

Hardies, S. C., Comeau, A. M., Serwer, P., and Suttle, C. A. (2003). The complete sequence of marine bacteriophage VpV262 infecting *Vibrio parahaemolyticus* indicates that an ancestral component of a T7 viral supergroup is widespread in the marine environment. *Virology* **310,** 359-371.

Harrison, S. C., Caspar, D. L., Camerini-Otero, R. D., and Franklin, R. M. (1971). Lipid and protein arrangement in bacteriophage PM2. *Nat New Biol* **229,** 197-201.

Hayashi, M., Aoyama, A., Richardson Jr., D. L., and Hayashi, M. N. (1988). Biology of the bacteriophage ϕX174. *In* "The Bacteriophages, vol 2" (R. Calendar, Ed.), pp. 1-71. Plenum Press, New York and London.

Heller, K. J. (1984). Identification of the phage gene for host receptor specificity by analyzing hybrid phages of T5 and BF23. *Virology* **139,** 11-21.

Heller, K. J. (1992). Molecular interaction between bacteriophage and the gram-negative cell envelope. *Arch Microbiol* **158,** 235-248.

Hendrix, R. W. (1978). Symmetry mismatch and DNA packaging in large bacteriophages. *Proc Natl Acad Sci U S A* **75,** 4779-4783.

Hendrix, R. W. (1998). Bacteriophage DNA packaging: RNA gears in a DNA transport machine. *Cell* **94,** 147-150.

Hendrix, R. W., Smith, M. C., Burns, R. N., Ford, M. E., and Hatfull, G. F. (1999). Evolutionary relationships among diverse bacteriophages and prophages: all the world's a phage. *Proc Natl Acad Sci U S A* **96,** 2192-2197.

Hendrix, R. W., Hatfull, G. F., and Smith, M. C. (2003). Bacteriophages with tails: chasing their origins and evolution. Res Microbiol 154, 253-257.

Hinnen, R., Schäfer, R., and Franklin, R. M. (1974). Structure and synthesis of lipid-containing bacteriophage. Preparation of virus and localization of the structural proteins. *Eur J Biochem* **50,** 1-14.

Hinnen, R., Chassin, R., Schäfer, R., Franklin, R. M., Hitz, H., and Schäfer, D. (1976). Structure and synthesis of a lipid-containing bacteriophage. Purification, chemical composition, and partial sequences of the structural proteins. *Eur J Biochem* **68,** 139-152.

Hofmann, K., and Stoffel, W. (1993). TMbase - A database of membrane spanning protein segments. *Biol Chem Hoppe-Seyler* **347,** 166.

Hogle, J. M., Chow, M., and Filman, D. J. (1985). Three-dimensional structure of poliovirus at 2.9 Å resolution. *Science* **229,** 1358-1365.

Holder, K. K., and Bull, J. J. (2001). Profiles of adaptation in two similar viruses. *Genetics* **159,** 1393-1404.

Höltje, J. V. (1998). Growth of the stress-bearing and shape-maintaining murein sacculus of *Escherichia coli*. *Microbiol Mol Biol Rev* **62,** 181-203.

Hugenholtz, P., Goebel, B. M., and Pace, N. R. (1998). Impact of culture-independent studies on the emerging phylogenetic view of bacterial diversity. *J Bacteriol* **180,** 4765-4774.

Ilyina, T. V., and Koonin, E. V. (1992). Conserved sequence motifs in the initiator proteins for rolling circle DNA replication encoded by diverse replicons from eubacteria, eucaryotes and archaebacteria. *Nucleic Acids Res* **20,** 3279-3285.

Ingraham, J. L., and Marr, A. G. (1996). Effect of temperature, pressure, pH, and osmotic stress on growth. *In* "*Escherichia coli* and *Salmonella typhimurium*: cellular and molecular biology, 2nd ed" (F. C. Neidhardt, R. Curtis, J. L. Ingraham, E. C. C. Lin, K. B. J. Low, B. Magasanic, W. S. Reznikoff, M. Riley, M. Schaechter, and H. E. Umbarger, Eds.), pp. 1570-1578. ASM, Washington, D. C.

Jazwinski, S. M., Lindberg, A. A., and Kornberg, A. (1975). The gene H spike protein of bacteriophages ϕX174 and S13. I. Functions in phage-receptor recognition and in transfection. *Virology* **66,** 283-293.

Jiang, S. C., and Paul, J. H. (1998). Significance of lysogeny in the marine environment: studies with isolates and a model of lysogenic phage production. *Microb Ecol* **35,** 235-243.

Jiang, S., Fu, W., Chu, W., and Fuhrman, J. A. (2003). The vertical distribution and diversity of marine bacteriophage at a station off Southern California. *Microb Ecol* **45,** 399-410.

Juhala, R. J., Ford, M. E., Duda, R. L., Youlton, A., Hatfull, G. F., and Hendrix, R. W. (2000). Genomic sequences of bacteriophages HK97 and HK022: pervasive genetic mosaicism in the lambdoid bacteriophages. *J Mol Biol* **299,** 27-51.

Kadner, R. J. (1996). Cytoplasmic membrane. *In* "*Echerichia coli* and *Salmonella typhimurium*: cellular and molecular biology, 2nd ed." (F. C. Neidhardt, R. Curtiss III, J. L. Ingraham, E. C. C. Lin, K. B. J. Low, B. Magasanik, W. S. Reznikoff, M. Riley, M. Schaechter, and H. E. Umberger, Eds.), pp. 58-87. ASM, Washington, DC.

Kalasauskaite, E. V., Kadisaite, D. L., Daugelavičius, R. J., Grinius, L. L., and Jasaitis, A. A. (1983). Studies on energy supply for genetic process. Requirement for membrane potential in *Escherichia coli* infection by phage T4. *Eur J Biochem* **130,** 123-130.

Kanamaru, S., Leiman, P. G., Kostyuchenko, V. A., Chipman, P. R., Mesyanzhinov, V. V., Arisaka, F., and Rossmann, M. G. (2002). Structure of the cell-puncturing device of bacteriophage T4. *Nature* **415,** 553-557.

Kao, S. H., and McClain, W. H. (1980). Baseplate protein of bacteriophage T4 with both structural and lytic functions. *J Virol* **34,** 95-103.

Kato, J., Amie, J., Kuroda, A., Mitsutani, A., and Ohtake, H. (1998). Development of a genetic transformation system for an algae-lysing bacterium. *Appl Environ Microbiol* **64,** 2061-2064.

King, J., and Chiu, W. (1997). The procapsid-to-capsid transition in double-stranded DNA bacteriophages. *In* "Structural biology of viruses" (W. Chiu, R. M. Burnett, and R. Garcea, Eds.), pp. 288-311. Oxford University Press, Inc., New York, Oxford.

Koebnik, R., Locher, K. P., and Van Gelder, P. (2000). Structure and function of bacterial outer membrane proteins: barrels in a nutshell. *Mol Microbiol* **37,** 239-253.

Koning, R., van den Worm, S., Plaisier, J. R., van Duin, J., Pieter Abrahams, J., and Koerten, H. (2003). Visualization by cryo-electron microscopy of genomic RNA that binds to the protein capsid inside bacteriophage MS2. *J Mol Biol* **332,** 415-422.

Koonin, E. V., and Rudd, K. E. (1994). A conserved domain in putative bacterial and bacteriophage transglycosylases. *Trends Biochem Sci* **19,** 106-107.

Kornberg, A., and Baker, T. A. (1992). Rolling-circle replication. *In* "DNA Replication", Vol. 2nd ed., pp. 502-503. Freeman, New York.

Kovalyova, I. V., and Kropinski, A. M. (2003). The complete genomic sequence of lytic bacteriophage gh-1 infecting *Pseudomonas putida*--evidence for close relationship to the T7 group. *Virology* **311,** 305-315.

Krogh, A., Larsson, B., von Heijne, G., and Sonnhammer, L. L. (2001). Predicting transmembrane protein topology with a hidden markov model: application to complete genomes. *J Mol Biol* **305,** 567-580.

Kuhn, R. J., Zhang, W., Rossmann, M. G., Pletnev, S. V., Corver, J., Lenches, E., Jones, C. T., Mukhopadhyay, S., Chipman, P. R., Strauss, E. G., Baker, T. S., and Strauss, J. H. (2002). Structure of dengue virus: implications for flavivirus organization, maturation, and fusion. *Cell* **108,** 717-725.

Labedan, B., Heller, K. B., Jasaitis, A. A., Wilson, T. H., and Goldberg, E. B. (1980). A membrane potential threshold for phage T4 DNA injection. *Biochem Biophys Res Commun* **93,** 625-630.

Labischinski, H., Goodell, E. W., Goodell, A., and Hochberg, M. L. (1991). Direct proof of a "more-than-single-layered" peptidoglycan architecture of *Escherichia coli* W7: a neutron small-angle scattering study. *J Bacteriol* **173,** 751-756.

Laemmli, U. K. (1970). Cleavage of structural proteins during the assembly of the head bacteriophage T4. *Nature* **227,** 680-685.

Lambert, O., Plancon, L., Rigaud, J. L., and Letellier, L. (1998). Protein-mediated DNA transfer into liposomes. *Mol Microbiol* **30,** 761-765.

Lanni, Y. T. (1965). DNA transfer from phage T5 to host cells: dependence on intercurrent protein synthesis. *Proc Natl Acad Sci U S A* **53,** 969-973.

Larson, S. B., and McPherson, A. (2001). Satellite tobacco mosaic virus RNA: structure and implications for assembly. *Curr Opin Struct Biol* **11,** 59-65.

Lata, R., Conway, J. F., Cheng, N., Duda, R. L., Hendrix, R. W., Wikoff, W. R., Johnson, J. E., Tsuruta, H., and Steven, A. C. (2000). Maturation dynamics of a viral capsid: visualization of transitional intermediate states. *Cell* **100,** 253-263.

Lawrence, J. G., Hatfull, G. F., and Hendrix, R. W. (2002). Imbroglios of viral taxonomy: genetic exchange and failings of phenetic approaches. *J Bacteriol* **184,** 4891-4905.

Lehnherr, H., Hansen, A. M., and Ilyina, T. (1998). Penetration of the bacterial cell wall: a family of lytic transglycosylases in bacteriophages and conjugative plasmids. *Mol Microbiol* **30,** 454-457.

Lepault, J., Dubochet, J., Baschong, W., and Kellenberger, E. (1987). Organization of double-stranded DNA in bacteriophages: a study by cryo-electron microscopy of vitrified samples. *EMBO J* **6,** 1507-1512.

Lescar, J., Roussel, A., Wien, M. W., Navaza, J., Fuller, S. D., Wengler, G., and Rey, F. A. (2001). The fusion glycoprotein shell of Semliki Forest virus: an icosahedral assembly primed for fusogenic activation at endosomal pH. *Cell* **105,** 137-148.

Letellier, L., Plancon, L., Bonhivers, M., and Boulanger, P. (1999). Phage DNA transport across membranes. *Res Microbiol* **150,** 499-505.

Letellier, L., Boulanger, P., de Frutos, M., and Jacquot, P. (2003). Channeling phage DNA through membranes: from *in vivo* to *in vitro*. *Res Microbiol* **154,** 283-287.

Liddington, R. C., Yan, Y., Moulai, J., Sahli, R., Benjamin, T. L., and Harrison, S. C. (1991). Structure of simian virus 40 at 3.8-Å resolution. *Nature* **354,** 278-284.

Lucas, R. W., Larson, S. B., McPherson, A. (2002). The crystallographic structure of brome mosaic virus. *J Mol Biol* **317,** 95-108.

Lundström, K. H., Bamford, D. H., Palva, E. T., and Lounatmaa, K. (1979). Lipid-containing bacteriophage PR4: structure and life cycle. *J Gen Virol* **43,** 583-592.

Mancini, E. J., Clarke, M., Gowen, B. E., Rutten, T., and Fuller, S. D. (2000). Cryo-electron microscopy reveals the functional organization of an enveloped virus, Semliki Forest virus. *Mol Cell* **5,** 255-266.

Mann, N. H. (2003). Phages of the marine cyanobacterial picophytoplankton. *FEMS Microbiol Rev* **27,** 17-34.

Männistö, R. H., Kivelä, H. M., Paulin, L., Bamford, D. H., and Bamford, J. K. H. (1999). The complete genome sequence of PM2, the first lipid-containing bacterial virus to be isolated. *Virology* **262,** 355-363.

Männistö, R. H., Grahn, A. M., Bamford, D. H., and Bamford, J. K. H. (2003). Transcription of bacteriophage PM2 involves phage-encoded regulators of heterologous origin. *J Bacteriol* **185,** 3278-3287.

Marcoli, R., Pirrotta, V., and Franklin, R. M. (1979). Interaction between bacteriophage PM2 protein IV and DNA. *J Mol Biol* **131,** 107-131.

Marsh, M., and Helenius, A. (1989). Virus entry into animal cells. *Adv Virus Res* **36,** 107-151.

McCorquodale, D. J., Shaw, A. R., Shaw, P. K., and Chinnadurai, G. (1977). Pre-early polypeptides of bacteriophages T5 and BF23. *J Virol* **22,** 480-488.

McKenna, R., Ilag, L. L., and Rossmann, M. G. (1994). Analysis of the single-stranded DNA bacteriophage ϕX174, refined at a resolution of 3.0 Å. *J Mol Biol* **237,** 517-543.

McKenna, R., Xia, D., Willingmann, P., Ilag, L. L., Krishnaswamy, S., Rossmann, M. G., Olson, N. H., Baker, T. S., and Incardona, N. L. (1992). Atomic structure of single-stranded DNA bacteriophage ϕX174 and its functional implications. *Nature* **355,** 137-143.

Mindich, L. (1999). Precise packaging of the three genomic segments of the double-stranded-RNA bacteriophage ϕ6. *Microbiol Mol Biol Rev* **63,** 149-160.

Mindich, L., and Lehman, J. (1979). Cell wall lysin as a component of the bacteriophage ϕ6 virion. *J Virol* **30,** 489-496.

Mindich, L., Sinclair, J. F., and Cohen, J. (1976). The morphogenesis of bacteriophage ϕ6: particles formed by nonsense mutants. *Virology* **75,** 224-231.

Mindich, L., Bamford, D., McGraw, T., and Mackenzie, G. (1982). Assembly of bacteriophage PRD1: particle formation with wild-type and mutant viruses. *J Virol* **44,** 1021-1030.

Moak, M., and Molineux, I. J. (2000). Role of the Gp16 lytic transglycosylase motif in bacteriophage T7 virions at the initiation of infection. *Mol Microbiol* **37,** 345-355.

Moak, M., and Molineux, I. J. (2004). Peptidoglycan hydrolytic activities associated with bacteriophage virions. *Mol. Microbiol.* **51,**1169-1183.

Moeck, G. S., and Coulton, J. W. (1998). TonB-dependent iron acquisition: mechanisms of siderophore-mediated active transport. *Mol Microbiol* **28,** 675-681.

Moffatt, B. A., and Studier, F. W. (1988). Entry of bacteriophage T7 DNA into the cell and escape from host restriction. *J Bacteriol* **170,** 2095-2105.

Molineux, I. J. (2001). No syringes please, ejection of phage T7 DNA from the virion is enzyme driven. *Mol Microbiol* **40,** 1-8.

Moore, E. R. B., Mau, M., Arnscheidt, A., Boettger, E. C., Hutson, R. A., Collins, M. D., Van de Peer, Y., De Wachter, R., and Timmis, K. N. (1996). The determination and comparison of the 16S rRNA gene sequences of species of the genus *Pseudomonas* (sensu stricto) and estimation of the natural intrageneric relationships. *Syst Appl Microbiol* **19,** 478-496.

Morais, M. C., Kanamaru, S., Badasso, M. O., Koti, J. S., Owen, B. A., McMurray, C. T., Anderson, D. L., and Rossmann, M. G. (2003). Bacteriophage ϕ29 scaffolding protein gp7 before and after prohead assembly. *Nat Struct Biol* **10,** 572-576.

Mosig, G., and Eiserling, F. (1988). Phage T4 structure and metabolism. *In* "The bacteriophages, vol 2" (R. Calendar, Ed.), pp. 521-606. Plenum Press, New York and London.

Nakagawa, H., Arisaka, F., and Ishii, S. (1985). Isolation and characterization of the bacteriophage T4 tail-associated lysozyme. *J Virol* **54,** 460-466.

Nandhagopal, N., Simpson, A. A., Gurnon, J. R., Yan, X., Baker, T. S., Graves, M. V., Van Etten, J. L., and Rossmann, M. G. (2002). The structure and evolution of the major capsid protein of a large, lipid-containing DNA virus. *Proc Natl Acad Sci U S A* **99,** 14758-14763.

Newcomb, W. W., Trus, B. L., Cheng, N., Steven, A. C., Sheaffer, A. K., Tenney, D. J., Weller, S. K., and Brown, J. C. (2000). Isolation of herpes simplex virus procapsids from cells infected with a protease-deficient mutant virus. *J Virol* **74,** 1663-1673.

Newcomb, W. W., Juhas, R. M., Thomsen, D. R., Homa, F. L., Burch, A. D., Weller, S. K., and Brown, J. C. (2001). The UL6 gene product forms the portal for entry of DNA into the herpes simplex virus capsid. *J Virol* **75,** 10923-10932.

Newcomb, W. W., Thomsen, D. R., Homa, F. L., and Brown, J. C. (2003). Assembly of the herpes simplex virus capsid: identification of soluble scaffold-portal complexes and their role in formation of portal-containing capsids. *J Virol* **77,** 9862-9871.

Nikaido, H. (1992). Porins and specific channels of bacterial outer membranes. *Mol Microbiol* **6,** 435-442.

Nikaido, H. (1996). Outer membrane. *In* "*Echerichia coli* and *Salmonella typhimurium*: cellular and molecular biology, 2nd ed." (F. C. Neidhardt, R. Curtiss III, J. L. Ingraham, E. C. C. Lin, K. B. J. Low, B. Magasanik, W. S. Reznikoff, M. Riley, M. Schaechter, and H. E. Umberger, Eds.), pp. 29-47. ASM, Washington, DC.

Nikaido, H., and Vaara, M. (1985). Molecular basis of bacterial outer membrane permeability. *Microbiol Rev* **49,** 1-32.

Ojala, P. M., Juuti, J. T., and Bamford, D. H. (1993). Protein P4 of double-stranded RNA bacteriophage ϕ6 is accessible on the nucleocapsid surface: epitope mapping and orientation of the protein. *J Virol* **67,** 2879-2886.

Olkkonen, V. M., and Bamford, D. H. (1989). Quantitation of the adsorption and penetration stages of bacteriophage ϕ6 infection. *Virology* **171,** 229-238.

Olkkonen, V. M., Ojala, P. M., and Bamford, D. H. (1991). Generation of infectious nucleocapsids by *in vitro* assembly of the shell protein on to the polymerase complex of the dsRNA bacteriophage ϕ6. *J Mol Biol* **218,** 569-581.

Olson, A. J., Bricogne, G., and Harrison, S. C. (1983). Structure of tomato busy stunt virus IV. The virus particle at 2.9 Å resolution. *J Mol Biol* **171,** 61-93.

Olson, N. H., Gingery, M., Eiserling, F. A., and Baker, T. S. (2001). The structure of isometric capsids of bacteriophage T4. *Virology* **279,** 385-391.

Ostrander, D. A., and Gray, H. B., Jr. (1974). Superhelix density heterogeneity in closed circular intracellular PM2 DNA. *Biopolymers* **13,** 955-975.

Palmen, R., Driessen, A. J., and Hellingwerf, K. J. (1994). Bioenergetic aspects of the translocation of macromolecules across bacterial membranes. *Biochim Biophys Acta* **1183,** 417-451.

Paul, J. H. (1999). Microbial gene transfer: an ecological perspective. *J Mol Microbiol Biotechnol* **1,** 45-50.

Paul, J. H., Sullivan, M. B., Segall, A. M., and Rohwer, F. (2002). Marine phage genomics. *Comp Biochem Physiol B Biochem Mol Biol* **133,** 463-476.

Pirttimaa, M. J., and Bamford, D. H. (2000). RNA secondary structures of the bacteriophage ϕ6 packaging regions. *RNA* **6,** 880-889.

Pirttimaa, M. J., Paatero, A. O., Frilander, M. J., and Bamford, D. H. (2002). Nonspecific nucleoside triphosphatase P4 of double-stranded RNA bacteriophage ϕ6 is required for single-stranded RNA packaging and transcription. *J Virol* **76,** 10122-10127.

Plancon, L., Janmot, C., le Maire, M., Desmadril, M., Bonhivers, M., Letellier, L., and Boulanger, P. (2002). Characterization of a high-affinity complex between the bacterial outer membrane protein FhuA and the phage T5 protein pb5. *J Mol Biol* **318,** 557-569.

Pletnev, S. V., Zhang, W., Mukhopadhyay, S., Fisher, B. R., Hernandez, R., Brown, D. T., Baker, T. S., Rossmann, M. G., and Kuhn, R. J. (2001). Locations of carbohydrate sites on alphavirus glycoproteins show that E1 forms an icosahedral scaffold. *Cell* **105,** 127-136.

Poranen, M. M., Daugelavičius, R., Ojala, P. M., Hess, M. W., and Bamford, D. H. (1999). A novel virus-host cell membrane interaction. Membrane voltage-dependent endocytic-like entry of bacteriophage ϕ6 nucleocapsid. *J Cell Biol* **147,** 671-682.

Poranen, M. M., Daugelavičius, R., and Bamford, D. H. (2002). Common principles in viral entry. *Annu Rev Microbiol* **56,** 521-538.

Prevelige, P. E., Jr., Thomas, D., and King, J. (1988). Scaffolding protein regulates the polymerization of P22 coat subunits into icosahedral shells in vitro. *J Mol Biol* **202,** 743-757.

Prevelige, P. E., Jr., Thomas, D., and King, J. (1993). Nucleation and growth phases in the polymerization of coat and scaffolding subunits into icosahedral procapsid shells. *Biophys J* **64,** 824-835.

Qian, X., Jeon, C., Yoon, H., Agarwal, K., and Weiss, M. A. (1993). Structure of a new nucleic-acid-binding motif in eukaryotic transcriptional elongation factor TFIIS. *Nature* **365,** 277-279.

Raetz, C. R., and Whitfield, C. (2002). Lipopolysaccharide endotoxins. *Annu Rev Biochem* **71,** 635-700.

Randall-Hazelbauer, L., and Schwartz, M. (1973). Isolation of the bacteriophage lambda receptor from *Escherichia coli*. *J Bacteriol* **116,** 1436-1446.

Rau, D. C., Lee, B., and Parsegian, V. A. (1984). Measurement of the repulsive force between polyelectrolyte molecules in ionic solution: hydration forces between parallel DNA double helices. *Proc Natl Acad Sci U S A* **81,** 2621-2625.

Ravantti, J. J., Gaidelyte, A., Bamford, D. H., and Bamford, J. K. H. (2003). Comparative analysis of bacterial viruses Bam35, infecting a gram-positive host, and PRD1, infecting gram-negative hosts, demonstrates a viral lineage. *Virology* **313,** 401-414.

Reinisch, K. M., Nibert, M. L., and Harrison, S. C. (2000). Structure of the reovirus core at 3.6 Å resolution. *Nature* **404,** 960-967.

Richardson, J. P. (1974). Effects of supercoiling on transcription from bacteriophage PM2 deoxyribonucleic acid. *Biochemistry* **13,** 3164-3169.

Richardson, J. P. (1975). Initiation of transcription by *Escherichia coli* RNA polymerase from supercoiled and non-supercoiled bacteriophage PM2 DNA. *J Mol Biol* **91,** 477-487.

Riede, I. (1987). Receptor specificity of the short tail fibres (gp12) of T-even type *Escherichia coli* phages. *Mol Gen Genet* **206,** 110-115.

Roessner, C. A., and Ihler, G. M. (1986). Formation of transmembrane channels in liposomes during injection of lambda DNA. *J Biol Chem* **261,** 386-390.

Rohwer, F. (2003). Global phage diversity. *Cell* **113,** 141.

Rohwer, F. L., Segall, A. M., Steward, G., Seguritan, V., Breitbart, M., Wolven, F., and Azam, F. (2000). The complete genomic sequence of the marine phage Roseophage SIO1 shares homology with nonmarine phages. *Limnol Oceanogr* **45,** 408-418.

Rost, B., and Sander, C. (1993). Prediction of protein secondary structure at better than 70% accuracy. *J Mol Biol* **232,** 584-599.

Rost, B., Fariselli, P., and Casadio, R. (1996). Topology prediction for helical transmembrane proteins at 86% accuracy. *Protein Sci* **5,** 1704-1718.

Ruiz, M. C., Charpilienne, A., Liprandi, F., Gajardo, R., Michelangeli, F., and Cohen, J. (1996). The concentration of Ca^{2+} that solubilizes outer capsid proteins from rotavirus particles is dependent on the strain. *J Virol* **70,** 4877-4883.

Rydman, P. S., and Bamford, D. H. (2000). Bacteriophage PRD1 DNA entry uses a viral membrane-associated transglycosylase activity. *Mol Microbiol* **37,** 356-363.

Rydman, P. S., and Bamford, D. H. (2002). The lytic enzyme of bacteriophage PRD1 is associated with the viral membrane. *J Bacteriol* **184,** 104-110.

Rydman, P. S., Bamford, J. K. H., and Bamford, D. H. (2001). A minor capsid protein P30 is essential for bacteriophage PRD1 capsid assembly. *J Mol Biol* **313,** 785-795.

Rydman, P. S., Caldentey, J., Butcher, S. J., Fuller, S. D., Rutten, T., and Bamford, D. H. (1999). Bacteriophage PRD1 contains a labile receptor-binding structure at each vertex. *J Mol Biol* **291,** 575-587.

Salditt, M., Braunstein, S. N., Camerini-Otero, R. D., and Franklin, R. M. (1972). Structure and synthesis of a lipid-containing bacteriophage. X. Improved techniques for the purification of bacteriophage PM2. *Virology* **48,** 259-262.

Sambrook, J., and Russell, D. W. (2001). "Molecular Cloning: A Laboratory Manual, 3rd ed." Cold Spring Harbor Laboratory Press, Cold Spring Harbor, New York.

San Martín, C., Burnett, R. M., de Haas, F., Heinkel, R., Rutten, T., Fuller, S. D., Butcher, S. J., and Bamford, D. H. (2001). Combined EM/X-ray imaging yields a quasi-atomic model of the adenovirus-related bacteriophage PRD1 and shows key capsid and membrane interactions. *Structure (Camb)* **9,** 917-930.

San Martín, C., Huiskonen, J. T., Bamford, J. K., Butcher, S. J., Fuller, S. D., Bamford, D. H., and Burnett, R. M. (2002). Minor proteins, mobile arms and membrane-capsid interactions in the bacteriophage PRD1 capsid. *Nat Struct Biol* **9,** 756-763.

Satake, H., Akutsu, H., Kania, M., and Franklin, R. M. (1980). Structure and synthesis of a lipid-containing bacteriophage. Studies on the structure of the bacteriophage PM2 nucleocapsid. *Eur J Biochem* **108,** 193-201.

Satake, H., Kania, M., and Franklin, R. M. (1981). Structure and synthesis of a lipid-containing bacteriophage. Amphiphilic properties of protein IV of bacteriophage PM2. *Eur J Biochem* **114,** 623-628.

Schäfer, R., and Franklin, R. M. (1975). Structure and synthesis of a lipid-containing bacteriophage. XIX. Reconstitution of bacteriophage PM2 *in vitro*. *J Mol Biol* **97,** 21-34.

Schäfer, R., and Franklin, R. M. (1978). Structure and synthesis of a lipid-containing bacteriophage. Total reconstitution of bacteriophage PM2 *in vitro*. *Eur J Biochem* **92,** 589-596.

Schäfer, R., Hinnen, R., and Franklin, R. M. (1974). Structure and synthesis of a lipid-containing bacteriophage. Properties of the structural proteins and distribution of the phospholipid. *Eur J Biochem* **50,** 15-27.

Schäfer, R., Kunzler, P., Lustig, A., and Franklin, R. M. (1978). Structure and synthesis of a lipid-containing bacteriophage. Dissociation of bacteriophage PM2 into its morphological subunits. *Eur J Biochem* **92,** 579-588.

Schägger, H., and von Jagow, G. (1987). Tricine-sodium dodecyl sulfate-polyacrylamide gel electrophoresis for the separation of proteins in the range from 1 to 100 kDa. *Anal Biochem* **166,** 368-379.

Shu, W., Liu, J., Ji, H., and Lu, M. (2000). Core structure of the outer membrane lipoprotein from *Escherichia coli* at 1.9 Å resolution. *J Mol Biol* **299,** 1101-1112.

Silbert, J. A., Salditt, M., and Franklin, R. M. (1969). Structure and synthesis of a lipid-containing bacteriophage. III. Purification of bacteriophage PM2 and some structural studies on the virion. *Virology* **39,** 666-681.

Simidu, U., Kita-Tsukamoto, K., Yasumoto, T., and Yotsu, M. (1990). Taxomony of four bacterial strains that produce tetrodotoxin. *Int J Syst Bacteriol* **40,** 331-336.

Simpson, A. A., Tao, Y., Leiman, P. G., Badasso, M. O., He, Y., Jardine, P. J., Olson, N. H., Morais, M. C., Grimes, S., Anderson, D. L., Baker, T. S., and Rossmann, M. G. (2000). Structure of the bacteriophage ϕ29 DNA packaging motor. *Nature* **408,** 745-750.

Sleytr, U. B., and Beveridge, T. J. (1999). Bacterial S-layers. *Trends Microbiol* **7,** 253-260.

Smith, D. E., Tans, S. J., Smith, S. B., Grimes, S., Anderson, D. L., and Bustamante, C. (2001). The bacteriophage ϕ29 portal motor can package DNA against a large internal force. *Nature* **413,** 748-752.

Snipes, W., Cupp, J., Sands, J. A., Keith, A., and Davis, A. (1974). Calcium requirement for assemby of the lipid-containing bacteriophage PM2. *Biochim Biophys Acta* **339,** 311-322.

Spencer, R. (1955). A marine bacteriophage. *Nature* **175,** 690-691.

Stehle, T., Gamblin, S. J., Yan, Y., and Harrison, S. C. (1996). The structure of simian virus 40 refined at 3.1 Å resolution. *Structure* **4,** 165-182.

Stewart, P. L., Burnett, R. M., Cyrklaff, M., and Fuller, S. D. (1991). Image reconstruction reveals the complex molecular organization of adenovirus. *Cell* **67,** 145-154.

Strauss, J. H., and Strauss, E. G. (2001). Virus evolution: how does an enveloped virus make a regular structure? *Cell* **105,** 5-8.

Strömsten, N. J., Bamford, D. H., and Bamford, J. K. H. (2003). The unique vertex of bacterial virus PRD1 is connected to the viral internal membrane. *J Virol* **77,** 6314-6321.

Studier, F. W., and Moffatt, B. A. (1986). Use of bacteriophage T7 RNA polymerase to direct selective high-level expression of cloned genes. *J Mol Biol* **189,** 113-130.

Takeda, N., Tanimura, M., and Miyamura, K. (1994). Molecular evolution of the major capsid protein VP1 of enterovirus 70. *J Virol* **68,** 854-862.

Tarahovsky, Y. S., Khusainov, A. A., Deev, A. A., and Kim, Y. V. (1991). Membrane fusion during infection of *Escherichia coli* cells by phage T4. *FEBS Lett* **289,** 18-22.

Tetart, F., Desplats, C., Kutateladze, M., Monod, C., Ackermann, H. W., and Krisch, H. M. (2001). Phylogeny of the major head and tail genes of the wide-ranging T4-type bacteriophages. *J Bacteriol* **183,** 358-366.

Thomassen, E., Gielen, G., Schutz, M., Schoehn, G., Abrahams, J. P., Miller, S., and van Raaij, M. J. (2003). The structure of the receptor-binding domain of the bacteriophage T4 short tail fibre reveals a knitted trimeric metal-binding fold. *J Mol Biol* **331,** 361-373.

Tsukagoshi, N., Kania, M. N., and Franklin, R. M. (1976). Identification of acyl phosphatidylglycerol as a minor phospholipid of *Pseudomonas* BAL-31. *Biochim Biophys Acta* **450,** 131-136.

Tsukagoshi, N., Schäfer, R., and Franklin, R. M. (1977). Structure and synthesis of a lipid-containing bacteriophage. An endolysin activity associated with bacteriophage PM2. *Eur J Biochem* **77,** 585-588.

Tuma, R., Tsuruta, H., Benevides, J. M., Prevelige, P. E., Jr., and Thomas, G. J., Jr. (2001). Characterization of subunit structural changes accompanying assembly of the bacteriophage P22 procapsid. *Biochemistry* **40,** 665-674.

Turner, D. R., Joyce, L. E., and Butler, P. J. (1988). The tobacco mosaic virus assembly origin RNA. Functional characteristics defined by directed mutagenesis. *J Mol Biol* **203,** 531-547.

Vaara, M. (1992). Agents that increase the permeability of the outer membrane. *Microbiol Rev* **56,** 395-411.

Valpuesta, J. M., and Carrascosa, J. L. (1994). Structure of viral connectors and their function in bacteriophage assembly and DNA packaging. *Q Rev Biophys* **27,** 107-155.

Vanden Boom, T., and Cronan, J. E., Jr. (1988). Enrichment of the bacteriophage PR4 membrane in phosphatidylglycerol is not essential for phage assembly and infectivity. *J Bacteriol* **170,** 2866-2869.

van der Schans, G. P., Weyermans, J. P., and Bleichrodt, J. F. (1971). Infection of spheroplasts of *Pseudomonas* with DNA of bacteriophage PM2. *Mol Gen Genet* **110,** 263-371.

van Mansfeld, A. D., Langeveld, S. A., Baas, P. D., Jansz, H. S., van der Marel, G. A., Veeneman, G. H., and van Boom, J. H. (1980). Recognition sequence of bacteriophage ϕX174 gene A protein-an initiator of DNA replication. *Nature* **288,** 561-566.

van Regenmortel, M. H. V., Fauquet, C. M., Bishop, D. H. L., Carstens, E. B., Estes, M. K., Lemon, S. M., Maniloff, J., Mayo, M. A., McGeoch, D. J., Princle, C. R., and Wickner, R. B. (2000). "Virus taxonomy, classification and nomenclature of viruses. Seventh report of the international committee on taxonomy of viruses." Academic Press, San Diego, San Francisco, New York, Boston, London, Sydney, Tokyo.

von Heijne, G. (1992). Membrane protein structure prediction. Hydrophobicity analysis and the positive-inside rule. *J Mol Biol* **225,** 487-494.

Waldor, M. K., and Mekalanos, J. J. (1996). Lysogenic conversion by a filamentous phage encoding cholera toxin. *Science* **272,** 1910-1914.

Walin, L., Tuma, R., Thomas, G. J., and Bamford, D. H. (1994). Purification of viruses and macromolecular assemblies for structural investigations using a novel ion exchange method. *Virology* **201,** 1-7.

Wang, B., Jones, D. N., Kaine, B. P., and Weiss, M. A. (1998). High-resolution structure of an archaeal zinc ribbon defines a general architectural motif in eukaryotic RNA polymerases. *Structure* **6,** 555-569.

Waterbury, J. B., and Valois, F. W. (1993). Resistance to co-occurring phages enables marine *Synechococcus* communities to coexist with cyanophages abundant in seawater. *Appl Environ Microbiol* **59,** 3393-3399.

Weaver, S. C., Kang, W., Shirako, Y., Rumenapf, T., Strauss, E. G., and Strauss, J. H. (1997). Recombinational history and molecular evolution of western equine encephalomyelitis complex alphaviruses. *J Virol* **71,** 613-623.

White, A. H. (1940). A bacterial discoloration of print butter. *Sci Agric* **20,** 638-645.

Whitfield, C., and Roberts, I. S. (1999). Structure, assembly and regulation of expression of capsules in *Escherichia coli*. *Mol Microbiol* **31,** 1307-1319.

Wikoff, W. R., Liljas, L., Duda, R. L., Tsuruta, H., Hendrix, R. W., and Johnson, J. E. (2000). Topologically linked protein rings in the bacteriophage HK97 capsid. *Science* **289,** 2129-2133.

Wildy, P. (1971). Classification and Nomenclature of Viruses. First Report of the International Committee on Taxonomy of Viruses., Vol. Monogr Virol 5, pp. 1-65.

Wommack, K. E., and Colwell, R. R. (2000). Virioplankton: viruses in aquatic ecosystems. *Microbiol Mol Biol Rev* **64,** 69-114.

Xie, Z., and Hendrix, R. W. (1995). Assembly *in vitro* of bacteriophage HK97 proheads. *J Mol Biol* **253,** 74-85.

Xu, L., Benson, S. D., Butcher, S. J., Bamford, D. H., and Burnett, R. M. (2003). The receptor binding protein P2 of PRD1, a virus targeting antibiotic-resistant bacteria, has a novel fold suggesting multiple functions. *Structure (Camb)* **11,** 309-322.

Yamamoto, K. R., Alberts, B. M., Benzinger, R., Lawhorne, L., and Treiber, G. (1970). Rapid bacteriophage sedimentation in the presence of polyethylene glycol and its application to large-scale virus purification. *Virology* **40,** 734-744.

Zavriev, S. K., and Shemyakin, M. F. (1982). RNA polymerase-dependent mechanism for the stepwise T7 phage DNA transport from the virion into *E. coli*. *Nucleic Acids Res* **10,** 1635-1652.

Zhang, W., Chipman, P. R., Corver, J., Johnson, P. R., Zhang, Y., Mukhopadhyay, S., Baker, T. S., Strauss, J. H., Rossmann, M. G., and Kuhn, R. J. (2003). Visualization of membrane protein domains by cryo-electron microscopy of dengue virus. *Nat Struct Biol* **10**, 907-912

Zimmer, S. G., and Millette, R. L. (1975a). DNA-dependent RNA polymerase from *Pseudomonas* BAL-31. II. Transcription of the allomorphic forms of bacteriophage PM2 DNA. *Biochemistry* **14,** 300-307.

Zimmer, S. G., and Millette, R. L. (1975b). DNA-dependent RNA polymerase from *Pseudomonas* BAL-31. I. Purification and properties of the enzyme. *Biochemistry* **14,** 290-299.

ZoBell, C. E., and Upham, H. C. (1944). A list of marine bacteria including description of sixty new species. *Bull Scripps Inst Oceanogr Univ Calif* **5,** 239-292.